Universidade do Minho
Escola de Ciências

Liliana Patrícia da Silva Araújo

Optimization of culture medium composition using agro-industrial by-products for the production of Silk-Elastin-Like Proteins by *Escherichia coli*

junho de 2022

Optimization of culture medium composition using agro-industrial by-products for the production of Silk-Elastin-Like Proteins by *Escherichia coli*

Liliana Araújo

UMinho | 2022

FUN2CNT
FCT Fundação para a Ciência e a Tecnologia
Governo da República Portuguesa
UNIÃO EUROPEIA
Fundo Europeu de Desenvolvimento Regional

Universidade do Minho
Escola de Ciências

Liliana Patrícia da Silva Araújo

Optimization of culture medium composition using agro-industrial by-products for the production of Silk-Elastin-Like Proteins by *Escherichia coli*

Dissertação de Mestrado
Mestrado em Bioquímica Aplicada – Ramo Biotecnologia

Trabalho efetuado sob a orientação do
Doutor André da Costa
Doutor Raul Machado

junho de 2022

DIREITOS DE AUTOR E CONDIÇÕES DE UTILIZAÇÃO DO TRABALHO POR TERCEIROS

Este é um trabalho académico que pode ser utilizado por terceiros desde que respeitadas as regras e boas práticas internacionalmente aceites, no que concerne aos direitos de autor e direitos conexos. Assim, o presente trabalho pode ser utilizado nos termos previstos na licença abaixo indicada. Caso o utilizador necessite de permissão para poder fazer um uso do trabalho em condições não previstas no licenciamento indicado, deverá contactar o autor, através do RepositóriUM da Universidade do Minho.

Licença concedida aos utilizadores deste trabalho

Atribuição-NãoComercial-SemDerivações

CC BY-NC-ND

https://creativecommons.org/licenses/by-nc-nd/4.0/

ACKNOWLEDGEMENTS

As the final months are near and the clock ticking out, putting the final points on the thesis, the everlasting masters is ending, and as this hard chapter is closing nothing but more than grateful comes to mind for the multiple of people who helped and supported through this journey.

First and foremost, I want to thank Dr. André Costa for teaching me so much during my master's program and for having the patience and dedication to sit with me whenever I had any questions and for guiding me through each step. Also, I'd like to thank Dr. Raul Machado for all of his assistance, availability, guidance, and encouragement from the beginning to the end of these. I am grateful to both of my advisors, Dr. André Costa and Dr. Raul Machado, for providing this opportunity. I am grateful for every day of this project because I learned something new every day. Thank you for being such excellent advisors!

Secondly, I would like to thank the University of Minho for receiving me, in particular to CBMA and IB-S and to the LBM II, which welcomed me with open arms.

I would like to express my gratitude to my colleagues (Diana, João, Luís, Anabela, Vanessa, and Bárbara). Also, I must express my appreciation for the technicians of the department of biology, in specific to Inês, Márcia and Lídia.

To my parents, Joaquim and Helena, I thank them for the support, dedication and education they have given me all these years. And, for unconditional love, Thank you.

To my two brothers, Catarina and Kevin, thank you for putting up with me all these years, I know it wasn't easy.

To my friends (especially: Alexandra, Ana Barbosa, Kelly and Rute) because sometimes the most important things in life are not knowledge, but friendship. Thank you for every adventure.

And, finally, I would like to express appreciation to the most comprehensible person that I know Pedro Fernandes, was always available and ready to help even when I am being irrational, thank you.

This work was supported by national funds through FCT – Fundação para a Ciência e a Tecnologia, IP, under the project “FUN2CYT - Harnessing the potential for biomedical applications of pleiotropic cytokines LIF and oncostatin M” with reference POCI-01-0145- FEDER-030568.

To all my sincere and deep, **Thank you very much**!

STATEMENT OF INTEGRITY

I hereby declare having conducted this academic work with integrity. I confirm that I have not used plagiarism or any form of undue use of information or falsification of results along the process leading to its elaboration.

I further declare that I have fully acknowledged the Code of Ethical Conduct of the University of Minho.

Otimização da composição do meio de cultura utilizando subprodutos agroindustriais para a produção de proteínas Seda-Elastina por *Escherichia coli*

Resumo

Nos últimos anos, a investigação associada ao desenvolvimento de biopolímeros tem vindo a ganhar um ímpeto significativo, impulsionada pela necessidade de encontrar materiais inovadores, com propriedades aprimoradas e menor impacto ecológico. Os polímeros proteicos recombinantes (rPPs) são um exemplo de novos materiais inovadores e, entre eles, as proteínas do tipo Seda-Elastina (*silk-elastin-like proteins*, SELPs) demonstram propriedades únicas. Estes polímeros são compostos por blocos de aminoácidos encontrados na seda e na elastina e são produzidos em fábricas celulares microbianas, em processos tipicamente à escala laboratorial. Para o escalonamento a nível industrial a níveis economicamente viáveis, é de extrema importância otimizar o processo de bioprodução. Adicionalmente, a crescente consciência ambiental implica o desenvolvimento de processos sustentáveis recorrendo a, por exemplo, abordagens de economia circular. A substituição de componentes do meio de cultura por subprodutos/resíduos de setores como o agroindustrial permite reduzir os custos associados ao meio fermentativo e contribuir para uma economia circular.

O presente projeto visou otimizar a bioprodução de SELPs em condições de fermentação descontínua, utilizando *Escherichia coli* como modelo microbiano (fábrica celular microbiana), e meios de cultura formulados com subprodutos/resíduos agroindustriais nomeadamente, soro de queijo, glicerol e licor de maceração de milho. A otimização do meio de fermentação foi analisada com recurso a técnicas clássicas nomeadamente, '*one-factor-at-a-time*' e '*central composite design'* (CCD). Para além da otimização do meio de cultura, procedeu-se à seleção de mutantes com produção reduzida de ácidos orgânicos através da técnica de '*proton suicide'*, resultando na obtenção de um mutante de *E. coli* com a capacidade de produzir maior quantidade de SELP. As análises por CCD demonstraram que a utilização de subprodutos industriais foi eficiente para sustentar o crescimento bacteriano e promover a elevada produção de SELP, resultando numa diminuição dramática dos custos associados ao meio de fermentação.

Palavras-chave: rPPs; proteína do tipo seda-elastina; otimização da produção; OFAT; CCD; suicídio de protões.

Optimization of culture medium composition using agro-industrial by-products for the production of Silk-Elastin-Like Proteins by *Escherichia coli*

Abstract

In recent years, research and development of biopolymers have been gaining significant momentum, driven by the need to find innovative and promising new bio-based materials. Recombinant protein polymers (rPPs) are an example of such innovation-driven outcomes and, among them, Silk-Elastin-Like Proteins (SELPs) demonstrate unique properties and have been used for an assortment of different applications. In order to scale up to industrial levels and achieve economically feasibility, it is important to improve the efficiency of the bioprocesses, ideally, by reducing the costs of protein production and improve production yields. Moreover, the increasing environmental consciousness favours the consideration of circular economy approaches for the design of sustainable processes. Accordingly, the use of industrial residues/by-products in the fermentation bioprocesses represents a convenient approach, not only to replace expensive media ingredients, but also to comply with the circular economy framework.

The present dissertation targeted the optimization of SELP bioproduction in batch fermentation conditions, using *Escherichia coli* as microbial cell factory and alternative culture media formulated with agro-industrial residues/by-products namely, cheese whey, glycerol and corn steep liquor. The optimization of the media based on these agro-industrial by-products was analysed through classical medium optimization techniques namely, one-factor-at-a-time (OFAT) and statistical design with central composite design (CCD). Also, we explored the use of a proton-suicide approach for the high-level biosynthesis of SELP by generating mutants with the ability to produce lower amounts of organic acids, pushing forward the high expression of heterologous recombinant proteins. CCD studies demonstrated that the utilization of undervalued industrial by-products was efficient to sustain bacterial growth and promote the high expression of SELP, leading to great improvements over protein expression and a dramatic decrease of costs associated with fermentation media.

Keywords: recombinant biopolymers; silk-elastin-like protein; industrial by-products; production optimization; OFAT; CCD; proton suicide.

Table of Contents

List of Abbreviations

APS – Ammonium Persulphate

BCA – Bicinchoninic acid assay

Br^-/BrO^-_3 – equimolar concentrations of Bromide and Bromate

Br^- – Bromide

Br_2 – Bromine

BrO^- – hypobromite

BrO_2^- – Bromite

BrO_3^- – Bromate

BSA – Bovine Serum Albumin

Ca – Calcium

CCD – Central composite design

CSL – Corn steep liquor

Cu – Cooper

CW – Cheese Whey

DMSO – Dimethyl sulfoxide

DNA – Deoxyribonucleic acid

***E. coli* –** *Escherichia coli*

EFT – Elapsed fermentation time

ELPs – Elastin-like polypeptides

ELR – Elastin-like recombinamers

EPS – Polystyrene

Fe – Iron

HA – Hyaluronic acid

HFIP – Hexafluoroisopropanol

HPLC – High Performance Liquid Chromatography

IPTG – Isopropyl-β-D-thiogalactopyranoside

K – Potassium

Lac – Lactose

***lacI* –** Lac repressor

***lac*Y –** Lactose permease

LB – Lysogeny Broth

LB+CW – Lysogeny Broth supplemented with cheese whey

LB+IPTG – Lysogeny Broth supplemented with IPTG

LB+Lac – Lysogeny Broth supplemented with lactose

LBA – Lysogeny Broth agar medium.

Mac – MacConkey agar medium

Mg – Magnesium

Mn – Manganese

Mo – Molybdenum

N – Nitrogen

OA – Organic acids

OD_{600nm} – Optical density at 600 nm

OFAT – One-factor-at-a-time method

P – Phosphorus

PE – Polyethylene

PEG – Polyethylene glycol

PEP – phosphoenolpyruvate.

PS – Polystyrene

RNA – Ribonucleic acid

rPPs – Recombinant protein polymers

S – Sulfur

SDS-PAGE – Sodium dodecyl sulphate-polyacrylamide gel electrophoresis

Se – Selenium.

SELPs – Silk-elastin-like proteins

SF/K – Silk fibroin/keratin

SLP – Silk-like protein

TB – Terrific Broth

TB+CW – Terrific Broth supplemented with cheese whey

TB+IPTG – Terrific Broth supplemented with IPTG

TB+Lac – Terrific Broth supplemented with lactose

TEMED – Tetramethylethylenediamine

TP – Tryptone

V – Vanadium

WR – Working reagent

YE – Yeast Extract

Zn – Zinc

List of Figures

List of Tables

1. Introduction

1.1. Brief introduction

The technological developments in chemistry, and materials science and engineering resulted in a new class of materials, called plastics (a class of polymers) (Padinjakkara *et al.,* 2019). The modern plastic industry started with Bakeland*,* (1909) creating the first solely synthetic plastic called Bakelite (Bakeland, 1909). Since then, plastic has evolved alongside with society, developed to make peoples life easier, turning daily tasks more practical, convenient and safe. Presently, there are several plastic formulations available (*e.g.*, Polyethylene (PE), Polystyrene (PS) Polystyrene (PS), etc.) (Meikle, 1995). Most of these materials are petroleum-based and extremely resistant to natural decomposition, generating a great impact on ecosystems. Therefore, the development of bio-based and biodegradable polymers as an alternative to petroleum-based polymers urged advances in the research for natural biopolymers (Tang *et al.,* 2012).

Natural biopolymers are obtained from natural sources and can be classified into three major classes according to the monomeric unit: polysaccharides (monosaccharide units joined together by glycosidic linkages), polynucleotides (DNA and RNA) or polypeptides (amino acid monomers linked by peptide bonds) (Runnels *et al.*, 2018; Tamang 2021). Natural biopolymers are commonly found in today markets, for instance, starch is a polysaccharide with potential to replace polyolefins and is used as additive in food, cosmetics, and pharmaceuticals (Cheng *et al.,* 2021). Silk is another example of a protein biopolymer, with a shining past in the textile industry, but also as a biomedical material (*e.g.* surgical sutures, drug delivery, scaffolds for tissue engineering) (Numata, 2020; Vollrath *et al.,* 2009). Within natural biopolymers, fibrous/structural proteins are of special interest due to the remarkable properties of mechanical performance, great biocompatibility and associated biodegradability (Casal *et al.*, 2013). Fibrous proteins such as silk, collagen, gelatin and elastin, have evolved in nature to fulfil the primary function of forming structural materials in living organisms. Hence, in recent years, the research and development of biopolymers based on proteins have been gaining significant momentum, driven by green practices and sustainability principles that are increasingly adopted by industry (Khalaf, 2016).

Although many of these fibrous proteins are already at use, recombinant DNA technology offers the opportunity to create custom-designed protein materials by reengineering the molecular architecture (Yang, *et al.,* 2017). By using recombinant biotechnology approaches, it is possible to program artificial genes to create novel bioinspired biopolymers – the recombinant protein

polymers (rPPs) – with well-defined monodispersity and structure (Casal *et al.*, 2013). These bioinspired recombinant biopolymers are based on the minimal consensus repeats, commonly found in natural fibrous proteins (Yang, *et al.*, 2017), and are obtained by genetic engineering and biological synthesis (Frandsen & Ghandehari, 2012). This approach allows to achieve a precise control over the genetic sequence, conferring the ability to custom-design the structure of rPPs with defined composition and size (Tjin *et al.,* 2014). Moreover, since rPPs are composed of only amino acids and produced in microbial cell factories, are inherently biodegradable with production not dependent on natural or oil based resources. An example of these genetically engineered recombinant protein polymers, and the main focus in this work, are Silk-Elastin-Like Proteins (SELPs); these recombinant protein polymers combine the physicochemical and biological properties of silk fibroin and mammalian tropoelastin in a single molecule (Huang, *et al.,* 2015; Machado *et al.,* 2015).

SELPs have been extensively implemented in a variety of applications, mainly for biomedical purposes (Pradhan *et al.,* 2017). Among these, SELPs are used as scaffolds for tissue engineering (Qiu *et al.*, 2010; Dias *et al.,* 2021; Kundu *et al.*, 2020), drug delivery systems (Burcin *et al.,* 2019; Soni *et al.,* 2021) or in wound healing devices (Vasconcelos *et al.,* 2012; Chouhan *et al.,* 2019). Nevertheless, the remarkable properties of SELPs (*e.g.,* mechanical, optical, biological) further expanded their use for other purposes such as in the development of biosensors (Kavetskyy *et al.,* 2019; Arlyapov *et al.,* 2021), microfluidic systems (Shiekh *et al.,* 2021), contact lenses (Xinming *et al.,* 2008) and multifunctional biocomposites (Pereira *et al.,* 2016; Fernandes *et al.,* 2018; Correia *et al.,* 2019). Despite the great potential, the widespread applicability of SELPs (and other recombinant protein polymers) is highly limited due to production costs and productivity issues (Collins *et al.,* 2013; Machado *et al.*, 2013a; Collins *et al.,* 2014). Therefore, finding cheaper alternative media can be a plus for decreasing overall production costs.

Over the past few years, the scientific community has been looking at agro-industrial wastes or residues as a cheap alternative for fermentation broths, since the practices used in the agro-industry processes are well known to generate huge quantities of some type of waste or by-products (Panesar *et al.*, 2015). The agro-industrial residues consist of many and varied products from agriculture and food industry (Vandamme, 2009), which are rich in organic matter and can be explored as ingredients for culture media formulation (Bacha & Nasir, 2011; Alexandri *et al.*, 2018). Thus, the employment of industrial residues has the potential to reduce the costs of the upstream

process of bulk chemicals while contributing to reduce the environmental impact of agro-industrial practices.

1.2. Polymers and biopolymers

Polymers are macromolecules composed of monomeric units combined in different ways and linked together through covalent bonds. In some cases, the bonds lead to a linear chain (figure 1.1A), with or without branches (figure 1.1B) and in particular cases, the chains cross-link to form three-dimensional structures (figure 1.1C).

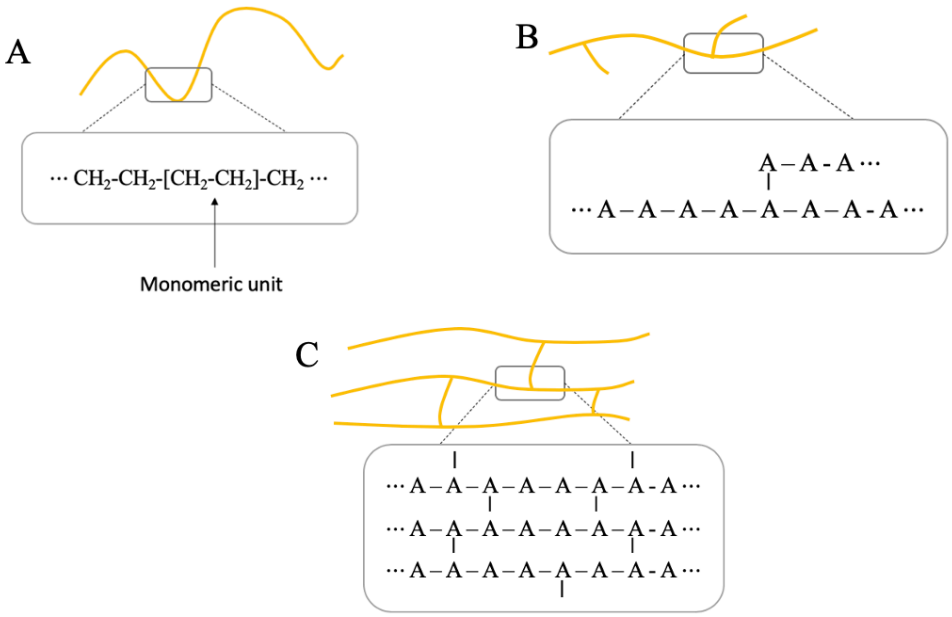

Figure 1.1 – Structural representation of the different ways the monomeric units can link together. A - linear chain; B - with or without branches; C - three-dimensional structures (chains cross-linked together).

Polymers can be synthetic or of natural origin. Most of the polymers used globally are synthetic and non-biodegradable, leading to serious environmental issues (Padinjakkara *et al.,* 2019). In response to this increasing awareness, the term "green chemistry" appeared in the mid-to-late 90's, focusing on the design and polymer production methods that diminishes or eliminates the use of hazardous materials for humans and the environment (Tănase *et al.*, 2014). This prompted researchers to develop and explore biopolymers as an alternative to the conventional petroleum-based solutions. With scientific and technological advances, biopolymers constitute an innovative

and promising eco-friendly alternative to diminish damages in the environment and ecosystems, reducing energy demand and the use of non-renewable resources.

Biopolymers are macromolecules found in Nature, either naturally produced by living organisms, like plants and animals (Gnanasekaran, 2019), or chemically synthesized from biological starting materials (*e.g.,* sugars, starch, etc.) (Padinjakkara *et al.,* 2019). These polymeric materials can be largely classified into three groups (figure 1.2): i) polynucleotides, composed of many nucleotide units (*e.g.,* RNA and DNA); ii) polypeptides, composed of amino acids; and iii) polysaccharides which are often linear or branched polymeric chains of carbohydrates (*e.g.,* alginates, cellulose, chitin, starch and chitosan) composed of many sugar units (Padinjakkara *et al.*, 2019; Elnashar, 2010).

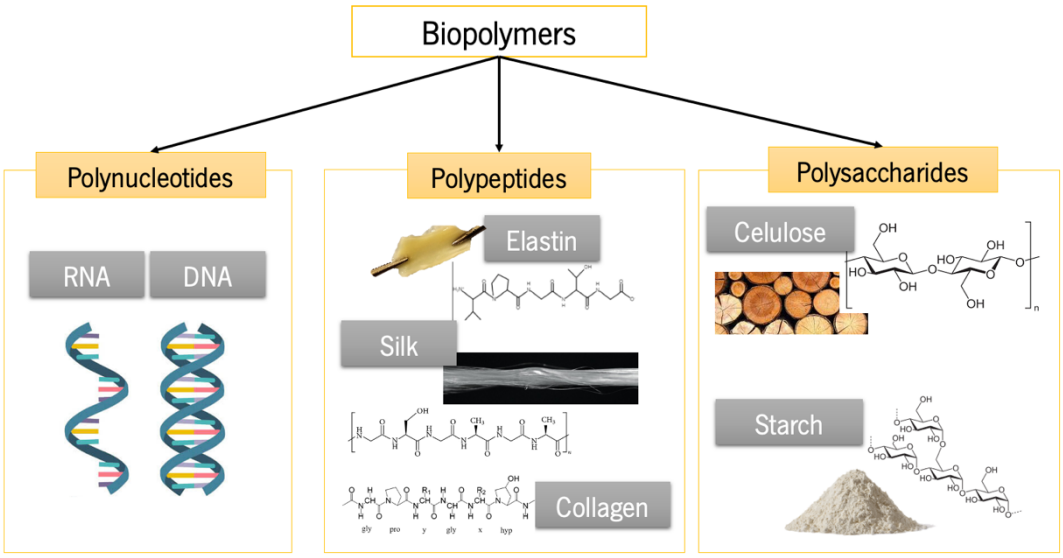

Figure 1.2 – General classification of biopolymers: polynucleotides, polypeptides and polysaccharides.

Biopolymers are biodegradable because of the oxygen and nitrogen atoms found in their structural backbone. Biodegradation converts them to CO_2, water, biomass, humid matter and other natural substances (Yadav *et al.,* 2015). Moreover, show fascinating properties (*e.g.*, nontoxicity, mechanical properties) and are of increasing importance for different applications in electronics, medical devices, energy, food packaging, drug delivery systems, wound healing, bioresorbable scaffolds for tissue engineering, among others (Elnashar, 2010; Yadav *et al.,* 2015).

1.3. Recombinant protein polymers (rPPs)

Recombinant protein polymers (rPPs) are genetically engineered protein macromolecules that emerged from advances in molecular biology techniques and traditional polymer science, allowing to create new biopolymer designs, with some examples represented in table 1.1. These recombinant proteinaceous materials consist of repeating blocks of amino acids based on the canonical repeats present in natural fibrous/structural proteins (Lutz & Bornscheuer, 2012; Casal *et al.*, 2013; Stevens, 2013).

The techniques in molecular biology are useful to create synthetic genes with a precise control over its sequence and direct the biosynthesis of protein polymers in recombinant microorganisms (Machado *et al.,* 2015). In general, rPPs are obtained by traditional recombinant DNA techniques, followed by protein expression and purification (Jana *et al.,* 2017).

Table 1.1 – Repeating sequences found in some natural structural/fibrous proteins (adapted from Casal *et al.*, 2013 and Werten *et al.,* 2001).

Protein family	Monomeric unit sequence
Elastin	GVGVP, VPGG, APGVGV
Silk fibroin	GAGAGS
Byssus	GPGGG
Flagelliform silk	GPGGX*
Dragline silk	GPGQQ, GPGGY, GGYGPGS
Collagen	GAPGAPGSQGAPGLQ, GAPGTPGPQGLPGSP
Keratin	AKLKLAEAKLELA
Titin (I-band)	PPAKVPEVPEPKKPVPEEKVPVPVPKKPEA
Abductin	GGFGGMGGGX*
Gelatin	GPPGEPGNPG

Note: *Sequences are given in single-letter amino acid code, where X is any amino acid.

1.4. Silk-Elastin-Like Proteins (SELPs)

Silk-Elastin-Like Proteins (SELPs) are a family of rPPs that combine the crystallinity and mechanical strength of silk blocks with the water solubility and resilience of elastin blocks, in the same polypeptide chain (Jana *et al.,* 2017). Typically, the silk sequence of SELPs is obtained from *Bombyx mori* silkworm silk with sequence GAGAGS (G: glycine, A: L-alanine, S: L-serine), whereas the elastin block relies on the pentamer sequence from mammalian tropoelastin with the sequence VPGVG (V: L-valine, P: L-proline) (Machado *et al.,* 2015; Tarakanova *et al.,* 2017). The diverse

mechanical and biological properties of SELPs are obtained by the various combinations of high tensile strength silk blocks with highly resilient elastin-like blocks (Machado *et al.,* 2013a; Machado *et al.,* 2015), with the number and sequence of these repeats directly related with the physicochemical properties of SELPs (Akash *et al.,* 2015). The silk-like blocks spontaneously form hydrogen-bonded β-sheets crystals that provide thermal and chemical stability as well as physical cross-linking sites, while the elastin block disrupts the overall crystallinity of the system and confers stimuli-responsiveness; meaning that SELPs can undergo structural transitions upon external stimuli such as temperature or pH (Chen *et al.*, 2017; Machado *et al.*, 2013a, Machado *et al.*, 2015). Moreover, the elastin blocks can form β-spirals conferring elasticity to the system, while also increasing the spacing between the silk blocks, resulting in increased flexibility, water solubility and resiliency (Machado *et al.,* 2013b; Casal *et al.,* 2013).

For the past years, genetically engineered SELPs demonstrated to be quite versatile, especially for biomedical purposes due to the remarkable biocompatibility and versatility of processing (Roberts *et al.,* 2018; Chambre *et al.,* 2020; Gustafson & Ghandehari, 2010). There are many techniques used for the fabrication of SELP-based materials originating a variety of different structures namely, nano or submicroparticles, fibers, films and hydrogels, to meet specific material applications (Tarakanova *et al.*, 2017). The manufacturing processes usually resort to the dissolution of the SELP into an adequate solvent mostly, water (Ner *et al.,* 2009; Machado *et al.,* 2015; Pereira *et al.,* 2021), hexafluoroisopropanol (HFIP) (Stephens *et al.,* 2005) or formic acid (Machado *et al.,* 2015; Correia *et al.,* 2019). Nevertheless, providing that SELPs present and adequate composition, the less environmentally friendly solvents HFIP and formic acid can be replaced by water, allowing the implementation of green processes (Machado *et al.,* 2015).

SELP nano or submicroparticles are mainly obtained by directed self-assembly of the block copolymers. The formation of SELP nanoparticles depends on the hydrophobicity difference between the silk and elastin blocks, the ratio between these two blocks as well as the hydrogen bonding between silk domains (Georgilis, *et al.,* 2020). For instance, Wang *et al.,* (2014b) formulated a series of SELPs with different silk-to-elastin block ratio and described their capacity to form micellar-like nanoparticles upon a thermal stimuli, for drug delivery purposes. Among the diverse uses, SELP micro- and nanofibers produced by electrospinning, have great potential for tissue engineering (Qiu *et al.*, 2010; Machado *et al.*, 2013b), with the benefit of avoiding the inconvenient use of synthetic polymers that can pose biocompatibility and toxicity risks. Electrospun SELP fibre mats demonstrated to be interesting as scaffolds in skin tissue repair and

in the fabrication of soft connective tissue substitutes (Machado *et al.*, 2013b; Ner *et al.*, 2009; Zhu *et al.,* 2016). Another potential application of SELPs are films or coatings that can be employed for different purposes, from sensors to biomedical applications. The formation of films is mainly achieved by solvent evaporation (solvent casting) and have been used for the development of transparent thin films that can be employed for ophthalmic applications (*e.g.* contact lenses, synthetic corneas, intraocular lenses, ophthalmic drug delivery matrices) and biosensors (Sun *et al.,* 2013; Teng *et al.,* 2011; Machado *et al.,* 2015). More recently, physically active SELP-based nanocomposites with magnetic and piezoelectric properties have been described, with potential applications as sensors (Fernandes *et al.,* 2018; Correia *et al.,* 2019). Unless submitted to a post-processing treatment, SELP fibre mats and films are soluble in water, limiting the range of potential applications. Structure stabilization is usually achieved by exposure to methanol that induces a dehydration-mediated physical cross-linking, resulting in crystallization of the silk blocks to render aqueous insolubility (Chen *et al.*, 2017; Machado *et al.*, 2013b; Machado *et al.,* 2015).

Finally, with adequate sequence and composition (*i.e.,* number of silk blocks, number of elastin blocks, silk:elastin ratio), SELPs can undergo an irreversible transition phase to form densely cross-linked hydrogels, initiated or accelerated by changes in temperature or pH (Gonzalez-Obeso *et al.,* 2021). In hydrogels, the silk:elastin ratio and the size of the silk block are important factors as the sol-gel transition occurs through crystallization of the silk units via hydrogen-bonding; thus, can be controlled by manipulating the silk:elastin ratio or changing the size of the silk block (Roberts *et al.,* 2018; Willems *et al.,* 2019). The hydrogel network formed by SELPs controls the release of incorporated therapeutic proteins from hours to days depending upon the concentration of SELP, charge on the released agents and the ionic strength of the release media (Greish *et al.,* 2009). Thus, allowing a variety of applications including matrix-mediated delivery systems for gene therapy, drug delivery systems, stimuli (pH, temperature and ionic strength) sensitive materials and as scaffolds (Akash *et al.,* 2015).

To sum up, the biocompatibility, biodegradability and mechanical properties of SELPs makes these protein polymers interesting versatile materials for a wide range of applications, although primary focus has been given to biomedical applications. Table 1.2 shows different biomedical applications for different types of SELP-based materials (Tarakanova *et al.,* 2017).

Table 1.2 – Examples of biomedical applications using SELP-based materials.

Type of Structure	Applications	Advantage	References
Nanoparticles	Drug delivery applications	To enhance targeting or therapeutic functionality	(Georgilis, *et al.,* 2020; Parker *et al.,* 2019)
Nanofibers	Precursors for scaffold and drug delivery systems	Mimic the structure and properties of the extracellular matrix	(Ner *et al.*, 2009)
Fibers	Tissue engineering -	Excellent mechanical properties and biocompatibility	(Qiu *et al.*, 2010)
Films	Drug delivery, contact lenses, synthetic corneas, intraocular lenses, ophthalmic drug delivery matrices, biosensors, tissue engineering, coatings, microfluidics and microelectronics	Biodegradable and bioactive materials	(Chen *et al.*, 2017; Sun *et al.*, 2013; Teng *et al.*, 2011; Fernandes *et al.*, 2018; Poursaid *et al.,* 2015)
Hydrogels	Administration delivery and release of drugs and genes by an in-situ gelling delivery system	Enhance delivery for cancer treatments, drugs and genes	(Jensen et al., 2019; Cappello *et al.*, 1998)

The structure of the SELP used in this dissertation is based on the work of Machado *et al.,* (2013a), termed as SELP-59-A, and was selected as representative biopolymer for the production studies. This protein polymer consists of 9 tandem repetitions of the sequence S_5E_9, where 'S' represents the silk block with sequence GAGAGS and 'E' the elastin block with sequence VPAVG (figure 1.3). The unique composition of SELP-59-A (*e.g.*, ratio of silk to elastin of 1:2 and size of the silk/elastin blocks) gives it unique biological and mechanical properties (Machado, *et al.,* 2013b). The high portion of elastin compared to silk confers properties like reduced tensile strength, higher resilience, lower propensity for hydrogel formation, increased solubility and reduced crystallinity (Machado *et al.,* 2013a).

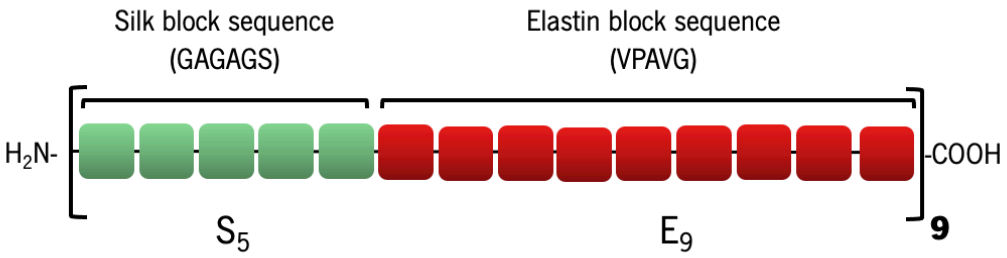

Figure 1.3 – Structural representation of SELP-59-A. Adapted from Machado *et al.*, (2013a).

1.5. Production of rPPs in *Escherichia coli* and optimization strategies.

1.5.1. A brief historical overview on heterologous protein production

The rise of the "new biotechnology" era started with the work of Paul Berg (Berg, 1971) when innovative research in gene splicing took place. It represented the first attempt to isolate a fragment of DNA from a bacterium and to insert it into a virus DNA, successfully creating the first DNA molecule with foreign DNA. This hallmark settled the basis for the subsequent research by Cohen, Chang, Boyer, and Helling (1973), which was the cornerstone of the biotechnology industry as we know today. This breakthrough was achieved when their combined knowledge of restriction endonucleases and plasmids was used to construct a recombinant plasmid (a plasmid containing recombined DNA from two different sources) (Cohen *et al.,* 1973). The insertion of the recombinant plasmid into *Escherichia coli* showed that the new transformed cell was biologically functional. With the upsurge of this combined techniques, a new age of terms was born, such as "foreign gene", "heterologous gene", and the "gene of interest". Interestingly, the first protein to be encoded in this system was described by terms like "heterologous protein", "foreign protein", and "recombinant protein".

The first recombinant protein to be synthesized by insertion of a heterologous gene in *E. coli* was Somatostatin (Itakura *et al.,* 1977) and, in the 80s, human insulin, the first biopharmaceutical (heterologous protein with therapeutic use), was approved by the FDA for medical use. After this, an increasing variety of heterologous proteins have been approved for medical use such as Protropin® (human growth hormone) and t-PA, Activase® (enzyme for blood clots) (Nielsen, 2013).

Recombinant proteins are used in various industries such as agro-industrial, chemical (*e.g.* detergents), cosmetic and pharmaceutical sectors. The sector of biomedical biotechnology is the backbone of recombinant protein production, used in medical treatments and as highly potent drugs. The biomedical industry for recombinant proteins has quickly grown. In recent years, almost two hundred recombinant proteins have been produced and utilized in medication around the world (Pham, 2018; Mitsui *et al.,* 2021). In 2020, the recombinant protein market was valued at approximately 108,680 € millions with a growth forecast of 11.2 % until 2026 (Mordor Intelligence, 2021), showing that, since the 70's, it was turned into a multimillionaire industry.

The next sections will focus on the production of recombinant protein polymers (rPPs).

1.5.2. Bioproduction of recombinant protein polymers (rPPs)

The design of an appropriate molecular cloning strategy is critical for the efficient synthesis of the protein encoding sequence and to produce a uniform protein product with an optimal yield. Usually, the biosynthesis of recombinant protein polymers (rPPs) namely, SELPs, involves the following steps (figure 1.4): (1) construction of a synthetic gene that encodes the SELP of interest in a plasmid with transcription control; (2) selection of the expression vector with the necessary transcriptional regulatory elements; (3) cloning of the recombinant gene into the expression vector; (4) transformation of the plasmid into competent expression host cells and the screening for positive clones, as well as confirmation of DNA sequence – SELPs are mainly produced in *Escherichia coli* using the *lac*I regulated T7 promoter-driven system; (5) growth of host cells at appropriate volume and induction of protein expression – generally, SELPs are produced in batch with a rich media; and (6) downstream processing operations involving the purification of the rPBPs of interest (Ducheyne *et al.,* 2015; Machado *et al.,* 2013a).

The next sections detail the most favourable fermentation variables such as cells, temperature, pH, agitation rates and oxygenation, and lastly, the composition of the growth media.

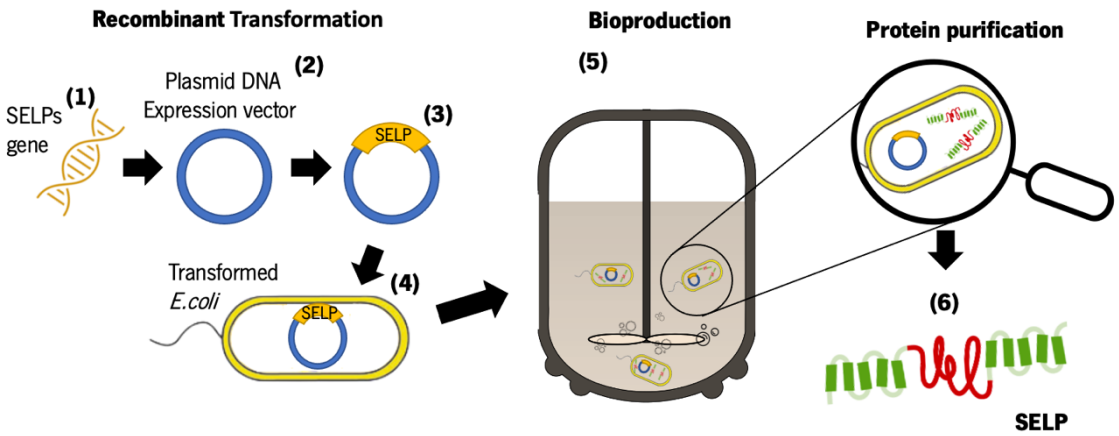

Figure 1.4 – Schematic representation of the biological production processes for SELPs. From selection and design of expression host and vectors (1- 4) to batch fermentation (5) and finally, SELPs purification (6).

1.5.2.1. Microbial cell factories

The widely disseminated usage of recombinant protein production and the amount of knowledge available on genetics and physiology of *E. coli* has made it to be the "microbial factory" of choice for the expression of rPPs (Chambre *et al.,* 2020). *E. coli* is a Gram-negative bacterium with high

growth rate and biomass yield (Boze *et al.,* 1995) that expedites the biotechnological processes for recombinant protein expression due to its relative simplicity, low-cost and well-known genetics with a large number of compatible tools available for biotechnology purposes (Sørensen & Mortensen, 2005).

Different rPPs have been produced in *E. coli* such as collagen, elastin-like polypeptides/recombinamers (ELPs/ELRs), silk-like proteins (SLPs) and silk-elastin-like proteins (SELPs) (Kinikoglu *et al.,* 2011; Xia *et al.,* 2011; Collins *et al*., 2013; Machado *et al.,* 2013a; Roberts *et al.,* 2018; Fernandes *et al.,* 2018). Another widely used microbial cell factory is *P. pastoris*, due to the ability to grow to high levels of biomass and protein expression, while also being appropriate for large-scale cultivation in bioreactors (Schipperus *et al.,* 2012). *P. pastoris* are able to grow in cheap defined media and can be easily manipulated at the genetic level, presenting the additional advantage of performing post-translational modifications, such as glycosylation, disulfide-bond formation, and proteolytic processing, in opposition to prokaryotic organisms (Cereghino *et al.,* 2002). Some studies describe the production of rPPs, such as recombinant spider silk and collagen (Fahnestock *et al.,* 1997; Teulé *et al.,* 2003), non-hydroxylated gelatins (Werten *et al.,* 1999) and elastin-like polypeptides (Sallach *et al.,* 2009; Schipperus *et al*., 2009). However, although representing an alternative to *E. coli*, there is a limited number of available plasmids and a limited choice of promoters (Yang *et al.,* 2017), and *E. coli* still remains the microorganism of choice for the expression of rPPs. In addition to the aforementioned, other hosts used for the expression of rPPs include transgenic plants (Scheller *et al.,* 2004), transgenic animals (Tang *et al.,* 2021), *Aspergillus nidulans* (Herzog *et al.,* 1997) and *Saccharomyces cerevisiae* (Sidoruk *et al*., 2015; Suástegui *et al*., 2017).

1.5.2.2. Expression systems

As mentioned, the main expression host used for the bioproduction of SELPs is *E. coli*, requiring.an expression system (plasmid DNA). The T7-based pET expression system (Novagen, 2006) with a *lac*I regulator is by far the most used in recombinant protein production (Machado *et al.,* 2013b; Collins *et al.,* 2013; Wang *et al.,* 2014b). Still, the expression host and vector should be carefully selected to maximize protein production. Accordingly, this expression system induces protein expression through the use of the synthetic lactose analogue isopropyl-β-D-thiogalactopyranoside (IPTG) (Machado *et al.,* 2013a). The T7 RNA polymerase is transcribed when IPTG (or allolactose)

binds and generates the release of tetrameric *LacI* from the lac operator. Transcription of the target gene from the T7 promoter (repressed by *LacI* as well) is then initiated by T7 RNA polymerase (Sørensen & Mortensen, 2005).

However, while IPTG is a well-known inducer for protein expression by *Lac* operons, it shows several disadvantages: is highly expensive, toxic to cells and requires additional culture handling for induction; in contrast, it is not metabolized meaning that concentration remains unchanged throughout the experiment (Machado *et al.,* 2013a; Studier, 2005). Natural sugars, such as lactose, are often used as alternative inducers, producing fewer toxic elements and generating less physiological stress to cells; consequently, removing some of the toxicity limitations associated with the addition of IPTG (Khani & Bagheri, 2020). The lactose is actively transported into the bacteria by a functional lac permease (lacY) and allolactose is converted from a part of lactose by the β-galactosidase enzyme (encoded by *lacZ* gene), to perform transgalactosidation reactions (Kotik *et al.,* 2004; Tan *et al.,* 2012).

The use of auto-induction media with lactose or lactose-containing compounds (industrial by-products such as permeated cheese whey) offers an inexpensive and efficient method for recombinant protein expression. It has been reported that lactose can serve as a substrate that can induce protein expression and contribute to the growth of *E. coli* (Crowley & Rafferty, 2019). Furthermore, the auto-induction method eliminates the need for follow-up growth at a certain time by adding an inducer, allowing the culture cells to grow to saturation and produce high protein yields without requiring additional steps (Machado *et al.*, 2013a).

Previously, Machado *et al.,* (2013a) demonstrated the usage of an auto-induction media for the production of SELPs, while using the pET25b-*E. coli* BL21 (DE3) expression system, reaching volumetric productivities within the range of 150 mg/L. In other works by the same group, the addition of an inducer like lactose or lactose-containing substrates (cheese whey) in the stationary phase of cell growth, allowed to achieve volumetric productivities as high as 500 mg/L (Collins *et al.,* 2013).

1.5.2.3. Cultivation modes

The biotechnological processes for the generation of microbial biomass by fermentation are generally grouped into three main methods: batch, fed-batch and continuous bioprocesses. From these, batch (Xia *et al.,* 2011; Machado *et al.,* 2013a) and fed-batch (Collins *et al.,* 2014) have

been the most commonly used fermentation processes for the production of SELPs in bacteria. The implementation of fed-batch processes always starts with a batch culture but with a subsequent input of substrate(s) in a later phase. Therefore, numerous culture parameters are first determined in batch cultures, such as media composition and environmental conditions (Boze *et al.,* 1995).

The main characteristic of a batch culture is that media components start at a given concentration until the microorganisms deplete the different available sources. In this 'closed system', there is no addition of substrates or removal of metabolites during culture (Roy, 2006) thus, the cells develop until there is a deficiency of nutrients or an accumulation of a toxic metabolite which stops growth (Collins *et al.,* 2013). The type of cultivation mode for the bioproduction of SELPs (and other recombinant proteins) is an important step as it influences toxic byproduct formation, plasmid stability, and can significantly impact polymer production. The authors Collins *et al.,* (2014) and Barroca *et al.*, (2016) demonstrated in their work a fed-batch process for the high-level production of a SELP in *E. coli* and importantly, suggest that the developed process can be scaled-up.

1.5.2.4. Environmental conditions

Temperature and pH

Temperature and pH are important factors for the expression of functional protein. It affects the growth rate, nutritional requirements, cell composition and cell permeability whereas, temperature also affects protein and lipid structure (Boze *et al.,* 1995). At this level, the optimum growth temperature for *E. coli* fluctuates from 20 °C to 37 °C (Herendeen *et al.,* 1978) with the optimum pH for most bacteria between 6.5 and 7.5 (Boze *et al.,* 1995). For the bioproduction of SELPs in *E. coli* the optimum growth temperature is around 37 °C at a pH of 6 - 7.5 (Collins *et al.,* 2013; Nagarsekar *et al.,* 2002).

Agitation and aeration

In a cell culture, oxygen affects cell growth, morphology, nutrient uptake and metabolite biosynthesis. The amount of dissolved oxygen (DO) is therefore an important variable in the fermentation process (Soccol *et al.,* 2013).

In aerobic metabolism, oxygen is a hydrogen acceptor that plays a critical role in the presence of hydrocarbons and aromatic compounds, not only for the production of energy but also for the

oxidation of the substrates, which requires more oxygen in fermentations using hydrocarbon sources than carbohydrates (Boze *et al.,* 1995). Thus, oxygen can be incorporated in carbon substrates (mostly hydrocarbons and aromatic compounds) during catabolism. The hydrocarbons and aromatic compounds in the presence of oxygen can be oxidised and can produce energy for the bacteria, resulting in the synthesis of ATP. Also, the oxidation of these organic compounds enables the generation of simpler organic compounds needed by the bacteria cell (Jurtshuk, 1996).

Most frequently, the concentration of dissolved oxygen (DO) in broths can be controlled by the speed of agitation. As such, the agitation rates should be adequately selected to meet the culture needs, by dispersing gas in small bubbles and hence, improve the contact area and maintain a high mass transfer with an even distribution of all the reagents (Stanbury *et al.,* 2013).

In the production of SELPs, the amount of oxygen dissolved in the media seems to play a critical factor for both bacterial cell growth and recombinant protein production yields. It is well-know that oxygen can affect cell densities in bacterial cell cultures. Therefore, the dissolved oxygen must be maintained at a concentration that meets the oxygen requirements of *E. coli* and avoid mixed acid fermentation. Consequently, elevated oxygen concentrations can also have negative effects on the process (oxidative damage) and can damage cells as a result of the high agitation rates (Collins *et al.,* 2014; Machado *et al.,* 2013a). Recombinant protein expression can be also affected by cell growth rate as the expression machinery (*e.g.,* RNA polymerases and ribosomes) of the cell is growth rate-dependent. However, it was found that for extreme growth rates, the protein/mass value decreases significantly, requiring the correct adjustment of growth rate for an adequate recombinant protein expression (Balbas & Lorence, 2004).

1.5.2.5. Key factors for protein production optimization

Media composition

The successful cultivation at high cell densities of a microorganism of interest (*e.g., E. coli*) depends on the type of culture media used. Liquid culture media or culture broth is the most commonly used; the nutrients are dissolved in water which facilitates their access by the cells (Bonnet *et al.*, 2019). Is also the most typically used media for the production of SELPs or recombinant protein polymers (Collins *et al.,* 2013; Collins *et al.,* 2014; Machado *et al.*, 2013a; Scheel *et al.,* 2021; Haider *et al.,* 2005).

The survival and growth of bacteria depends on an adequate supply of essential nutrients and favourable environmental conditions. Thus, the culture media is a nutritive substrate capable of allowing the nutrition and growth of microorganisms. The main substances can be classified in four categories: substrate, macro elements, trace elements and growth factors (Boze *et al.*, 1995).

The media must contain all necessary components for cell metabolism that allows the growth of the microorganism. Carbon substrates, such as glucose, can control the growth but are also limiting factors, as above certain concentrations (*e.g.*, above 50 g/L of glucose) can inhibit cell growth (Lee, 1996). On the other hand, its absence results in the opposite, leading to low cell densities (Soini *et al.,* 2008; Moulton, 2014; Stanbury *et al.,*1998). As such, a balanced media formulation is important for optimal cell density and protein expression.

The principal macro elements are nitrogen (N), phosphorus (P), potassium (K), magnesium (Mg), calcium (Ca), sulfur (S) and other salts (Ghasemi *et al.,* 2018). In fermentations without these macro elements the cells won't grow, since they are associated to energy transfer and cell permeability regulation functions (Sekar *et al.,* 2013), and cell structure maintenance (Moulton, 2014). Microorganisms require large amounts of these elements and the most used sources in fermentation processes are $K_2HPO_4$and $MgSO_4$ given that they provide the K, P, S and Mg elements in large quantities (Moulton, 2014).

The trace elements are important to improve microbial growth and biomass gain, playing a crucial role in biological processes by operating as a co-factor for enzymes (Soini *et al.,* 2008) and maintaining protein structures that use such elements (metalloproteins and selenoproteins) (Zhang *et al.,* 2010). The specific requirements for cell culturing can vary from strain and species, and although required in low concentrations, metal ions such as Fe, Mn, Zn, Se, Mo, V and Cu are fundamental for the microbial metabolism (Costa *et al.,* 2020).

In specific cases, a few microorganisms cannot synthesize some of their key cell components from the nitrogen and carbon sources, and there is the need to supplement the media with growth factors. The growth factors most commonly required are vitamins, specific amino acids, fatty acids, purines, pyrimidines and sterols (Walker, 2014). Occasionally, the deficiency of growth factors can be circumvented by choosing and blending certain substrates such as specific adjuncts of plant or animal origin, but normally the needs of growth factors are met by addition of yeast extract as a high B-vitamin source (Hui & Khachatourians, 1996).

In sum, bacterial growth is dependent on the type of cultures media used, and are essentially composed of basic elements (water, carbon, nitrogen, phosphate, hydrogen and oxygen). As the nutrient requirements for each microorganism may vary, the formulation of the culture medium should be properly considered, since it profoundly affects the growth rate (Jenkins & Maddocks, 2019). For instance, the concentration of a given nutrient (*e.g.,* carbon) can induce an inhibitory or toxic effect to the microorganism (Smolke, 2009). In production optimization studies focusing on SELPs, Collins *et al.,* (2013) demonstrated that the aerobic fermentation of *E. coli* in an excess of carbon source can produce high amounts of extracellular acetate, affecting the growth rate and SELP production.

Commercial and rich fermentation broths

Commercial and rich fermentation broths are synthetic media formulated to meet the nutritional needs of microorganisms. Generally, the culture media falls into two broad categories: chemically defined media or complex media (undefined media) (Jenkins & Maddocks, 2019). Nevertheless, regardless of the type of media, bacteria need a minimum of nutrients like substrate (water and a carbon source), macro elements (a nitrogen source and a phosphates sources), trace elements (mineral salts) and growths factors (Bonnet *et al.*, 2019), which are detailed in the next sections.

Defined media

Carbon

The carbon source is long been recognized as the most important for it acts as an energy source and plays an important role in the growth as well as in the production of primary and secondary metabolites. The growth of bacteria thus requires necessary energy with different strains requiring different sources of nutrients (Dubey, 2014; Singh *et al.,* 2017). Also, carbon is the most abundant constituent element in bacteria and it is a growth-limiting nutrient. So, the carbon present in the culture media is essential for bacteria to produce carbon-based molecules, such as fats, carbohydrates, proteins and nucleic acids. Bacteria can both use inorganic carbon sources, such as carbon dioxide, or organic sources such as sugars and alcohols (Bonnet *et al.,* 2019). Still, the preferred carbon source for *E. coli*, as for many other bacteria, is glucose that supports a faster growth rate compared with other sugars (Bren *et al.*, 2016).

Nitrogen

Nitrogen is an essential nutrient playing an important role in metabolite production (Singh *et al.,* 2017), allowing bacteria to synthesize proteins, nucleic acids and coenzymes (Godard *et al.*, 2007). As for nitrogen sources, they are numerous and can be found in a large number of compounds used for the formulation of a culture medium. One of the main sources of nitrogen of commercial origin is peptone, found in the organic form and nitrates in the inorganic form (Bonnet *et al.*, 2019); but it has been showed that the best nitrogen source for *E. coli* is ammonia (Bren *et al.,* 2016).

Phosphate

Inorganic phosphorus is also a growth-limiting nutrient and a basic component for microbial fermentation. In fermentation, phosphorus is necessary for the formation of nucleic acids, for the synthesis of high energy organic compounds - adenosine triphosphate (ATP) is required to produce phospholipids present in the microbial cell membrane (Sanchez *et al.,* 2002). Finally, the quantity of phosphorus in the fermentation broth depends upon the composition of the broth and the need of the organism, as well as according to the nature of the desired product and can be supplied in the form of phosphate salts for use by all microbial cells (Bonnet *et al.,* 2019; Singh *et al.,* 2017).

1.5.3. Methods for optimization

As mentioned, it is clear that changes in carbon or nitrogen sources of the fermentative broth or variation from their optimum required concentration may affect their productivity. Hence, the production media with all the essential components in an appropriate concentration is required for the production of the desired metabolite at large scale (Singh *et al.*, 2017). Therefore, in an attempt to standardize the production media, the concept of media optimization has emerged. So, usually, the media optimization is accomplished either by a one-factor-at-a-time approach (OFAT) or multiple factors or parameters by statistical methods such as Central Composite Design (CCD) (Brar *et al.,* 2019).

1.5.3.1. One-Factor-At-a-Time (OFAT)

The diversity of data sources and the different process development have required a variety in data analysis methods. In the classical medium optimization technique, one-factor-at-a-time (OFAT) experiment is a popular choice among researchers for defining media composition and used in the initial stages in diverse fields (Jacyna *et al.,* 2018). In OFAT, also known as single-factor design,

experiments are designed to vary only one factor at a time while keeping others constant (Eckert & Trinh, 2016). Meaning that the concentrations of the selected media components can be changed according to a desired range. Because of its ease and convenience, this methodology is still used today during the initial stages of media formulation for the production of new metabolites (Lee *et al.,* 2021; Othmana *et al.,* 2021).

1.5.3.2. Central Composite Design (CCD)

Central composite design (CCD) is a collection of mathematical and statistical techniques widely used to determine the effects of several variables, first described by George E. P. Box and K. B. Wilson in 1951 (Tran *et al.,* 2010).

Currently, CCD is widely used in response surface methodology (RSM), for building a second order (quadratic) model for the response variable without using a complete three-level factorial experiment. Nevertheless, the CCD method is a relatively simple method based on factorial design and yet meeting RSM principles (Jacyna *et al.,* 2018; Basavarajaiah & Murthy, 2020). The design consists of three distinct sets of experimental runs (figure 1.5):

1. a three parameter factorial design (blue dots) in each of the factors studied, each having two levels (+1 and −1).
2. centre points (0,0,0) (red dot in figure 1.5), where experimental runs have the median values of each factor used in the factorial design;
3. star points (α) (yellow dots in figure 1.5), experimental runs identical to the centre points except for one factor, which will take on values both below and above the median of the two factorial levels. The numbers of star points are the double the number of factors used in the design. This means the star point (α) has two factors with extreme, upper or lower level (Liu, 2020), making it possible to estimate the curvature of the response surface (Ait-Amir, 2015).

On the basis of the set of experiments and the level of factors there are 3 types of CCD designs, which depend on where the star points are placed: Circumscribed CCD (CCC), Inscribed CCD (CCI) and Face centred CCD (CCF) (Singh *et al.,* 2017).

Figure 1.5 depicts the circumscribed CCD (CCC), which has 5 levels for each factor and was the basis for planning the CCD experiments of the present dissertation. This model was chosen based on its rotatability, which is a better fit to study the main effects and the interactions of media

compositions (glycerol, cheese whey and corn steep liquor) and to find the combination of factors levels that give the optimum operating conditions (Liu, 2020; Djoudi *et al.,* 2007).

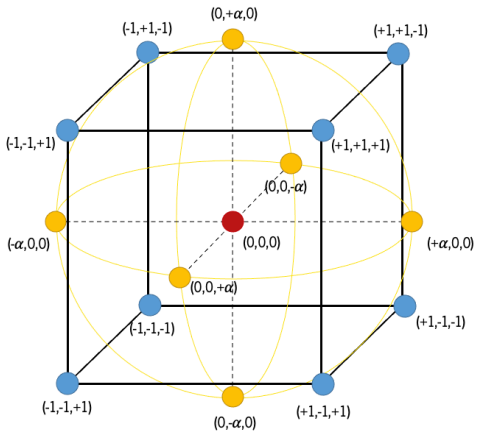

Figure 1.5 – Central Composite Design (15 experiments) for the optimization process with 3 parameters. The cube with blue dots represents the factorial design, the star points (α) are represented in yellow and central point in red.

1.6. Alternative media sources

1.6.1. Industrial by-products or residues

Fermentation processes typically employ artificial media that supports the optimal growth of microorganisms and ensures recombinant protein production (Rosano *et al.,* 2014). Media components cover the significant portion of the product cost and thus, selection of these components become an important task to minimize the economic burden associated with production (Singh *et al.,* 2017). Therefore, there is the necessity to find cheaper alternative sources for media composition, like by-products and residues from agro-industrial sectors. The usage of these 'wastes' offers not only a competitive cost advantage, but also contributes to reduce the environmental pressure/impact of agro-industrial processes through a circular economy approach by reusing/reintroducing residues into the industrial value chain.

There is a wide-range of by-products or residues derived from agro-industries that have been considered as potential carbon, nitrogen and mineral sources for fermentation processes targeting recombinant protein production. For instance, fruit pulp, glycerol, whey, molasses, corn steep liquor, bran and many others (Álvarez-Cao *et al.,* 2018; Leong *et al.,* 2014; Diaz *et al.,* 2018).

In the present dissertation, permeated cheese whey (from dairy industry), glycerol (from biodiesel production) and corn steep liquor (corn wet-milling) were selected as industrial by-

products/residues. Due to their low price, these components are very competitive for broth formulation, compared to expensive sugars, and can be used as alternative ingredients in fermentation media (Kumar *et al.,* 2019; Kim *et al.,* 2020). Moreover, these industrial by-products are produced in large quantities each year, posing an environmental risk and demanding a solution from an environmental, social and economic perspective (Torrezan *et al.*, 2020). The increasing awareness around environmental pollution and scientific knowledge results in the recovery of an extensive range of valuable and usable products, which were previously considered as waste. For example, corn steep liquor has a much lower price as a bulk agro-industrial by-product than traditional nitrogen resources such as yeast extract and tryptone, which constitute a cost burden in media formulation (figure 1.6). The use of low-cost residues/by-products like glycerol, corn steep liquor and cheese whey can thus be converted into value-added products and replace expensive carbon substrates required for fermentation production by microorganisms (Kaur *et al.*, 2020).

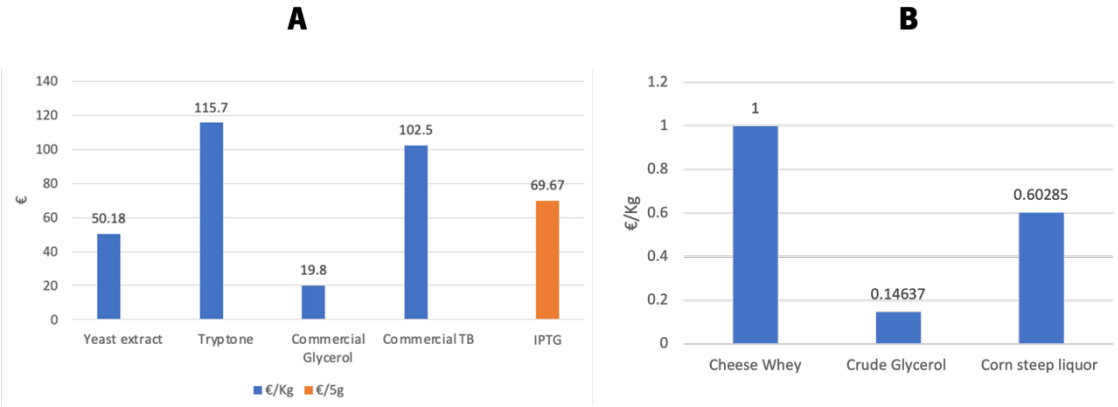

Figure 1.6 – Cost analysis of A) main commercial components used for media formulation and B) industrial residues/by-products. In figure A, yeast extract (Enzymatic, 2021), tryptone (Enzymatic, 2021), commercial glycerol (Enzymatic, 2021), Terrific broth GEN (Enzymatic, 2021) and IPTG (Price per 5 g; Enzymatic, 2021). In figure B, price per kilogram of cheese whey (European Commission, 2021), crude glycerol (Ruy *et al.,* 2021) and corn steep liquor (Made-in-china, 2021).

1.6.1.1. Cheese Whey

The dairy industry, based on the processing and manufacturing of milk and cheese, produces large volumes of by-products like cheese whey. Cheese whey is the liquid portion that is produced during the coagulation of milk casein in cheese making or in casein manufacture (Carvalho *et al.,* 2013). The cheese whey is abundant in nutrients retaining 55 % of milk nutrients, with the most abundant being lactose (4.5–5 % w/v), soluble proteins (0.6–0.8 % w/v), lipids (0.4–0.5 % w/v) and mineral salts (8–10 % of dried extract) (Guimarães *et al.*, 2010). The current total worldwide production of whey is estimated at about 180 to 190 million tons/year (Yadav *et al.*, 2015). These large amounts

lead to pollution load in rivers, therefore representing a significant environmental problem that could be reduced by its use as microbial growth media ingredient.

1.6.1.2. Glycerol

Another by-product is glycerol, also known as 1,2,3-propanetriol. It is an oily liquid with viscous, odourless and colourless properties. Glycerol is primarily synthesized from biodiesel production, produced through trans-esterification (reactions of acyl glycerides from oils and fats), which generates a tremendous amount of waste glycerol (million tons per year) (Luo *et al.,* 2016;), and the expectancy for biodiesel production to increase 4.5 % annually, glycerol production is also expected to increase (Monteiro *et al.,* 2018). For every 10 kg of biodiesel produced, around one kg of glycerol is generated (Kumar *et al.,* 2019). Also, it can be produced from saponification (soap production) and by hydrolysis of fatty acids. The worldwide glycerol production is estimated to be 41,900 million litres each year, with 10 % generated from hydrolysis, 12 % from saponification and 50–80 % from transesterification processes (Kaur *et al.*, 2020; Ahmad *et al.,* 2021).

Glycerol production in the last decade has increased, mainly by the demand for petroleum-based products in consequence of the increasing industrialization and modernization (Quispe *et al.,* 2013). Ergo, it was generated large amounts of by-products (such as crude glycerol), in which researchers saw the potential to use as value-added products, not only from an economic but also from an environmental point of view. Subsequently, crude glycerol has been used as a potential carbon source in fermentation processes for the production of value-added products (Abad *et al.,* 2014) such as polymers (Ashby *et al.,* 2005), pigments, dicarboxylic acids (Selvakumari *et al.,* 2021) and fatty acids (Cavero-Olguin *et al.,* 2021).

1.6.1.3. Corn steep liquor

Corn steep liquor (CSL) is a viscous liquid mixture with light to dark brown colour, obtained as a by-product of wet corn milling, and consists entirely of the water-soluble components of corn steeped in water (Karigidi & Olaiya 2019; Li *et al.,* 2016). CSL has an ensiled odour and acidic pH (high lactic acid) (Azizi-Shotorkhoft *et al.,* 2016), contains high amounts of amino acids, organic acids (*e.g.*, lactic acid), polypeptides and B-complex vitamins, and is an excellent nitrogen source for microorganisms (Kim *et al.,* 2020; Hull *et al.,* 1996). However, the chemical composition (table 1.3) of corn steep liquor can be unpredictable, varying with corn specie, season and the wet milling

process (Hofer *et al.*, 2018). Despite the rich content, the use of CSL as ingredient in culture media brings some drawbacks. Usually, the liquor contains a high sugar content and low pH properties that are typically damaging to most bacterium, requiring an optimization of its content in the fermentative media (Wu *et al.,* 2020).

Table 1.3 – Chemical composition of corn steep liquor**.** Adapted from Mahr-Un-Nisa *et al.*, 2006 & Eckerle *et al.*, 2012.

Items (%) of Corn steep liquor	
Dry matter	48.71 ± 5.10
Organic matter	95.1
Crude protein	36.85 ± 7.42
Nitrogen free extract	16 ± 1.10
Lactic acid	21 ± 1.22
pH	3.7 ± 0.077

1.7. High-level expression of recombinant proteins in *Escherichia coli* using a proton-suicide approach

The proton suicide method was developed by J. W. Winkelman and D. P. Clark (1984), and as the name suggests, induces the "suicide" of cells by the presence of excessive protons (H^+) (Winkelman & Clark, 1984). During metabolism, microbial cells produce carboxylic acids such as lactic, acetic, formic, and succinic acids, that function as chemical donors of protons (H^+) (Ciani *et al.*, 2008; Trefil *et al.,* 2001). This method relies on the production of bromine (a powerful oxidant) from a mixture of bromide and bromate under the acidic conditions produced by the cell. Bromine is lethal to cells, showing a concentration-dependent lethality, affecting cells producing carboxylic acids; thus, survivors are expected to present mutations affecting acid synthesis (Tanner & Pitner, 1939; Gerba, 2015). This method is detailed in the following sections.

1.7.1. Proton Suicide approach

As mentioned earlier, the amount of knowledge available on genetics and physiology of *E. coli* has made it to be a widely used "microbial factory" for recombinant protein production. The high amount of information on gene expression and regulation makes *E. coli* as the most commonly used cell factory in the scientific community (Lee, 1996; Pontrelli *et al.,* 2018). Although aerobic,

E. coli can also be a facultative anaerobic Gram-negative organism, capable of using a wide variety of organic carbon sources for heterotrophic growth. The available sugars are fermented to originate a mixture of acids (*e.g.,* lactic, acetic, formic, and succinic acids) and ethanol that are catabolized to H^2 and CO_2 via the Krebs cycle, correlated pathways and the electron transport chain (Ciani *et al., 2008)*. The mixed acid fermentation under aerobic conditions occurs in two phases. In the first phase, occurs glycolysis in which, through a chain of different reactions, one molecule of glucose is converted into two molecules of pyruvate with an energetic gain of two ATP and two NADH molecules (figure 1.7). In a second phase, the pyruvate molecules are converted into acetyl-CoA and carbon dioxide by the pyruvate dehydrogenase complex. The acetyl-CoA is then transformed into different acids (*e.g.* acetic, formic and succinic acid) (Clark, 1989; Förster & Gescher, 2014). These distinctive pathways of mixed-acids consumes great amounts of sugar, restricting the amount of sugar available for cell growth and protein production. Therefore, the efficiency of the conversion of carbon source into biomass and recombinant protein production can be increased by reducing the production of mixed acids during fermentation (Jian *et al.,* 2010; Enjalbert *et al.,* 2017; Jung *et al.*, 2019).

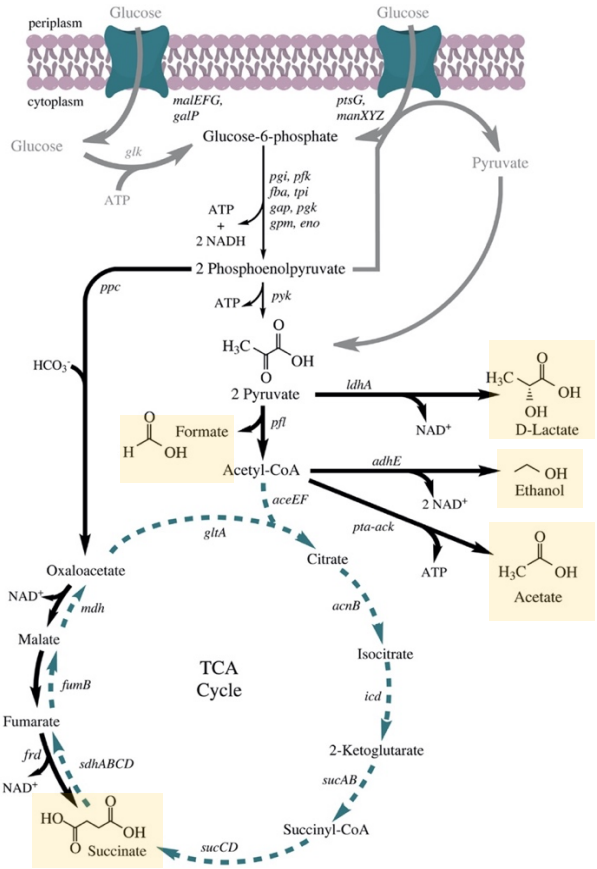

Figure 1.7 – Representation of the mixed acid fermentation in *E. coli*. The main products of mixed-acid fermentation are represented in yellow. Adapted from Förster & Gescher, 2014.

The proton suicide method is a selection method based on the isolation of *E. coli* mutants submitted to a lethal concentration of bromine (Br_2) and hypobromite (BrO^-), deriving from bromide (Br^-) and bromate (BrO_3^-) supplemented into the medium. The isolated viable mutants produce low amounts of organic acids from sugars and therefore, there is less stress for cell growth at higher densities, potentially resulting in higher protein production (Pais *et al.*, 2014).

In the presence of excess protons, the bromide (Br^-) and bromate (BrO_3^-) ions react to release elemental bromine (Br_2) and bromite (BrO_2^-) (equation 1); whereas, these latter two species react to produce elemental bromine (Br_2) and hypobromite (BrO^-) (equation 2):

$$BrO_3^- + 2Br^- + 2H^+ \rightarrow Br_2 + BrO_2^- + H_2O \quad \text{(eq. 1)}$$

$$BrO_2^- + 2Br^- + 2H^+ \rightarrow Br_2 + BrO^- + H_2O \quad \text{(eq. 2)}$$

In the cell, sugars are converted into acids (acetic, formic and succinic acids) that are excreted, resulting in acidification of the medium. In the presence of bromate and bromide, cells with excess production of protons (due to acid release) are killed as a result of the reaction of protons (H^+) with bromate and bromide, which produces bromine and hypobromite (Winkelman & Clark, 1984). These two chemical species are formed only in acidified environments (cells producing high amounts of acids) and highly toxic to the cell, especially bromine (Abbad-Andaloussi *et al.,* 1995; White, 1998). Bromine is highly reactive and a strong oxidant that reacts with any organic molecule including proteins, lipids, carbohydrates and nucleic acids, disrupting their structure (White, 1998). Bromine can result in cell membrane disruption resulting in leakage of cell components and loss of membrane functions, nucleic acid denaturation, and inactivation of enzymes and damage to critical proteins (Gerba, 2015). Therefore, the supplementation of bromate and bromide into the growth medium results in proton suicide of cells producing high amounts of acids, whereas cells producing low amounts of acid production remain viable.

1.7.2. Isolation of colonies producing low amounts of acids

Colonies of *E. coli* showing a low production of organic acids can be distinguished from those with higher yields by using the MacConkey agar (MAC) medium. The main discriminating components of the MacConkey agar are crystal violet dye, bile salts, lactose, and neutral red (pH indicator). The

crystal violet dye and bile salts are selective components of the media and inhibit the growth of Gram-positive bacteria (Estevez, 1984). The presence of lactose in MAC medium allows to select colonies based on their lactose metabolism and neutral red acts as pH indicator, turning red under acidic conditions (pH below 6.8). Therefore, in the presence of Gram-negative bacteria that produces organic acids by fermenting lactose (*e.g.,* lactic acid), the pH of the solid medium will decrease, conferring it a neutral red colour (figure 1.8). However, Gram-negative bacteria that are non-fermenters of lactose (low production of organic acids) will form pink/yellow colonies under more alkali conditions (above 8.0) (Wanger *et al.*, 2017).

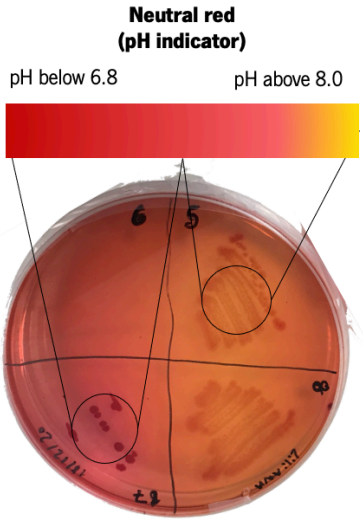

Figure 1.8 – Plate of MacConkey agar with colonies of *E. coli*. The neutral red in the agar differentiates colonies by color: pink/yellow colonies produce a lower amount of acids while red colonies produce a greater amount of acids.

.

2. Objectives

SELPs are recombinant protein polymers with noteworthy properties that can be employed for a diversity of different applications. However, their potential industrial applicability is restricted at some extent by the production costs. Although successfully produced in typical biological production processes with standard laboratory methods, to scale-up production to an industrial level, there is the need to improve efficiency by reducing costs of protein production and to improve productivity yields. To reduce the overall costs associated with the production bioprocesses, one can take advantage of agro-industrial by-products and/or residues to replace expensive media ingredients, while adopting a circular economy mindset.

In this sense, this work targets the optimization of SELP bioproduction in batch fermentation conditions, using alternative culture media formulated with agro-industrial by-products or residues (*e.g.*, cheese whey, glycerol and corn steep liquor). In addition, this work also targets the improvement of recombinant protein production levels through the implementation of a method to select cells producing low amounts of acids. To achieve the goals, this work proposes the following main objectives:

1. Formulation of a low-cost media using industrial by-products;
2. Determination of the best formulation parameters using classical medium optimization techniques namely, one-factor- at-a-time (OFAT) and central composite design (CCD);
3. Establishment of a Proton Suicide Method (PSM) to obtain an *E. coli* mutant producing low amounts of organic acids, providing less stress and driving bacterial metabolism towards SELP production.

3. Materials and Methods

3.1. Transformation of *E. coli* BL21(DE3)

The genetic construction used in this work namely, pCM13-SELP-59-A, was previously obtained by our group and provided for the realization of this study (Machado *et al.*, 2013b). The recombinant protein SELP-59-A, was designed to have a molecular weight of 55 kDa, consisting of 9 tandem repeats of a monomeric unit comprising 5 silk-like (sequence GAGAGS) and 9 elastin-like (sequence VPAVG) blocks (figure 1.3). Before initiating the production studies, *E. coli* BL21(DE3) cells were firstly transformed with pCM13-SELP-59-A already established in *E. coli* XL1-Blue.

For plasmid extraction, *E. coli* strain XL1-Blue harboring pCM13-SELP-59-A was inoculated in Lysogeny Broth (LB) (10 g tryptone, 5 g yeast extract and 5 g NaCl, per liter) supplemented with 100 µg/mL ampicillin and grown overnight at 37 °C and 200 rpm. Plasmid extraction was performed using a commercial plasmid extraction kit according to manufacturer's instructions (NZYtech) and quantified by spectrophotometry (Nanodrop). The extracted plasmid was then used to transform competent *E. coli* BL21(DE3) cells (protocol detailed in appendix A) by following standard (thermal shock) transformation protocol (Sambrook & Russel, 2006). Briefly, 200 µL of competent cells were thawed on ice and 0.5 µL of pCM13-SELP3 were added. The cells were kept on ice for 30 min and heat shocked at 42 °C for 90 sec, followed by an incubation on ice for 10 min. Then, 900 µL of LB medium was added and incubated at 37 °C for 1 h with agitation (200 rpm). Finally, the cells were spread on solid Lysogeny Broth agar (LBA) medium (LB with 20 % of agar), supplemented with 100 µg/mL ampicillin and incubated at 37 °C overnight. After overnight incubation, 6 colonies were selected and transferred to LBA plates supplemented with ampicillin, and incubated at 37 °C overnight. Each colony was then used for protein expression studies (expression screening) and inoculated in 10 mL of Terrific Broth supplemented with lactose (TB+Lac; 12 g tryptone, 24 g yeast extract, 0.17 M KH_2PO_4, 0.72 M K_2HPO_4, 5 g glycerol, 2 g lactose, per liter) and 100 µg/mL ampicillin for 18 h at 37 °C.

3.2. Direct selection of low-OA producing mutants by Proton Suicide Method

To obtain bacterial cells unable to produce, or producing low amounts of organic acids (OA), a positive selection approach resorting to the proton suicide method was envisaged. *E. coli* BL21(DE3) cells were grown overnight in 10 mL of LB medium at 37 °C and 200 rpm. The cells were then centrifuged at 12,108 xg for 5 min, and the pellet was resuspended in NaCl 0.89 %

(w/v) and plated onto solid LBA supplemented with Bromide (Br^-) and bromate (BrO_3^-). Different equimolar concentrations of each ion were tested (0, 50, 125, 175, 200, 225 and 250 mM). To calculate cell viability, colony-forming units (CFU) were enumerated after incubation for 48 h and 144 h at 37 °C. The lowest concentration of Br^- /BrO_3^- for which no cell growth was observed was selected and used in the subsequent experiments.

For isolation of mutants, a single colony of *E. coli* BL21(DE3) was inoculated into 10 mL of LB and incubated overnight at 37 °C and 200 rpm. Cells were collected and resuspended in 10 mL of fresh LB medium supplemented with 175 mM equimolar Br^- /BrO_3^- (lowest concentration showing no colonies) and incubated for 96 h. After incubation, cells were collected and resuspended in 10 mL NaCl 0.89 % (w/v), followed by plating onto LBA for 48 h at 37 °C. To subject the cells to additional mutagenic pressure, the obtained CFUs were then plated onto solid LBA medium supplemented with increased bromide (Br^-) and bromate (BrO_3^-) concentrations (175, 200 and 225 mM) for 48 h and 144 h at 37 °C.

Finally, the obtained mutated cells were plated on MacConkey Agar Base medium (Difco™) and incubated overnight at 37 °C to evaluate organic acid (OA) production. Bacteria producing high amounts of OA are identified by the formation of pink colonies in the presence of the neutral red indicator present in the MacConkey medium; whereas, mutants unable to produce OA or with lower OA production are characterized by the formation of yellow/light pink colonies.

3.2.1. TSS transformation of *E. coli* BL21(DE3) mutants

Some colonies obtained via the proton suicide method were grown overnight at 37 °C and 200 rpm in 10 mL of LB. Colonies were selected based on the color obtained in the Difco™ MacConkey Agar Base medium: yellow/light pink for bacteria with low or inexistent OA production, and bright pink/red for cells producing high amounts of OA. The following day, 10 mL LB cultures were inoculated at an adjusted optical density (OD_{600nm}) of 0.1 and incubated at 37 °C and 200 rpm until reaching OD_{600nm}= 0.3 - 0.4. The inoculums were then placed on ice for 5 min and transferred to 2 mL centrifuge tubes. Cells were collected by centrifugation at 1,100 xg for 10 min, 4 °C and resuspended in 1 mL of filtered ice cold TSS 1x (0.014 M PEG with mw 3,350; 0.30 M DMSO; 0.05 M $MgCl_2$; dissolved in LB, pH 6.5). One microliter of pCM13::SELP59-A plasmid was added, followed by incubation for 1 h on ice. A heat shock was given at 42 °C for 2 min, followed by ice incubation for 2 min. Afterwards, 1 mL of warm LB was added and allowed to incubate for 1 h at

37 °C and 200 rpm. Two hundred microliters of the transformation mix were then plated on solid LBA supplemented with 100 µg/mL ampicillin, and incubated for 20 h at 37 °C. After incubation, 3 colonies harboring the plasmid pCM13::SELP-59-A were selected - PS.2, PS.5 and PS.8 - and used for protein production testing assays.

3.2.2. Analysis of protein expression and growth

The *E. coli* BL21(DE3) mutants PS.2, PS.5 and PS.8 were evaluated for recombinant protein expression induced by lactose, and compared with the control (*E. coli* transformed with pCM13::SELP59-A). Bacteria were used to inoculate 10 mL TB+Lac, supplemented with 100 µg/mL ampicillin, and incubated for 22 h at 37 °C and 200 rpm. The optical density of the bacterial cultures was assessed and 1 mL of cells were collected by centrifugation for 3 min at 17 000 xg for further analysis by sodium dodecyl sulfate-polyacrylamide gel electrophoresis (SDS-PAGE, see section 3.4.1).

3.2.3. Growth curve of the best performing mutant

Growth curves of the non-mutated and the best performing mutant according to the protein expression profile (mutant PS.5) were performed using a 1:10 volume of medium to volume of flask ratio in standard 1 L flat-bottom glass Erlenmeyer flasks with 100 mL of Terrific Broth (TB) (12 g tryptone, 24 g yeast extract, 0.17 M KH_2PO_4, 0.72 M K_2HPO_4, 5 g glycerol, per liter) supplemented with of 100 µg/mL ampicillin. The starting inoculum was defined as 0.1 (OD_{600nm}) and samples were collected every 2 h until a maximum elapsed fermentation time (EFT) of 24 h. The absorbance for each time point was measured, and quantified for sugar and organic acid content by High Performance Liquid Chromatography (HPLC).

3.3. Production studies in shake flask cultures

3.3.1. Protein expression screening in auto-induction media

For analysis of protein expression in auto-induction media, a study was conducted using media supplemented with lactose and cheese whey. Cells of *E. coli* BL21(DE3) transformed with pCM13:SELP59-A were inoculated in a 50 mL centrifuge tube containing 10 mL of LB and incubated for 12 h at 37 °C and 200 rpm. The fresh cells were then diluted to an optical density

of 0.01 (OD_{600nm}) in standard 500 mL flat-bottom glass Erlenmeyer flasks with 125 mL (ratio 1:4) of media supplemented with 100 µg/mL ampicillin, and allowed to grow for 22 h at 37 °C.

Protein expression was assessed after 8 h of EFT in LB and TB supplemented with 2 g/L of α-lactose (LB+Lac, TB+Lac) or 12.8 g/L of cheese whey, corresponding to 2 g/L of Lactose (LB+CW, TB+CW). Samples were collected at 20, 22 and 24 h for absorbance measurements and cell crude extracts were analysed by SDS-PAGE in 10 % polyacrylamide gels (see section 3.4.1). For direct comparison of production levels, samples were normalized to the same optical density (OD_{600nm} = 0.1) according to equation 3:

$$OD_{600} \times Vi = OD_f \times Vf \qquad \text{(eq. 3)}$$

where, OD_{600nm} is the optical density of the cell culture at 600 nm, Vi is the volume of sample to be applied into the SDS-PAGE gel, OD_f is the normalization factor to 0.1, and Vf is the final volume used to resuspend the cell pellets (100 µL of TE + 25 µL of loading buffer, Vf=125 µL). Each gel was stained with copper chloride and BlueSafe Coomassie staining (NZYTech).

The cheese whey used in this study is a more concentrated variant termed as cheese whey permeate, a byproduct obtained when cheese whey is passed through an ultrafiltration membrane to concentrate whey protein. The cheese whey was re-hydrated in deionized water and autoclaved to obtain a stock solution of 25 g/L. For media formulation, an adequate amount of stock solution was added into the medium to achieve a final concentration of 2 g/L lactose according to previous results by the group (data not shown).

3.3.2. Assessment of protein expression after induction at the beginning of the stationary phase

Pre-inoculum of *E. coli* BL21(DE3) harboring the plasmid pCM13::SELP59-A and non-transformed BL21(DE3) were prepared in 10 mL LB for 7 to 8 h at 37 °C. The freshly prepared cultures were used to inoculate 100 mL of LB in flat-bottom glass Erlenmeyer flasks (250 mL) and grown overnight. The cells were then collected by centrifugation (12,108 xg for 5 min), resuspended in fresh LB and used as pre-inoculum for the main cultures.

Protein production studies were conducted in standard flat-bottom glass Erlenmeyer flasks of 1L containing 100 mL of TB (ratio 1:10) supplemented with 100 µg/mL ampicillin. Cultures were

inoculated for an initial OD_{600nm} of 0.05 and grown for 24 h at 37 °C and 250 rpm. Protein expression was induced after 8 h EFT with IPTG (1 mM), α-lactose (Lac, 2 g/L) and cheese whey (CW corresponding to 2 g/L of Lactose). *E. coli* BL21(DE3) harboring the plasmid pCM13::SELP59-A with no inducer and non-transformed/empty BL21(DE3) were used as controls.

3.3.3. Exploitation of residues/by-products for bioproduction by one-factor-at-a-time (OFAT).

Different residues/by-products from the agri-food and industrial sectors were utilized for the formulation of culture media. Eleven different media compositions were tested (table 3.1) using a one-factor-at-a-time (OFAT) approach and the growth conditions described in the previous section (section 3.3.2). Preparation of pre-inoculum was conducted as mentioned in the previous section (section 3.3.2) and induction was performed as described in table 3.1, in auto-induction conditions (i.e. from the beginning of growth) or after 8h of ETF. The cheese whey was re-hydrated in distilled water to obtain stock solutions of 25 g/L. The corn steep liquor, glycerol and re-hydrated cheese whey were autoclaved separately and added at the desired concentration according to table 3.1. For medium #11 (table 3.1), production studies were conducted with mutant PS.5 obtained with the proton suicide method.

Samples were collected at 0, 2,4, 6, 8, 10, 12 and 24 h EFT for analysis including, measurement of optical density (OD_{600nm}), determination of dry-cell weight, content of total protein (BCA method, appendix B), determination of phosphates (see section 3.4.3) and free amino nitrogen (FAN; see section 3.4.4), and HPLC for assessing sugars and organic acids (see section 3.4.5). Also, samples at the time of induction (8h), and 4 (12 h EFT) and 16 h (24 h EFT) after induction were collected for SDS-PAGE analysis (see section 3.4.1).

Table 3.1 – Media composition used for OFAT experiments. The cells were induced at 8 h EFT. MM – minimal medium (4.1 g/L NaH_2PO_4; 11.16 g/L K_2HPO_4; 2 g/L $(NH_4)_2SO_4$; 0.012 g/L $MgSO_4$; 0.0011 g/L $CaCl_2$; 0.00025 g/L $FeSO_4.7H_2O$ and adjust pH to 6.8); IPTG – isopropyl β-D-1-thiogalactopyranoside; CW – cheese whey. PS.5 - best performing mutant obtained by proton suicide.

Media #	Description	Induction type
1	Terrific broth at optimized conditions (TB, positive control)	CW (induction after 8 h growth)
2	Commercially available auto-induction TB (TBAIM, GRiSP Research Solutions Lda.)	Auto-induction (lactose-containing medium)
3	MM + glycerol (5 g/L) + corn steep liquor (30 g/L) + H_2O	CW (induction after 8 h growth)
4	MM + glycerol (5 g/L) + corn steep liquor (30 g/L) + H_2O	Lactose (induction after 8 h growth)

(cont.) Table 3.1 – Media composition used for OFAT experiments. The cells were induced at 8 h EFT. MM – minimal medium (4.1 g/L NaH_2PO_4; 11.16 g/L K_2HPO_4; 2 g/L $(NH_4)_2SO_4$; 0.012 g/L $MgSO_4$; 0.0011 g/L $CaCl_2$; 0.00025 g/L $FeSO_4.7H_2O$ and adjust pH to 6.8); IPTG – isopropyl β-D-1-thiogalactopyranoside; CW – cheese whey. PS.5 - best performing mutant obtained by proton suicide.

5	MM + glycerol (5 g/L) + corn steep liquor (30 g/L) + H_2O	IPTG (induction after 8 h growth)
6	MM + glycerol (5 g/L) + corn steep liquor (30 g/L) + Yeast Extract (0.06 g/L) + H_2O	Lactose (induction after 8 h growth)
7	MM + glycerol (5 g/L) + corn steep liquor (30 g/L) + Yeast Extract (0.12 g/L) + H_2O	Lactose (induction after 8 h growth)
8	MM + glycerol (5 g/L) + corn steep liquor (60 g/L) + Yeast Extract (0.12 g/L) + H_2O	Lactose (induction after 8 h growth)
9	MM + glycerol (5 g/L) + corn steep liquor (30 g/L) + Tryptone (0.03 g/L) + H_2O	Lactose (induction after 8 h growth)
10	MM + glycerol (5 g/L) + corn steep liquor (60 g/L) + Yeast Extract (0.06 g/L) + H_2O	Lactose (induction after 8 h growth)
11	Terrific broth at optimized conditions (TB, *E. coli* mutant P.S.5)	CW (induction after 8 h growth)

3.3.4. Optimization of culture medium composition by Central Composite Design (CCD)

The culture medium composition using industrial residues/by-products was optimized by CCD and performed with *E. coli* BL21(DE3) and the mutant PS.5 obtained via proton suicide, both transformed with the plasmid pCM13::SELP59-A. The pre-cultures, inoculum and growth parameters followed the same procedures described in section 3.3.2. The conditions used for CCD are presented in table 3.2 and, for each condition, fresh cell cultures were inoculated to a starting optical density of 0.1 (OD_{600nm}) in standard flat-bottom glass Erlenmeyer flasks of 1L with 100 mL of media (ratio 1:10) supplemented with 100 µg/mL ampicillin. In all conditions, cells were allowed to grow for 24 h and induced after 8 h EFT. The cheese whey was re-hydrated in distilled water to obtain stock solutions for each level ($-\alpha$, -1, 0, +1, and $+\alpha$) in a way that only 20 mL of stock solution was required for each condition. The corn steep liquor, glycerol and re-hydrated cheese whey were autoclaved separately and added at the desired concentration according to table 3.2.

Samples were collected at 0, 2,4, 6, 8, 10, 12 and 24 h EFT for analysis that included measurement of optical density, determination of dry-cell weight, content of total protein (BCA method, appendix B), determination of phosphates (see section 3.4.3) and free amino nitrogen (see section 3.4.4), and HPLC for assessing organic acids (acetic acid) (see section 3.4.5). Also, samples at the time of induction (8h EFT), and 4 (12 h EFT) and 16 h (24 h EFT) after induction were collected for SDS-PAGE analysis (see section 3.4.1).

Table 3.2 – 2^3 central composite design experiment with variables glycerol ($\chi 1$), corn step liquor ($\chi 2$) and cheese whey ($\chi 3$).

Condition	Coded values			Real values		
	$\chi 1$	$\chi 2$	$\chi 3$	($\chi 1$) Glycerol (g/L)	($\chi 2$) Corn step liquor (g/L)	($\chi 3$) Cheese whey (induction after 8 h growth) (g/L)
1	-α	0	0	0	30	12.8
2	+1	+1	+1	9	45	19.2
3	0	0	0	6	30	12.8
4	0	+ α	0	6	60	12.8
5	+1	+1	+1	9	45	19.2
6	0	- α	0	6	0	12.8
7	-1	+1	-1	3	45	6.4
8	0	0	0	6	30	12.8
9	0	0	+ α	6	30	25.6
10	-1	+1	+1	3	45	19.2
11	0	0	- α	6	30	0
12	0	0	0	3	45	6.4
13	-1	-1	-1	3	15	6.4
14	+ α	0	0	12	30	12.8
15	-1	-1	+1	3	15	19.2
16	+1	-1	+1	9	15	19.2
17	-1	-1	+1	3	15	19.2
18	0	0	0	6	30	12.8
19	0	0	0	6	30	12.8
20	+1	+1	-1	9	45	6.4
21	-1	-1	-1	3	15	6.4
22	0	0	0	6	30	12.8
23	+1	+1	-1	9	45	6.4
24	+1	-1	-1	9	15	6.4
25	+1	-1	+1	9	15	19.2
26	+1	-1	-1	9	15	6.4
27	0	0	0	6	30	12.8
28	-1	+1	+1	3	45	19.2

3.4. Quantification methods

3.4.1. Protein analysis (SDS-PAGE)

Cell crude extracts were analysed by SDS-PAGE with 10 % polyacrylamide gels (appendix C) and stained with copper chloride 0.3 M and Blue Safe Coomassie stanning (Nzytech). For the preparation of samples, 1 mL of cell cultures were collected, centrifuged for 2 min at 17,000 xg and resuspended in 100 µL of TE buffer (50 mM Tris, 1 mM EDTA at pH 8.0) with an additional 25 µL of loading buffer (10 % w/v SDS, 10 mM beta-mercapto-ethanol, 20 % v/v glycerol, 0.2 M

Tris-HCl pH 6.8 and 0.05 % w/v bromophenol blue). Samples were mixed thoroughly and centrifuged for 10 min at 17,000 xg for separation of the soluble and insoluble fractions. Unless otherwise specified (as in the normalized samples described in section 3.3.1), 5 µL of the soluble fraction (supernatant) were loaded into the gel and run at 10 mA. NZYColour Protein Marker II (3.5 µL) was used for every gel. Digitally acquired images were analysed with the image processing software ImageJ (Schneider *et al.,* 2012) for protein quantification by densitometry.

3.4.2. Protein purification

Purification of SELP-59-A was achieved by employing well-established methodologies involving a two-step purification process: an initial acidification step for removal of a large portion of *E. coli* endogenous proteins, followed by recovery of SELP-59-A by salting-out using ammonium sulfate precipitation (Machado *et al.*, 2013a).

Cells were harvested by centrifugation for 30 min at 12,108 xg, resuspended in TE buffer and lysed by ultrasonic disruption/sonication (750 W, Vibra Cell 75043, Fisher S. Bioblock Scientific). Sonication was performed with 30 % amplitude, 3 s pulse on, 9 s pulse off, total sonication time of 40 min, while maintaining the cells on ice. To precipitate *E. coli* native proteins and improve cell lysis, the crude cell extract was adjusted to a pH of 3 - 3.5 with hydrochloric acid (HCl) 1.6 M, while on ice-cold temperature under agitation, followed by centrifugation at 12,108 xg for 20 min at 4 °C. The supernatant was transferred to a new tube and the insoluble debris (pellet) was discarded. Ammonium sulfate was then slowly added to the clear supernatant for a final saturation of 25 %, followed by an incubation for 30 min to allow the salting-out of SELP-59-A, while maintaining the sample on ice under agitation. The amount of ammonium sulfate was determined with the aid of the online tool Ammonium Sulfate Calculator (https://www.encorbio.com/protocols/AM-SO4.htm). For recovery of the recombinant biopolymer, the mixture was centrifuged for 30 min at 12,108 xg and 4 °C. After centrifugation, the precipitated protein was resolubilized in deionized water at 4 °C overnight and the resulting solution was dialysed against water to remove the excess of ammonium sulfate. Finally, the dialyzed solution was centrifuged at 12,108 xg for 30 min at 4 °C, to remove insoluble debris and frozen at –80 °C for subsequent lyophilization.

3.4.3. Quantification of phosphates by microplate reading

The method for quantification of phosphates was optimized and adapted for microplate reading (JET BIOFIL) by establishing a comparison with the standard methodology using cuvettes. Stock solutions of 10 % ascorbic acid (store at 4 °C); 2.5 % ammonium molybdate and 6 N sulfuric acid were prepared for preparation of reagent C (2 volumes of distilled water, 1 volume of 6 N sulfuric acid, 1 volume of 2.5 % ammonium molybdate, 1 volume of 10 % ascorbic acid, stored at 4 °C until use). Culture supernatants were diluted in water (1:2,000) and freshly prepared reagent C was added according to the volumes indicated in table 3.3. The samples were mixed thoroughly and incubated in the dark for 2 h at room temperature, prior to reading the absorbance at 820 nm. In the measurements acquired in microplates (JET BIOFIL), absorbances were recorded at 15 min, 30 min and 60 min. For phosphate quantification, a standard calibration curve was created using known concentrations of phosphates, ranging from 1 µM to 200 µM. Based on the results (Appendix E), 15 min of incubation were adequate to proceed with analyses and future analyses used microplate format.

Table 3.3 – Volumes used for the quantification of phosphates.

	Cuvettes (µL)	**Microplates (µL)**
Samples (1:2000)	500	100
Reagent C	500	100

3.4.4. Determination of Wort Free Amino Nitrogen (FAN)

Determination of FAN was based on the method described by Spedding *et al.*, 2013. A ninhydrin stock solution was prepared by adding 0.11 M ninhydrin into pure ethylene glycol and mixed until complete dissolution, followed by addition of 4N sodium acetate pH 5.5 (4 mM sodium acetate trihydrate, 6.66 M glacial acetic acid). A solution of stannous chloride ($SnCl_2$) was prepared by dissolving 0.52 M $SnCl_2$ into ethylene glycol. The ninhydrin reagent/working solution (25 µL of $SnCl_2$ for each 1 mL of ninhydrin) was prepared fresh each day.

A glycine stock was made by adding exactly 107.2 mg of glycine in 100 mL of distilled water and stored at 4 °C until use. For the glycine standard solution, 1 mL of stock solution was diluted 1:100 with ultra-pure water (corresponding to 2 mg/L of amino nitrogen). This standard solution was freshly made for each assay.

Determination of FAN was optimized by diluting the culture samples (1:10, 1:20, 1:50 and 1:100). In a normal assay, 2 µL of glycine standard or diluted samples were added to 96 well plate (Greiner) followed by the addition of 100 µL of pH 5.5 acetate-buffered ninhydrin reagent (working solution). Microplates were heated for 10 min at 104 °C and absorbance values were recorded at 575 nm in a microwell plate reader. For each sample, water blanks and glycine standards were made in triplicate. The free amino nitrogen was determined according to equation 4. Culture samples (Sample) and standard glycine values (Avg gly) were corrected by averaging the blank (Avg Blank) and subtracting it from readings. The average of each sample (blank corrected) is divided by the net absorbance of standard glycine (blank corrected) and multiplied by 2 and the dilution factor (100) (FD) to obtain FAN content in mg/L:

$$\mathrm{FAN(mg/L)} = \frac{(\mathrm{Sample - Avg\ Blank})}{(\mathrm{Avg\ gly - Avg\ Blank})} * \mathrm{FD} \qquad \text{(eq. 4)}$$

3.4.5. HPLC analysis

The chromatographic analyses of sugars and organic acids were carried out on a Hitachi LaChrom Elite® with automatic injector. The flow in the gradient pump was set at 0.7 mL/min in the first 8 min and adjusted to 0.3 mL/min for the remaining time of the experiment, for a total run time of 45 min. The samples were separated in a Rezex™ ROA-Organic Acid H^+ (8 %), LC Column 300 x 7.8 mm at 60 °C. The RI detection system was a model L-2490. The signal acquired from detector was recorded by EZChrom software. Previously defined calibration curves were performed for each of the sugars and acids evaluated.

4. Results and Discussion

4.1. Selection of mutants producing low amounts of organic acids via the proton suicide method

The production of mixed acids during fermentation poses a limiting factor for the growth of microbial cell factories at high cell densities, such as *E. coli* (Han *et al.*, 1992; Warnecke *et al.*, 2005). This affects the volumetric productivities of recombinant proteins as the number of available producing cells is reduced (Kim *et al.*, 2015). In this work, and in parallel to the optimization of culture media for improved SELP-59-A production, *E. coli* BL21(DE3) was subjected to the direct selection of mutants producing low amounts of organic acids by the proton suicide method.

The proton suicide method resides in the direct selection of mutants that changed its metabolism after being exposed to toxic compounds. Here, the aim was to obtain mutants able to grow at higher cell densities due to lower organic acid production, resulting in higher net values of produced SELP-59-A. As a consequence of the mutagenic pressure induced by lethal concentrations of bromine and hypobromite (resulting from the reaction of bromide and bromate with H^+), the viable mutated cells are incapable or produce low amounts of organics acids. This is expected to provide less stress for cell growth, resulting in higher protein production.

The first step in this method was to find the lowest lethal concentration of bromate and bromide (0 - 250 mM) that result in no *E. coli* growth. Herewith, different equimolar concentrations of Bromate and Bromide (Br^-/BrO_3^-) (0 - 250 mM) were tested in LB agar.

Preliminary results (table 4.1) showed that a concentration of 175 mM Br^-/BrO_3^- was lethal for the strain *E. coli* BL21(DE3). Hence, the concentration of 175 mM of Br^-/BrO_3^- was selected for the proton suicide method. A first mutagenic pressure was made from cells resuspended in saline solution and plated in solid LBA (LB+agar) supplemented with 175 mM of Br^-/BrO_3^-. Eight colonies were selected to proceed to the next stage, consisting of a second mutagenic pressure in LBA medium supplemented with Br^-/BrO_3^- (175, 200, 225 mM). In this second step, results demonstrated that cells were unable to grow at a concentration of 225 mM of bromate and bromide. However, all colonies demonstrated to grow at concentrations of 175 and 200 mM of bromate and bromide, with exception for colony 6 at 200 mM of Br^-/BrO_3^- (appendix D).

Table 4.1 – CFU enumeration in LB agar supplemented with different concentrations of bromide and bromate.

	Counted Growth (CFU/plate)		Real CFU (with dilution)	
Br^-/BrO_3^- (mM)	**48 h**	**144 h**	**48 h**	**144 h**
0	280	280	280 000 000	280 000 000
	170	171	170 000 000	171 000 000
	369	374	369 000 000	374 000 000
50	1	60	1 000 000	60 000 000
	1	39	1 000 000	39 000 000
	1	135	1 000 000	135 000 000
125	1	2	1 000 000	2 000 000
	1	1	1 000 000	1 000 000
	2	3	2 000 000	3 000 000
175	0	0	0	0
	0	0	0	0
	0	0	0	0
200	0	0	0	0
	0	0	0	0
	0	0	0	0
225	0	0	0	0
	0	0	0	0
	0	0	0	0
250	0	0	0	0
	0	0	0	0
	0	0	0	0

The mutants obtained from the second mutagenic pressure with 200 mM of Br^-/BrO_3^- were plated on MacConkey agar to identify *E. coli* mutants with low production of organic acids. The MacConkey agar medium is useful to distinguish Gram-negative bacteria that produces low amounts of organic acids from those producing high quantities, based on the color of colonies: colonies producing low amounts are characterized by pink/yellow color, whereas colonies producing high amounts of organic acids are characterized by dark pink/red colonies.

Considering the results, colonies 5 and 8 exhibited a faintly light pink or yellow color (figure 4.1 B), indicating that these bacteria produced low amounts of organic acids. On the other hand, colonies

1 - 4 and 7 demonstrated to produce higher amounts of organic acids, displaying dark pink/red colonies surrounded by a pink halo (figure 4.1 A).

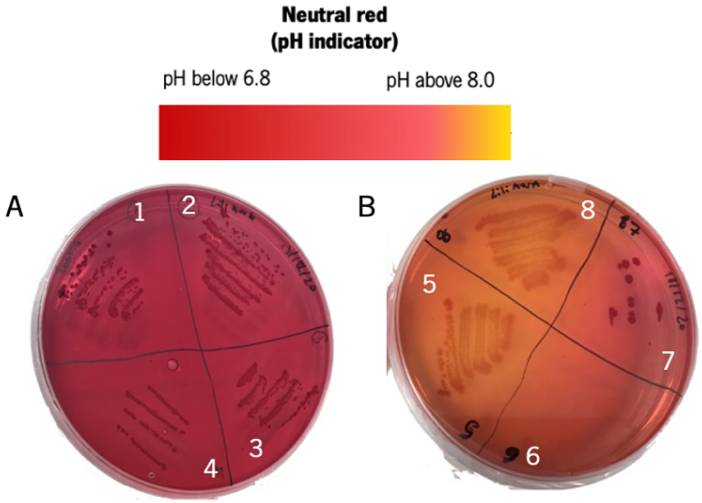

Figure 4.1 – Petri dish with MacConkey agar. A) colonies from 1 to 4 and B) colonies from 5 to 6. At pH below 6.8, the pH indicator (neutral red) of the medium presents a red color and above 8, displays light pink to yellow color.

The presence of bromine exerted a mutagenic pressure on the pathways leading to organic acid production, resulting in low organic acid production in colonies 5 and 8. The presence of colonies with red color indicates that colonies were able to adapt to bromine, likely by mutating in other parts of the genome, thus allowing organic acid production. For instance, colony 7 (Figure 4.1 B), grew at a slower rate than the other red-colored colonies (Figure 4.1 A). The fact that lactose is the only sugar available on the MacConkey plate suggests that colony 7 may display a mutation in the cell metabolism related with lactose uptake or breakdown. These findings suggest that proton suicide causes mutagenesis not only in organic acid synthesis and excretion, but also in other pathways.

According to the observations, mutants 5 (PS.5) and 8 (PS.8) were selected as low acid-producing *E. coli* BL21(DE3), and colony 2 (PS.2), displaying a dark pink color, was chosen to be used as control. The selected colonies PS.2, PS.5 and PS.8 were then transformed with the vector pCM13::SELP-59-A and subjected to protein expression studies.

4.1.1. Evaluation of protein expression and growth

Due to the potential impact of the proton suicide method on the lactose importer *lacY* (lactose permease gene), the ability of the mutants PS.2, PS.5 and PS.8 to be induced by lactose was assessed in auto-induction media, while using non-mutated samples as control. Accordingly,

bacteria were transformed with pCM13::SELP-59-A and protein expression was evaluated in TB supplemented with lactose (TB+Lac) as described in the materials and methods section. It should be noted that TB+Lac is routinely employed in our group to screen for rPP production.

SDS-PAGE analysis (figure 4.2) indicates that the mutants maintained the ability to transport lactose into the cells, inducing protein expression. The exception was for mutant PS.8 that seems to have lost the ability to grow after transformation. This was unexpected and could be a consequence of mutations in sugar uptake pathways, inhibiting its growth. Nevertheless, mutant PS.5 demonstrated high levels of protein expression and was selected for subsequent assays. To note that the abnormal gel mobility of SELP-59-A at higher molecular weight (*i.e.* approximately 70 kDa in opposition to the expected ≈ 50 kDa) has been observed by other authors and attributed to the hydrophobic nature of the protein polymer (Lyons *et al.*, 2007; Machado *et al.*, 2013a; da Costa *et al.*, 2015; Pereira *et al.*, 2021).

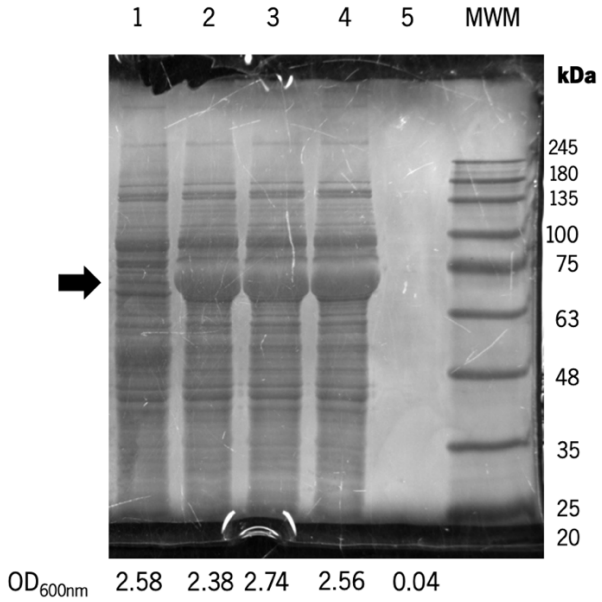

Figure 4.2 – Electrophoretic pattern of soluble crude cell extracts. 1) Non-transformed/without plasmid *E. coli* BL21(DE3), used as negative control; 2) Non-mutated *E. coli* BL21(DE3) transformed with pCM13::SELP-59-A, used as positive control; 3) *E. coli* BL21(DE3) mutant PS.2 transformed with pCM13::SELP-59-A; 4) *E. coli* BL21(DE3) mutant PS.5 transformed with pCM13::SELP-59-A; 5) *E. coli* BL21(DE3) mutant PS.8 transformed with pCM13::SELP-59-A; MWM: molecular weight marker (NZYColour Protein Marker II). Samples correspond to cultures after 22 h of elapsed fermentation time in TB+Lac at 37 °C and 200 rpm. Five microliters of soluble extract were loaded to the gel. The optical density at 600 nm (OD_{600nm}) is indicated below each lane and arrow points to the band corresponding to SELP-59-A.

After assessing protein expression, growth curves of the transformed bacteria were performed to compare cell growth between the non-mutated and the mutated variant PS.5. Both bacteria displayed similar cell growth profiles in culture media (TB) without inducer, reaching OD_{600nm} values of 8.7 and 8.5 for the non-mutated *E. coli* and mutant PS.5, respectively (figure 4.3).

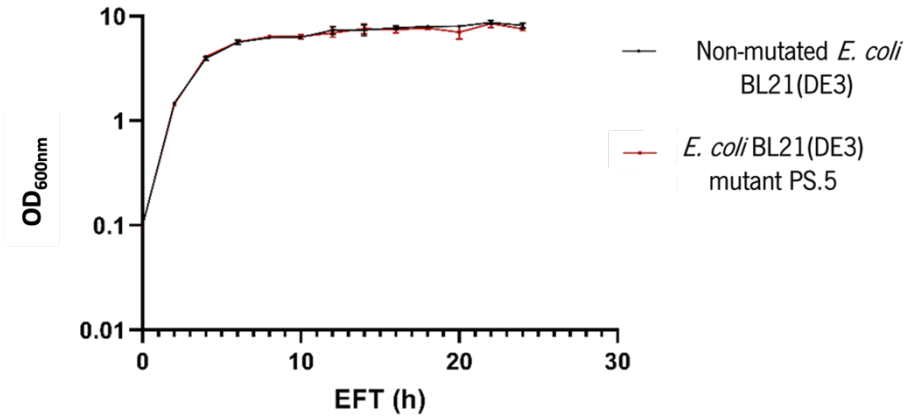

Figure 4.3 – Growth curves of non-mutated *E. coli* BL21(DE3) and mutant PS.5 in TB without inducer.

Analysis of pH along time revealed modest differences in pH levels, with mutant PS.5 displaying values slightly higher than the non-mutated *E. coli* (Figure 4.4). To investigate the differences between cultures in more detail, the content of glucose, glycerol, fructose, acetic acid, malic acid, succinic acid, lactic acid and ethanol was assessed by HPLC (Figure 4.5). Comparing the results obtained for the non-mutated and the mutated variant, results show a slightly lower production of organic acids (lactic, acetic, succinic and malic acids) for mutant PS-5 (figure 4.5).

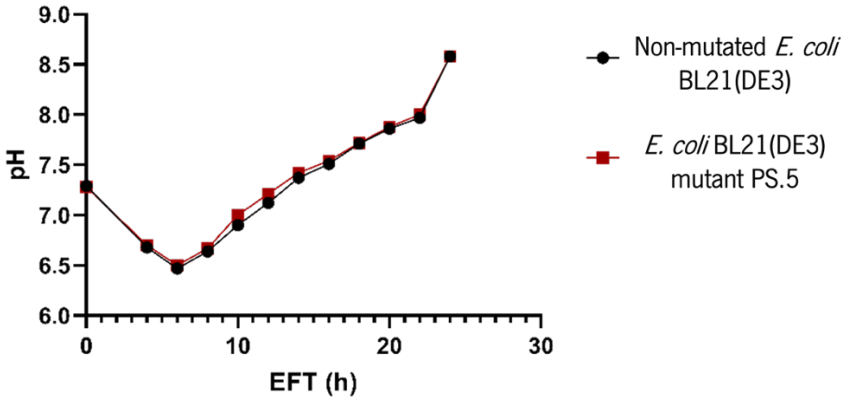

Figure 4.4 – pH variation of the cultures in TB without inducer.

After 24 h of fermentation, the original non-mutated strain showed values of 0.27 g/L for succinic acid and 0.2 g/L for acetic acid, while mutant PS.5 revealed contents of 0.16 g/L and 0.19 g/L for succinic and acetic acid, respectively. Regarding the determination of lactic and malic acids, there was no detectable concentration after 24 h. Overall, the proton suicide methodology demonstrated to affect organic acid production with an overall reduction of 25 %, without influencing the heterologous expression of SELP-59-A. A longer number of cycles with bromide/bromate could improve this reduction even further, and will be explored in future works by the group.

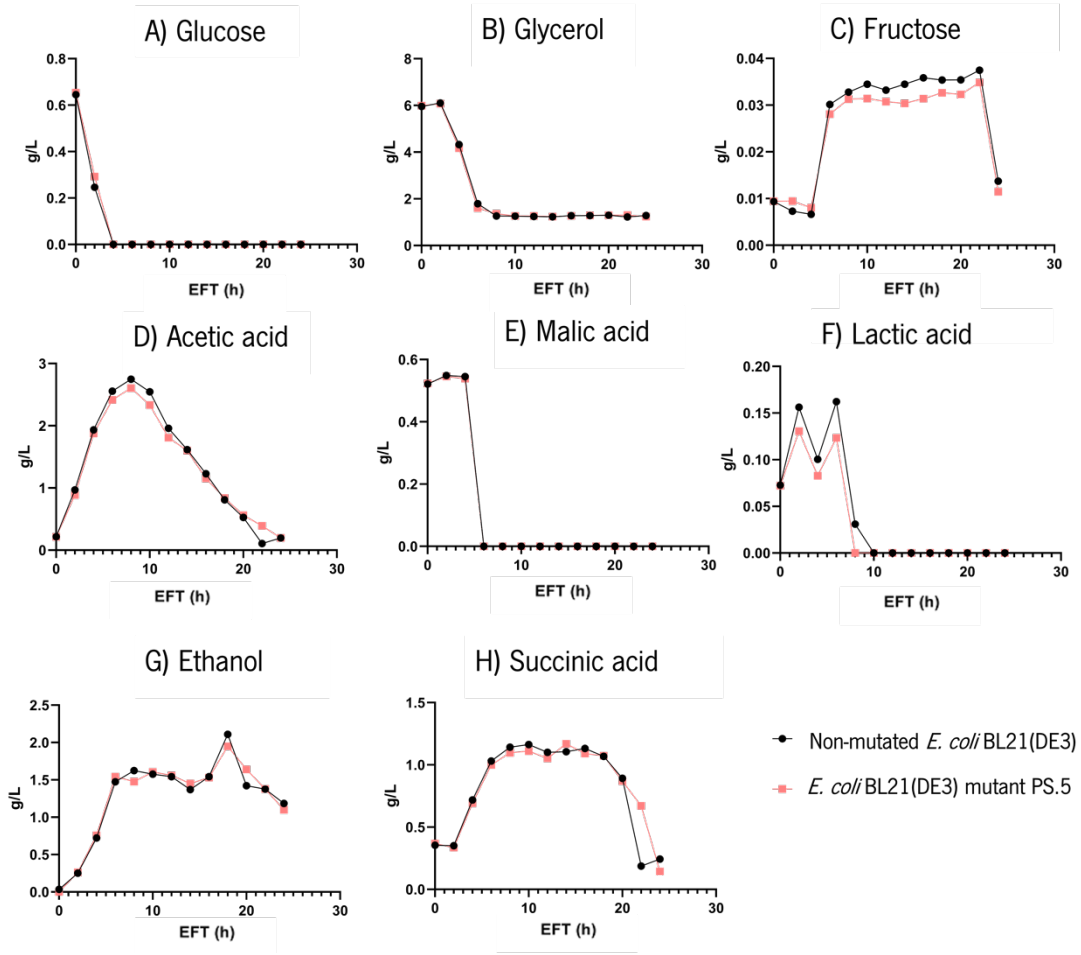

Figure 4.5 – HPLC analysis of sugars, carboxylic acids and ethanol during growth in TB.

4.2. Production studies in shake flask cultures

4.2.1. Screenings with auto-induction media

A first screening was performed to evaluate protein expression in non-mutated *E. coli* BL21(DE3) transformed with pCM13::SELP-59-A, grown in auto-induction media (TB or LB supplemented with lactose or cheese whey). In auto-induction media, protein expression is induced as soon as glucose is depleted without the need of additional culture handling, and is routinely employed in our group for the rapid screening of recombinant protein expression. As a brief note, when different sugars are available, cells prefer to use glucose first due to its high affinity for the phosphotransferase system (Kopp *et al.,* 2018). Cultures containing both glucose and lactose result in diauxic growth or catabolic repression, resulting in reduced lactose uptake when glucose is abundant (Wurm *et al.,* 2016). When glucose is depleted, cells are stimulated by lactose, which enters the cell by active transport via a lactose permease (Crowley & Rafferty, 2019).

After 24 h of EFT, the cultures in TB (OD_{600nm} = 3.27) showed a higher optical density when compared to LB media (OD_{600nm} = 2.45) (Figure 4.6). This can be explained by the greater nutrient value of TB in comparison to LB. TB contains higher concentrations of yeast extract and tryptone, which provide more nutrients and growth factors for rapid multiplication and increase plasmid yield by extending *E. coli's* exponential phase. Similarly, the cultures in TB supplemented with lactose (OD_{600nm} = 2.47) or CW (OD_{600nm} = 2.89) demonstrated higher cell densities after 24 h of fermentation than the equivalent in LB (OD_{600nm} = 0.94 and 1.18 for lactose and CW, respectively).

Comparing protein expression, it is possible to observe good expression levels of SELP-59-A in LB+Lac, TB+Lac and TB+CW for all the time points, whereas no protein expression was found for LB or LB+CW (figure 4.6). While the absence of SELP-59-A production in LB was not surprising due to the absence of inducer, this was not expected for the cells grown in LB supplemented with cheese whey. Since a large fraction of CW comprises lactose, we expected similar results as those obtained with LB+Lac. However, the reasons for this remain to be elucidated. Regarding the samples in TB, it was possible to observe a protein band corresponding to SELP-59-A at all the time points, especially after 22 h of fermentation. This was previously observed by our group and attributed to the presence of residual lactose in the medium components, especially yeast extract. Indeed, it has been argued that yeast extract may contain traces of lactose, depending of the manufacturer (Zhang *et al.,* 2003; Fu *et al.*, 2006; Nair *et al.*, 2009). The high amount of yeast extract in TB, compared with LB, can provide sufficient lactose to induce protein expression, thus

explaining our results. Analysis of protein expression along time revealed that the intensity of the SELP-59-A bands was comparable between 20 and 22 h of EFT, with an apparent reduction after 24 h of fermentation.

To further support the assignment of the bands to SELP-59-A, the SDS-PAGE gels were also stained with Coomassie blue (figure 4.6, images on the left in blue color). Due to the limited amino acid variability in SELPs (as well as on other rPPs), gels stained with Coomassie appear with diffuse or 'ghost' bands. Coomassie blue binds more strongly to charged and aromatic amino acids that are absent from SELP-59-A composition, which comprises mainly glycine, L-alanine, L-serine, L-valine and L-proline, and at a lower extent, L-histidine due to the poly 6x-his tag. This results in bands with a 'ghost' faded appearance (Pereira *et al.,* 2021; Machado *et al.,* 2013a). As mentioned in section 4.1.1., the abnormal gel mobility of SELP-59-A at higher molecular weight is attributed to the hydrophobic nature of the protein.

Considering all the results, the best expression levels were observed for TB+CW, showing similar expression levels to cultures induced by lactose (TB+Lac); however, the cultures in TB+CW were able to reach cell densities a bit higher than in TB+Lac. This indicates that cheese whey is an adequate inducer for the expression of SELPs (as well as for other recombinant proteins). The use of lactose as inducer provides advantages over the commonly used IPTG by reducing costs and avoiding the negative effects associated with the toxicity of IPTG (Viitanen *et al.*, 2003). Also, the use of lactose as alternative inducer demonstrated expression levels of recombinant proteins comparable to IPTG (Machado *et al.*, 2013a; Gombert & Kilikian, 1998; Woyski & Cupp-Vickery, 2001; Neubauer *et al.,* 1992). Lactose is readily available in industrial by-products/residues such as CW, circumventing the need to use purified lactose as inducer. Therefore, the use of CW as inducer provides not only advantages both at the economic and environmental levels, but also an efficient solution to induce protein expression.

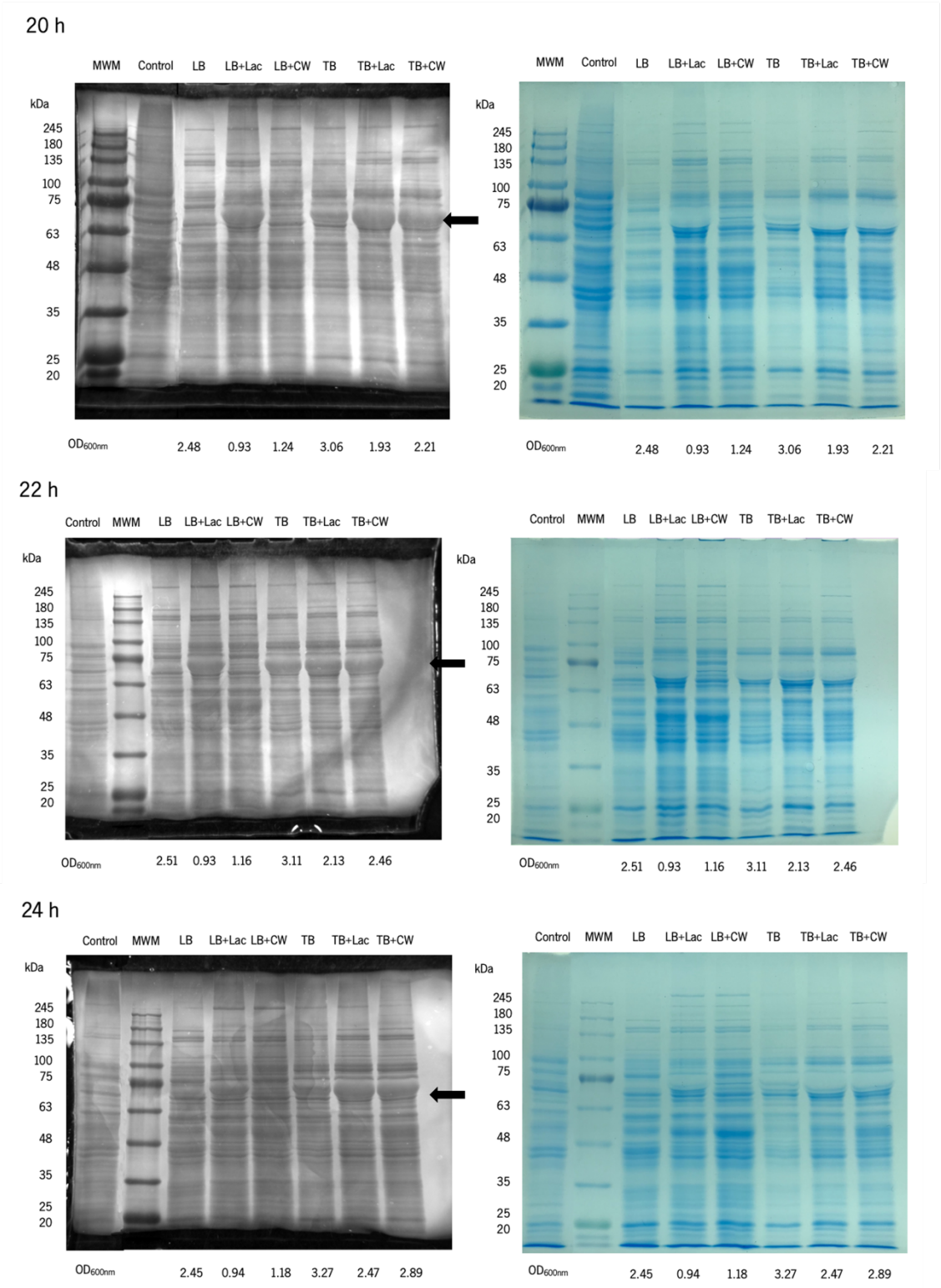

Figure 4.6 – Electrophoretic patterns of soluble crude cell extracts during growth by auto-induction at 20 h, 22 h and 24 h of EFT. The cell crude extracts of *E. coli* BL21(DE3) transformed with pCM13::SELP-59-A were assessed in LB (LB); LB with Lactose (LB+Lac); LB with cheese whey (LB+CW); TB (TB); TB with Lactose (TB+Lac) and TB with cheese whey (TB+CW). Non-transformed *E. coli* BL21(DE3) was used as control. All samples were normalised for the same cell density of 0.1 before loading. The optical density OD_{600nm} is indicated below each lane. Target recombinant protein is indicated by arrows and molecular weight marker is represented in of each gel by MWM (NZYColour Protein Marker II).

4.2.2. Optimization of induction conditions

While the use of auto-induction media offers a convenient approach for the expression of recombinant proteins, it also generates much lower cell densities compared to those obtained in fermentors. Our group has previously optimized the growth and expression of SELPs with an inducible methodology and improved production in batch conditions (Collins *et al.,* 2013). Following this previous work, and using the same methodology, different inducers such as IPTG, lactose (Lac) and cheese whey (CW) were tested using the best conditions in TB medium. In this method, instead of using auto-induction for protein expression, the inducer was added after 8 h of EFT. Two controls were used: non-transformed/empty *E. coli* BL21(DE3) and *E. coli* BL21(DE3) transformed with pCM13-SELP-59-A without induction.

The growth rate for all samples remained similar up to 12 h, with all cultures reaching the stationary phase between 8 h to 10 h EFT (figure 4.7). After this point, the cultures induced with CW at 8 h EFT reached a slightly higher density. Quantification of total protein content further supports this observation as the cultures induced by CW present a higher value after 24 h EFT (figure 4.8).

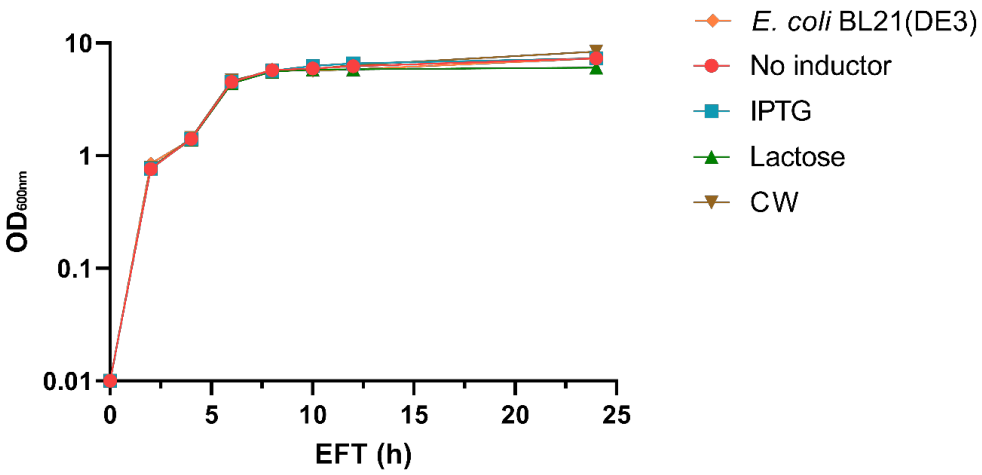

Figure 4.7 – Growth curves of *E. coli* BL21(DE3) transformed with pCM13::SELP-59-A after 24 h EFT using different inducers. The optical density (OD_{600nm}) was measured at different timepoints during the 24 h of elapsed fermentation time (EFT).

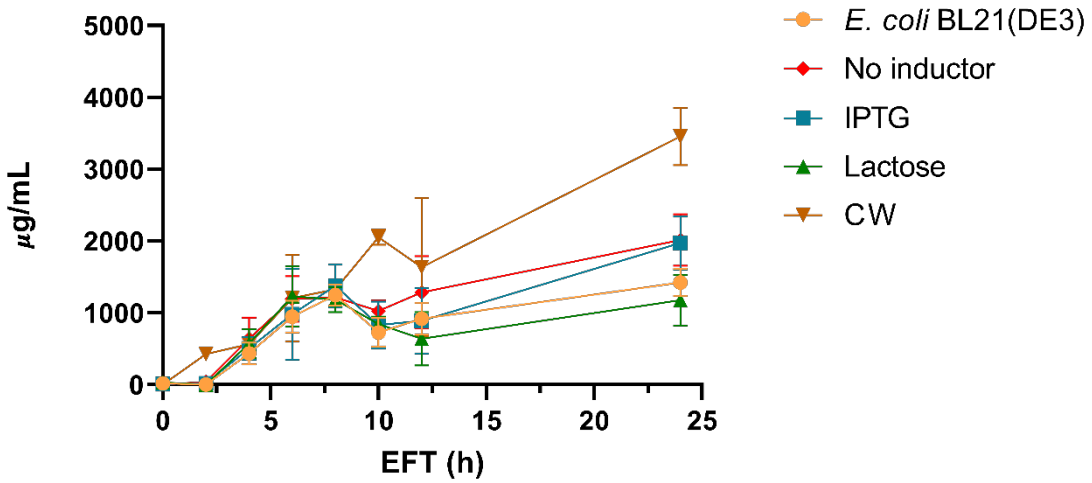

Figure 4.8 – Total protein quantification of *E. coli* BL21(DE3) transformed with pCM13::SELP-59-A with different inducers. The protein levels (µg/mL) were measured at different timepoints during the 24 h of elapsed fermentation time (EFT). Protein quantification was determined using Pierce BCA Protein Assay kit (Thermo Scientific).

Analysis of total protein content (figure 4.8) demonstrates that the quantity of produced protein was in general proportional to the growth, up to the stationary phase. After induction at 8 h EFT, it was possible to observe differences. The CW sample presents a drastic increase in protein due to its high protein content, while the other conditions showed a decrease up to 12 h, before starting to increase again. The quantification of total protein also suggests that the stationary phase was reached at 8 h of fermentation, in agreement with the growth curve and the peak of acid acetic concentration at 8 h, observed by HPLC (figure 4.9). This is due to the rapid uptake of the carbon source, which is converted into products and biomass (Sun *et al.*, 2020), depleting almost all of the carbon sources available in the medium, namely glucose (figure 4.9 A) and glycerol (figure 4.9 B).

Overall, HPLC analysis revealed a similar trend for all the measured parameters and conditions (figure 4.9). Of notice, between 8 to 12 h EFT, it is possible to observe an accumulation of acetic acid at values above 2 g/L, which can be harmful to cells. It has been reported that acetate at concentrations greater than 1 g/L exerts a negative influence in cell growth and protein expression, affecting the stability of internal proteins (Pinhal *et al.*, 2019). Moreover, in a previous study reporting the production of SELP-59-A in batch conditions, Collins *et al.,* (2013) demonstrates that higher concentrations of acetic acid (1 – 4 g/L) appear to have a bacteriostatic effect on bacterial cell cultures of *E. coli,* thus affecting cell growth. Interestingly, it was observed an increase of lactic acid concentration after IPTG induction. This observation was previously observed in our group, but the reasons remain to be elucidated.

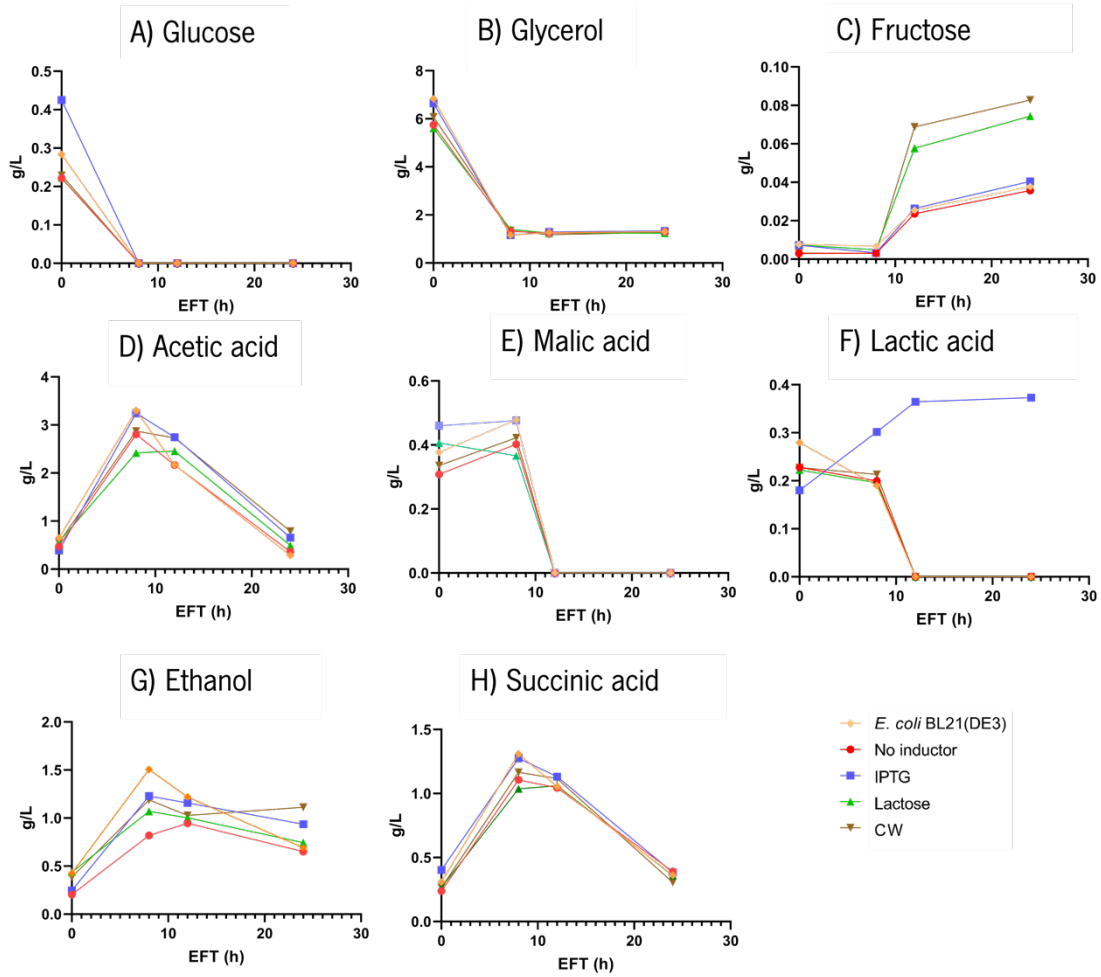

Figure 4.9 – HPLC analysis of sugars, ethanol and carboxylic acids during growth of SELP-producing *E. coli* tested with different inducers.

To depict a more comprehensive picture of the possible limiting factors affecting growth, the concentration of phosphates and free amino nitrogen (FAN) was determined using methodologies optimized for microplate reading (appendix E and F for phosphate and FAN, respectively).

The results of phosphate concentration (figure 4.10 A) demonstrate that the concentration of phosphates is maintained at some extent throughout the time course of the experiment, except for CW. For the latter, there is a prominent decrease in phosphate concentration after 12 h EFT. As for the content in free amino nitrogen, all samples contained yeast extract and tryptone as source of nitrogen that is slowly consumed up to 8 h EFT (figure 4.10 B). The initial burst in FAN content observed at 2 h EFT is due to the inoculum that contains yeast extract and tryptone. After induction, there is a noticeable increase of FAN content in the CW sample due to the complex richness of cheese whey.

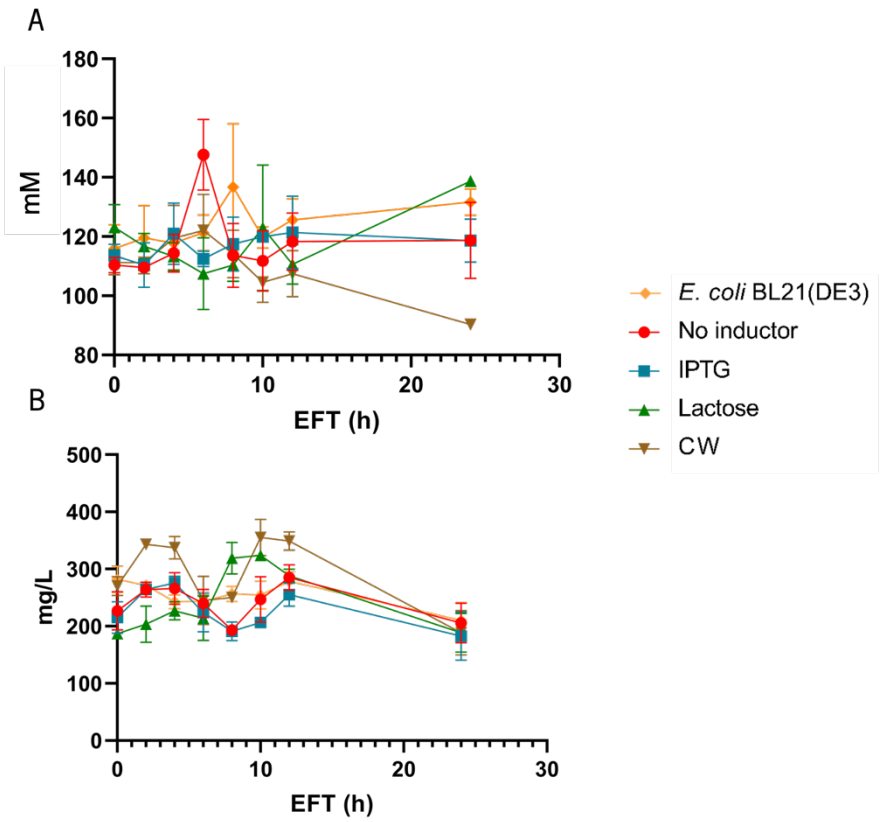

Figure 4.10 – Free amino nitrogen (FAN) and phosphate concentration: A) values for phosphate concentration during 24 h of fermentation. B) values of FAN during 24 h of fermentation.

To relate the aforementioned results with SELP-59-A production, the samples were analysed by SDS-PAGE after 8, 12 and 24 h EFT, and assessed in terms of band intensity with the aid of ImageJ (figure 4.11). Analysis of the crude cell extracts before induction revealed very low levels of SELP-59-A for all the conditions tested (figure 4.11 A; 8 h EFT). To note that *E. coli* BL21(DE3) lacking the plasmid was used as control. After induction, all the induced conditions (IPTG, Lac and CW) demonstrated to result in the overexpression of SELP-59-A after 4 h of induction (12 h EFT) (figure 4.11 B). After 16 h of induction (24 h EFT), it was observed an increase of SELP-59-A production, reflected by an increase of band intensity (figure 4.11 C).

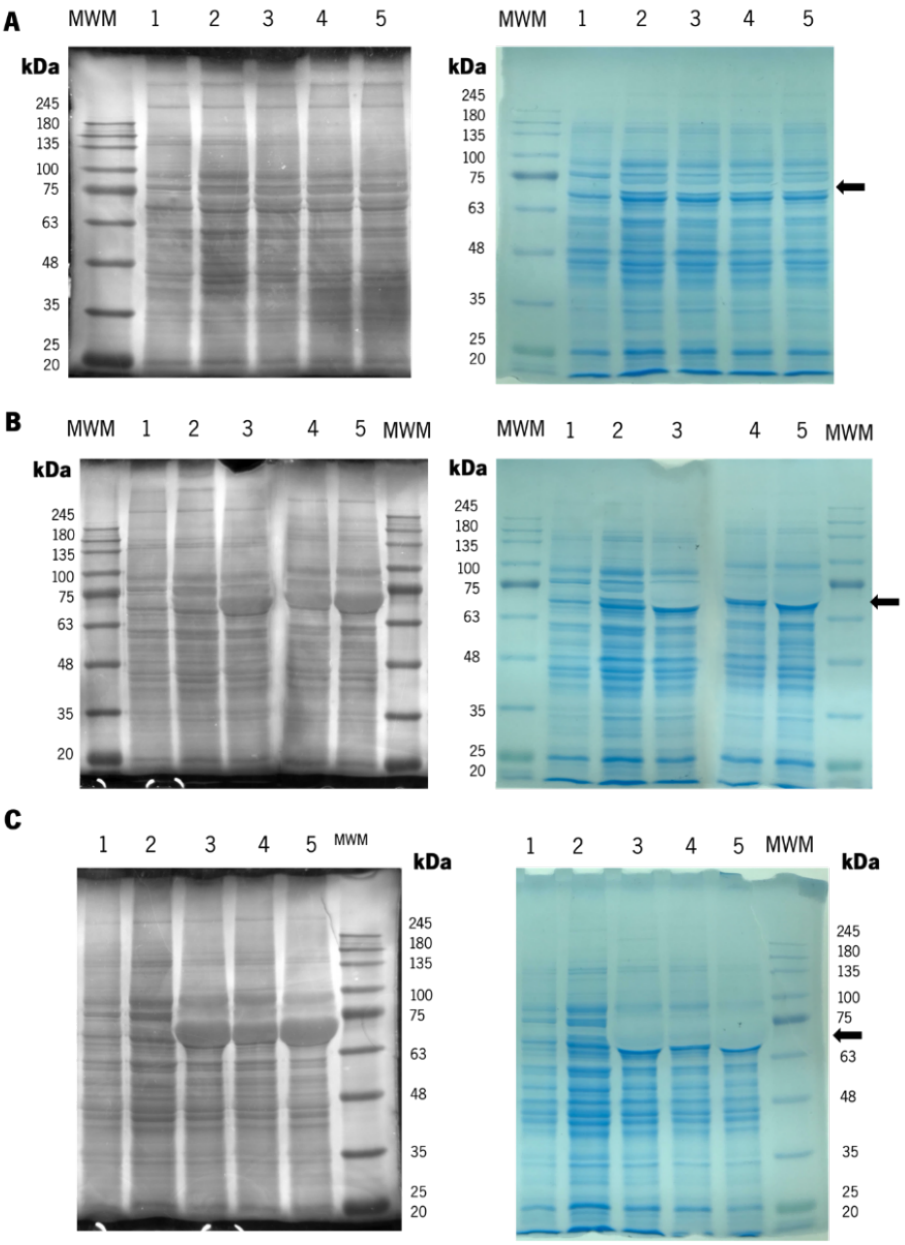

Figure 4.11 – Electrophoretic patterns of soluble crude cell extracts at A) 0 h, B) 4 h and C) 16 h of induction. Cells were allowed to grow for 8 h in TB prior to induction. 1) control - non-transformed *E. coli* BL21(DE3); 2) culture without induction; 3) culture induced with IPTG; 4) culture induced with lactose (Lac); 5) culture induced with cheese whey (CW); MWM - molecular weight marker (NZYColour Protein Marker II). All samples were normalised for the same quantity (5 µL) before loading on gel. Gels were stained with copper chloride (left column) and with Coomassie blue staining (BlueSafe, NzyTech). SELP-59-A is indicated by arrows.

Noteworthy, induction with cheese whey presented bands with more intensity when compared to the other inducers, indicating that more SELP-59-A was produced in that condition. These observations have been also reported by other authors. Viitanen *et al.,* (2003) reported the feasibility of using CW as alternative inducer for the expression of an alcohol dehydrogenase, showing expression levels equivalent to induction by IPTG. More recently, Mobayed *et al.,* (2020) reported the use of CW as inducer for the expression of β-galactosidase with expression levels

higher than IPTG. Regarding the electrophoretic pattern of *E. coli* cultures in TB without inducer, the discrepancy with the results obtained in figure 4.6, is a consequence of the different medium to volume ratio (1:4 corresponding to 125 mL in 1L flask *vs* 1:10 corresponding to 100 mL in 1L flask) that results in different aeration. In the experiments devised in the study with auto-induction media (section 4.2.1), we used protocols established in our group for the rapid screening of rPPs (without the need of additional culture handling) that allow for high protein expression, in detriment of cell growth ($OD_{600nm.} \approx 2.2 \pm 0.94$ after 24 h, figure 4.6). In this section, induction is performed after 8 h of fermentation using aeration conditions that allow reaching high cell densities ($OD_{600nm} \approx 7.3 \pm 0.83$ after 24 h, figure 4.7). The lower oxygen levels in the auto-induction conditions result in reduced cell growth, allowing leakage expression (Ukkonen *et al.*, 2013).

4.2.3. Exploitation of residues/by-products for the bioproduction of SELP-59-A via one-factor-at-a-time

After assessing the potential of using cheese whey as inducer for protein expression, other residues/by-products such as glycerol and corn steep liquor (CSL), were tested for their viability to be used as media components. Based on previous findings, the concentration of glycerol and cheese whey/lactose were fixed to a concentration of 5 g/L and 2 g/L, respectively (data not shown). Following a one-factor-at-a-time methodology, the concentration of corn steep liquor was varied and, in some conditions, was supplemented with yeast extract and tryptone, while maintaining the rest constant. In this approach, we used optimized TB conditions (12 g tryptone, 24 g yeast extract, 0.17 M KH_2PO_4, 0.72 M K_2HPO_4, 5 g glycerol per liter) as positive control and included a commercially available auto-induction TB medium (TBAIM) for comparison purposes. In addition, mutant PS.5 was also included in the experimental design.

The growth curve for all the tested conditions and OD_{600nm} values obtained after 24 h EFT are depicted in figure 4.12. All conditions reached the stationary phase within 6 to 8 h EFT, with TB (both with the non-mutated and the mutated variant) allowing to achieve the highest cell densities before induction (8 h EFT) with OD_{600nm} around 8.5 (formulations #1 and #11, figure 4.12); the remaining media formulations reached similar cell densities before induction ($OD_{600nm} \approx 4.4 \pm 0.32$). After induction, major changes were observed for media formulations #3, #4, #6, #7 and #9, showing a remarkable decrease in OD_{600nm} values after 4 h of induction (12 h EFT). Regarding conditions #8 and #10, it was possible to observe a slight increase in growth after 4 h of induction and, for the rest of the conditions, the cell densities for media #1, #2, #5 and #11 were relatively

constant up to the end of the experiment (16 h of induction; 24 h EFT). Although the highest cell densities were observed with TB, the high OD_{600nm} values observed for media #8, #10 and #5 are promising, especially considering that these outperformed the commercial TBAIM. Moreover, the addition of very small amounts of yeast extract demonstrated to slightly increase growth.

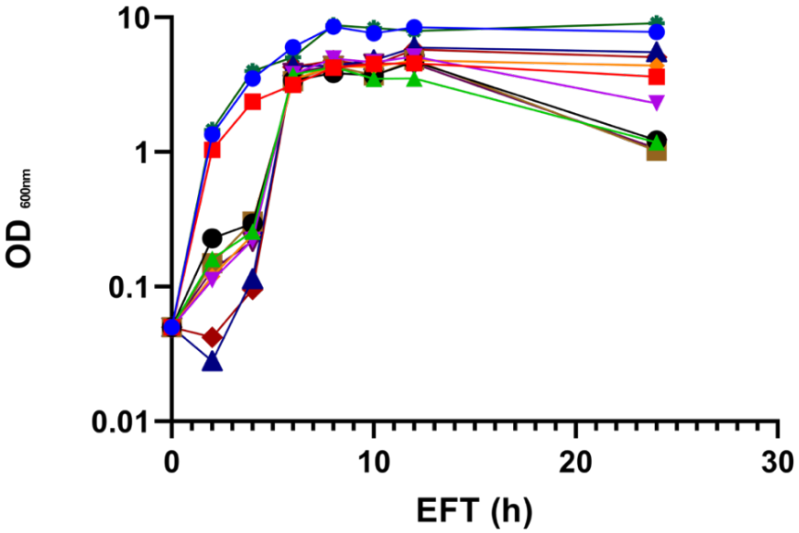

	Description	Inducer	OD_{600nm} after 24 h EFT
1	TB, positive control	CW	7.8
2	TBAIM	Auto-induction	3.625
3	Glycerol (5 g/L) + CSL (30 g/L)	CW	1.18
4	Glycerol (5 g/L) + CSL (30 g/L)	Lactose	2.3
5	Glycerol (5 g/L) + CSL (30 g/L)	IPTG	4.38
6	Glycerol (5 g/L) + CSL (30 g/L) + YE (0.06 g/L)	Lactose	1.22
7	Glycerol (5 g/L) + CSL (30 g/L) + YE (0.12 g/L)	Lactose	1.02
8	Glycerol (5 g/L) + CSL (60 g/L) + YE (0.12 g/L)	Lactose	5.52
9	Glycerol (5 g/L) + CSL (30 g/L) + TR (0.03 g/L)	Lactose	1.06
10	Glycerol (5 g/L) + CSL (60 g/L) + YE (0.06 g/L)	Lactose	5.06
11	TB, *E.coli*, P.S.5	CW	9.025

Figure 4.12 – Growth curves of the media formulations used in the OFAT approach. Cell densities (OD_{600nm}) were measured after 24 h of elapsed fermentation time (EFT). CSL – corn steep liquor; YE – yeast extract; TR – tryptone.

Analysis of total protein content is depicted in figure 4.13. Since addition of CW for induction at 8 h EFT influences the results due to its high protein content, the amount of protein added was subtracted from the associated measurements. Based on the average total protein results, analysis of mean values after 24 h suggest two clusters: one with high total protein content above 2 g/L comprising media formulations #1, #2, #3 and #11, and another with lower total protein content comprising the remaining media. Still, the high standard deviations do not allow for an accurate assessment of results.

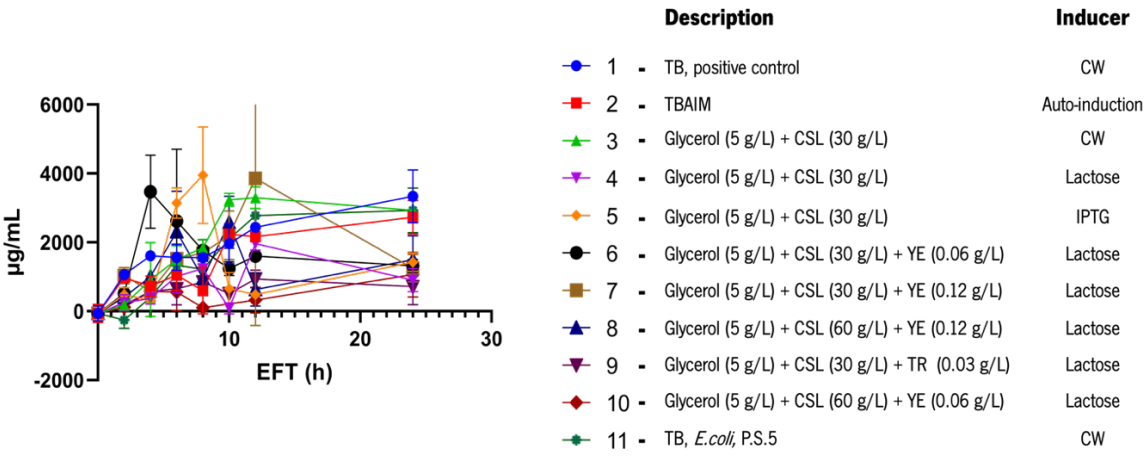

Figure 4.13 – Total protein content of *E. coli* cells grown in media formulations used in the OFAT approach.

Phosphate concentration demonstrated little changes over the time of fermentation, indicating that the media has enough concentration to sustain cell growth and media buffering (figure 4.14 A). However, in contrast to the phosphate concentration, the free amino nitrogen (FAN) values varied over time, with TBAIM showing the highest concentration of FAN (figure 4.14 B).

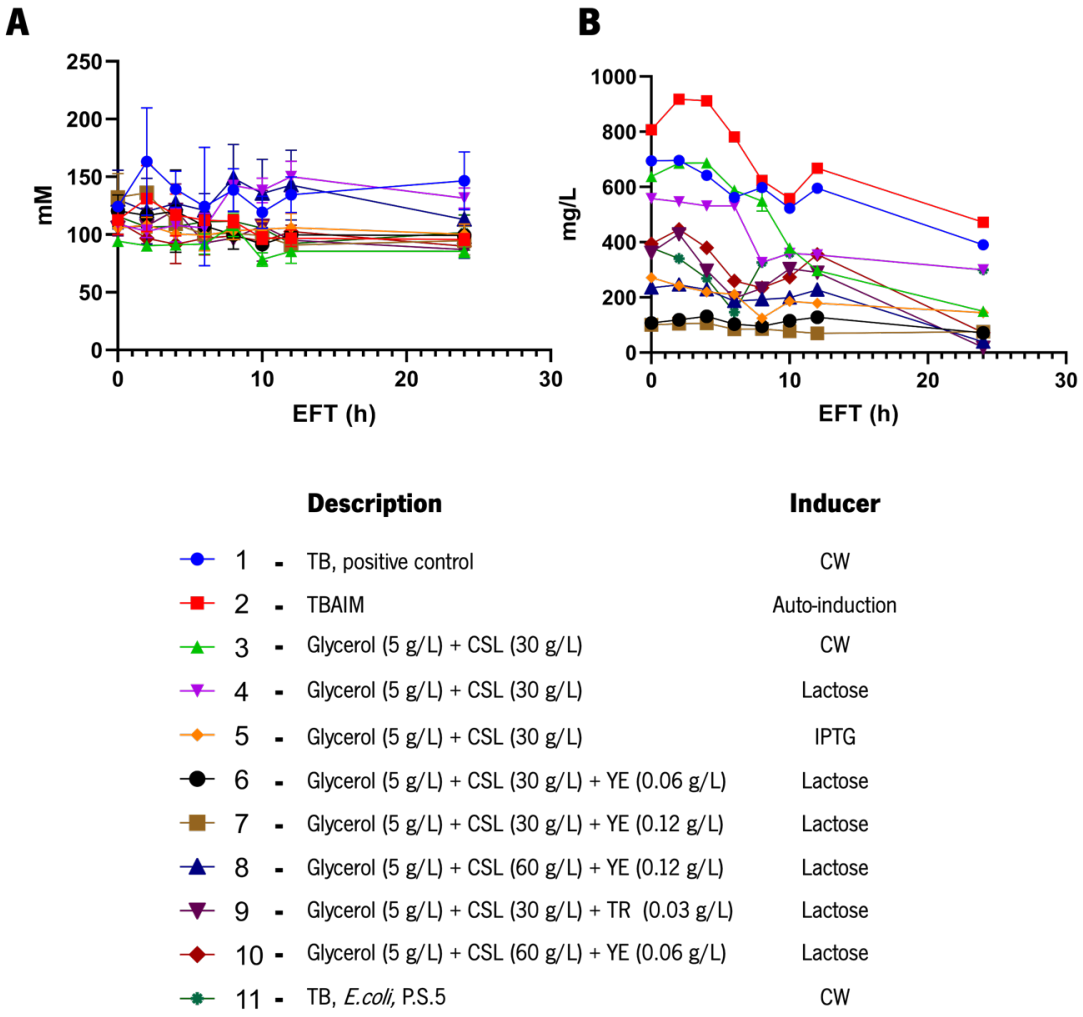

Figure 4.14 – Phosphate and free amino nitrogen (FAN) concentration variation: A) phosphate and B) FAN concentration during the 24 h of fermentation.

Evaluation of the SDS-PAGE results revealed surprising results for the formulations comprising the by-products/residues. All the media formulations displayed high levels of protein expression, even before induction (figure 4.15 A). These demonstrated to be comparable, or even higher, to the commercial TBAIM (lane 2, figure 4.15 A), which was expected to show expression due to the presence of lactose in medium composition. Regarding the other samples and as previously observed in (figure 4.11), the use of TB resulted in very low levels of protein expression before induction (lanes 1 and 11 in figure 4.15. After induction for 4 h, the expression levels remained similar for TBAIM and for the media formulations comprising glycerol and CSL, with all samples overall exhibiting equivalent expression levels for SELP-59-A (figure 4.15 B). Noteworthy, after 16 h of induction (24 h EFT), the sample with mutant PS.5 showed the highest SELP-59-A expression levels, outperforming all the remaining conditions (figure 4.15 C). However, except for media

formulations #1, #8, #10 and #11, the bands corresponding to SELP-59-A seem to have disappeared after 16 h of induction (24 h EFT) (figure 4.15 C). This was unexpected and may indicate a degradation (or consumption by *E. coli*) of the recombinant protein.

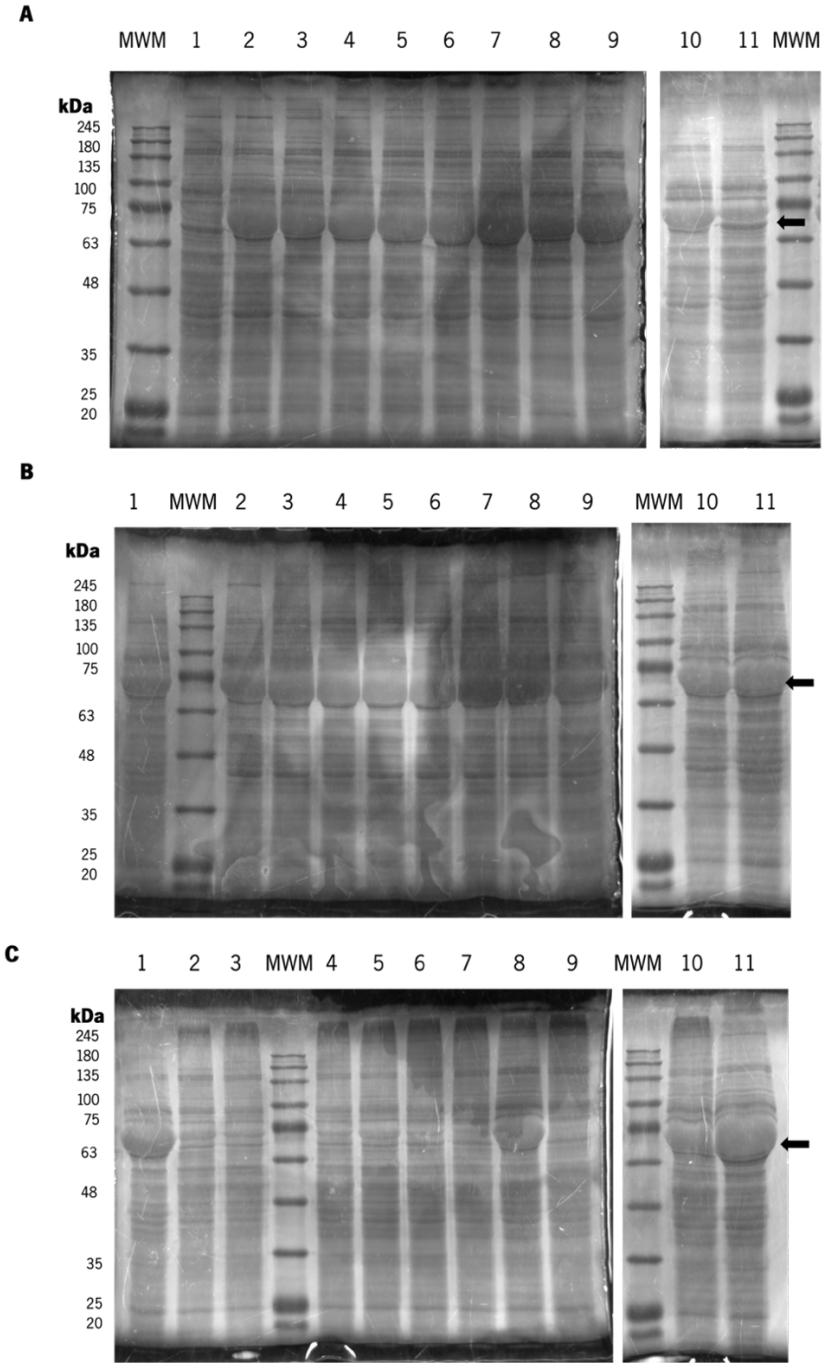

Figure 4.15 - Electrophoretic patterns of soluble crude cell extracts A) before induction (8 h EFT) and after B) 4 h (12 h EFT) and C) 16 h of induction (24 h EFT). 1) TB (TB), corresponding to formulation #1 using non-mutated *E. coli* BL21(DE3); 2) commercial auto-induction medium TBAIM (GRiSP Research Solutions Lda.), corresponding to formulation #2; Lanes 3 to 10 correspond to media formulations #3 to #10, respectively; 11) TB (TB) with *E. coli* BL21(DE3) mutant PS.5. All samples were normalised for the same quantity (5 µL) before loading on gel. Target recombinant protein is indicated by arrows and molecular weight marker is represented by MWM (NZYColour Protein Marker II). Gels were stained with copper chloride.

For each of the conditions, SELP-59-A was purified (appendix G) and pure protein fractions were lyophilized and weighed for determination of the volumetric productivities after 24 h EFT (figure 4.19). Comparing the different media compositions, the best volumetric productivities were obtained with media formulation #1 (consisting of TB), formulation #8 (5 g/L glycerol + 60 g/L CSL + 0.12 g/L YE) and formulation #10 (5 g/L glycerol + 60 g/L CSL + 0.06 g/L YE), with values of 87, 151 and 129 mg/L, respectively. A remarkable result was the volumetric productivity obtained with the mutant PS.5 that allowed to achieve volumetric productivities near 3-fold higher (380 mg/L).

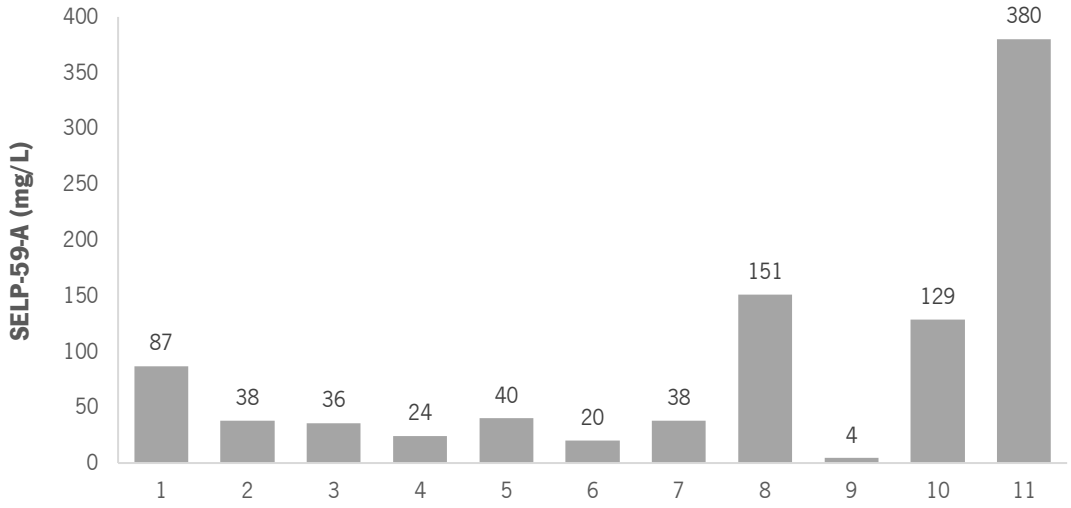

Figure 4.16 - Volumetric productivities (mg/L) obtained for SELP-59-A after purification. Categories in the x-axis correspond to media formulations #1 to #11.

Analyzing the results obtained from HPLC, it is possible to observe that glucose in TB media (formulation #1 and #11) and TBAIM (formulation #2) is almost or completely depleted within the first hours of fermentation (figure 4.17 A); whereas, glucose is maintained in the media containing CSL and glycerol (figure 4.17 A). The media comprising CSL (formulations #3 to #10) also demonstrate slower glycerol consumption (figure 4.17 B) and a higher accumulation of malic acid than TB (figure 4.17 E). Lactic acid oxidation generates CO_2, which is a regulator of the phosphoenolpyruvate carboxylase (Zhang *et al.,* 2009). This enzyme transforms phosphoenolpyruvate (PEP) and bicarbonate to oxaloacetate and inorganic phosphorus in an irreversible manner in the presence of Mg^{2+}. Increased carboxylation of PEP to generate oxaloacetate rather than pyruvate occurs more frequently in the presence of CO_2, making malic acid synthesis from oxaloacetate more likely (Song *et al.,* 2006). The concentration of lactic acid

was higher for formulations #8 to #10 (figure 4.17F), which is due to the presence of CSL. Corn step liquor is obtained after the corn has been softened and swollen in warm water and the soluble parts of the grain have been extracted into steep water (Hull *et al.*, 1996). This extracted water is rich in organic matter and lactic acid, which is then evaporated to obtain the liquor (Liggett *et al.,* 1948; Loy & Lundy, 2019). The reduction of lactic acid concentration along fermentation time suggests that lactic acid is used as carbon source, likely through the conversion of lactate into pyruvate (for each mole of lactate formed, one mole of pyruvate was formed) (Haugaard, 1959). The concentration of succinic acid was higher for TB, suggesting that malic acid was not converted to succinic acid in TCA cycle.

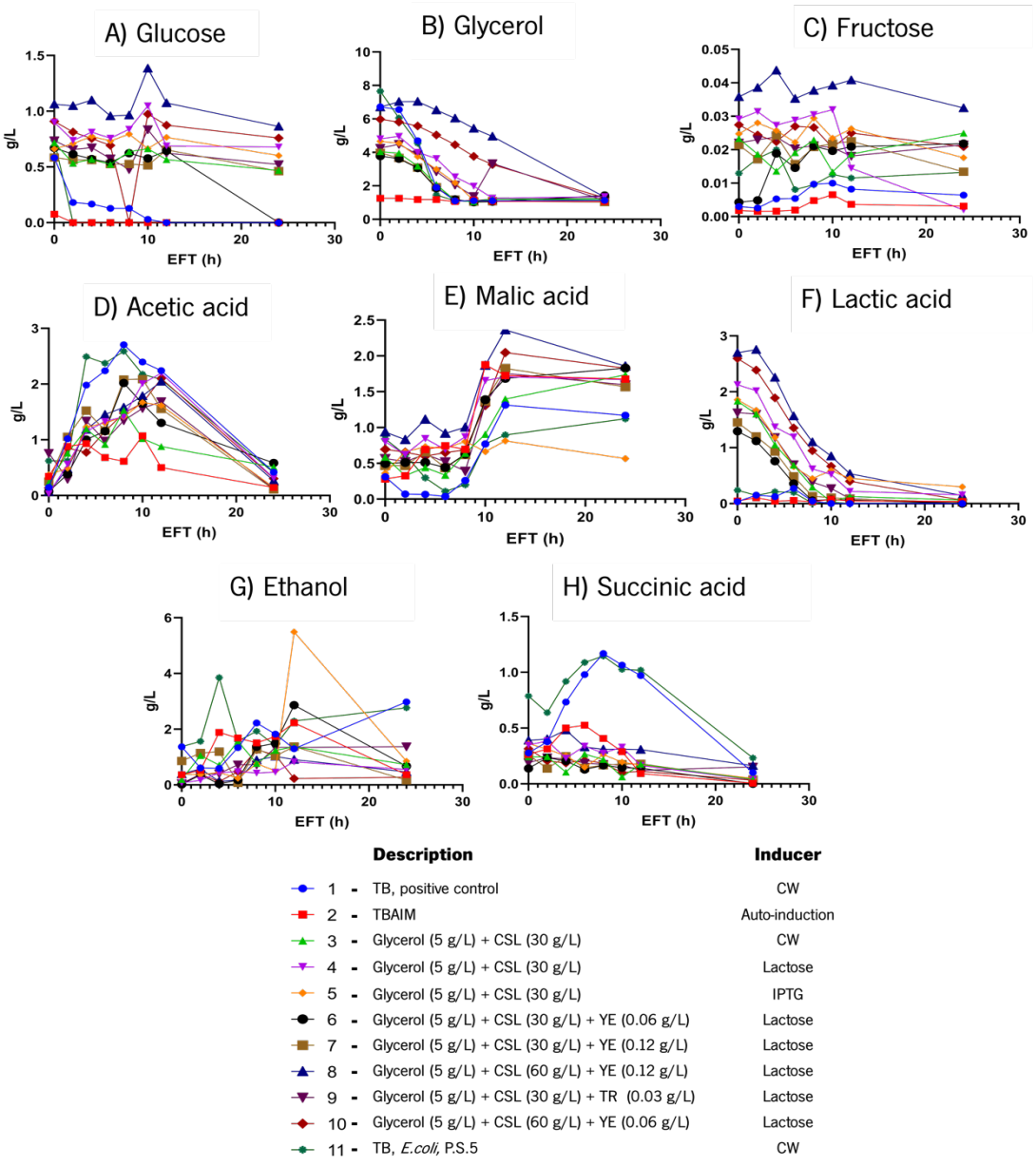

Figure 4.17 – HPLC analysis of sugars, ethanol and carboxylic acids during growth in the different media.

4.3. Optimization of culture medium composition through multivariate statistical analysis

This chapter reports the optimization of media composition using the selected industrial residues/by-products by central composite design. As in the OFAT approach, the optimization studies included both the original *E. coli* BL21(DE3) (section 4.3.1) and the mutant PS.5 (section 4.3.2). The studies used a circumscribed central composite design with five levels for each factor, and considered the results obtained in the aforementioned section (*e.g.,* induction at 8 h EFT with CW; use of glycerol and CSL as media components; 12 h and 24 h EFT). The model was chosen to investigate the key interactions between media compositions (glycerol, CW and CSL), as well as to determine the best operating settings. Glycerol concentrations were tested at 0, 3, 6, 9 and 12 g/L, CSL concentrations at 0, 15, 30, 45, and 60 g/L, and CW concentrations at 0, 6.4, 12.8, 19.2, and 25.6 g/L, according to the conditions defined in table 3.2, for a total of 28 different conditions. For each experiment, one of the variables was fixed at the central point (CW: 12.8 g/L; CSL: 30 g/L; glycerol: 6 g/L) and the other two were allowed to vary. For instance, in figure 4.18 A-1, the cell density was studied at a fixed concentration of 12.8 g/L of CW while the concentrations of CSL and glycerol were allowed to vary between 0 – 60 g/L and 0 – 12 g/L, respectively.

4.3.1. Original, non-mutated *E. coli* BL21(DE3) strain

4.3.1.1. CCD analysis of growth conditions

The first step on the CCD study, was to characterize the growth and assess total protein content of the original non-mutated *E. coli* BL21(DE3), transformed with pCM13::SELP-59-A (figure 4.18). In addition, the variation in phosphate concentration and free amino nitrogen (figure 4.19) were also assessed to provide a more complete profile on cell growth.

Figure 4.18 depicts the 3D contour plots for cell densities (OD_{600nm}) and total protein content via the BCA method after 24 h EFT (corresponding to 16 h of induction). Analysis of the 3D plots indicates that cell density is mostly influenced by the amount of CSL and CW. For instance, at high concentration of glycerol and no CSL, the OD_{600nm} presents the lowest value (figure 4.18 A-1). A similar behavior is found for the conditions with high concentrations of glycerol and no CW (figure 4.18 A-2). Regarding the analysis of total protein content, the results partially agree with those obtained for cell density. High values of total protein were found for the conditions with high

concentration of CW and CSL (figure 4.18 B-3). Still, the best results were obtained for the conditions with high concentrations of glycerol and CW (figure 4.18 B-2). The peak observed at the conditions with no CSL and glycerol was unexpected and the reasons for that remain to be elucidated.

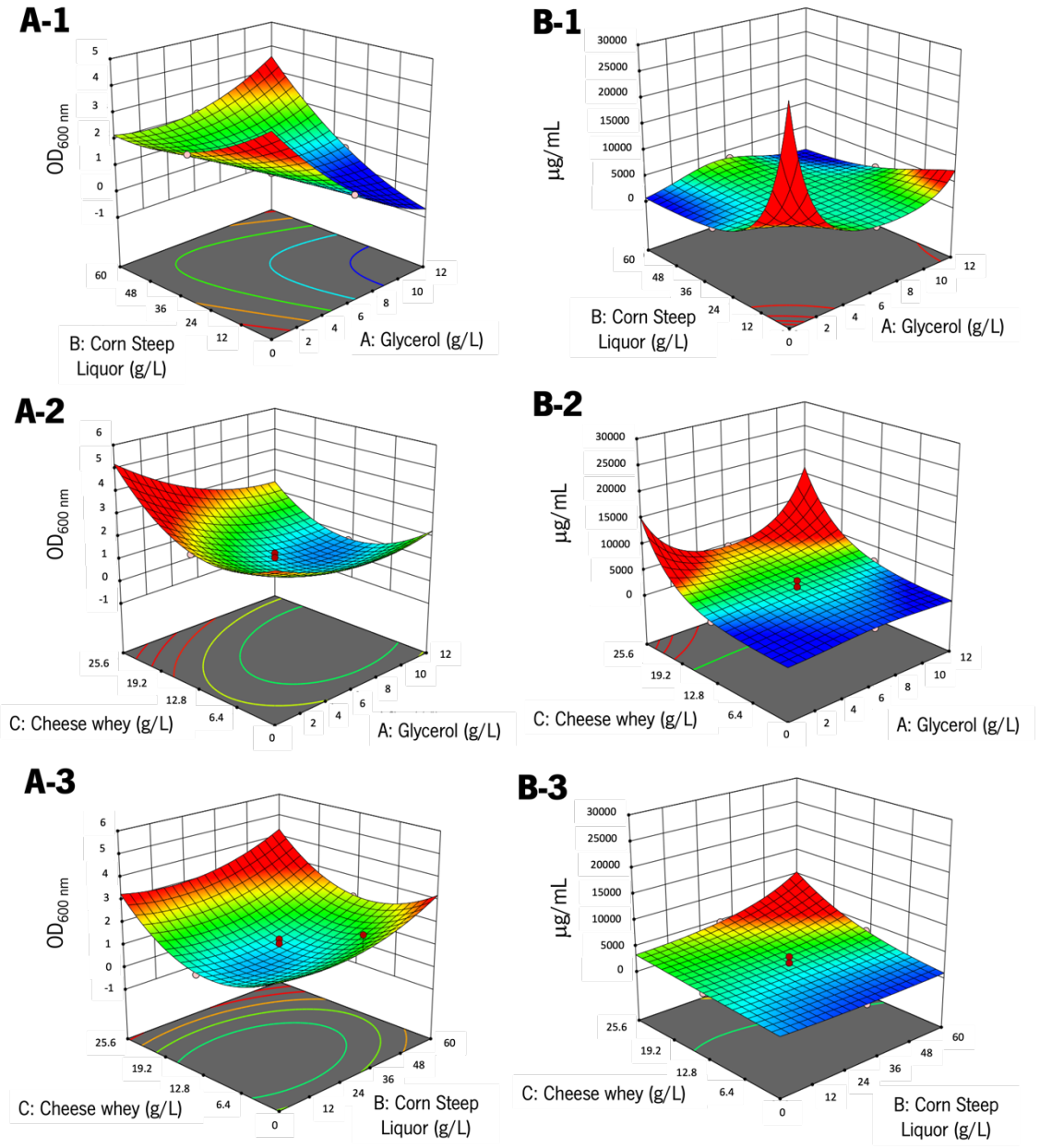

Figure 4.18 – 3D contour plots representing the variations in cell density (left column) and total protein content (right column) of non-mutated *E. coli* BL21(DE3) at different concentrations of CW, CSL and glycerol after 24 h EFT. A) Cell densities of the 28 different conditions defined in the CCD were determined by assessing the optical density at 600 nm (OD_{600nm}). B) The protein levels (µg/mL) of the 28 different conditions defined in the CCD were quantified using the Pierce BCA Protein Assay (Thermo Scientific). In dark red (●) are the points above the surface and in light red (●), the points below the surface.

The nitrogenous compounds such as amino acids, peptides, and ammonium ions are known as free amino nitrogen (FAN). Analysis of the total values of phosphate and FAN after 24 h, demonstrated that the concentration of phosphates slightly decreases with increased glycerol content whereas, FAN concentration remained relatively constant (appendix H, figure 7.6). For a better assessment of the variations in phosphate and nitrogen concentration, the consumption of phosphates and nitrogen after 24 h EFT was determined and represented in figure 4.19. For this, the initial concentration of phosphates and FAN at 0 h EFT were subtracted from the values obtained after 24 h. Increased CSL concentrations resulted in lower levels of phosphate consumption (figure 4.19 A-1 and figure 4.19 A-3), while increasing glycerol and CW resulted in high phosphate consumption (figure 4.19, left column). Regarding FAN consumption, both CSL and glycerol demonstrated a low to moderate impact on consumption levels (figure 4.19 B1-3). In contrast, increasing the concentration of CW demonstrated a dramatic increase of FAN consumption (figure 4.19 B-2 and figure 4.19 B-3). Nevertheless, the highest consumption levels were observed at the highest concentrations of CW and CSL (figure 4.19 B-3). These results are in agreement with analysis of cell growth after 24 h EFT, since biomass levels demonstrated to be highly dependent of CW and CSL concentration (figure 4.18). As for glycerol, high concentrations demonstrated to result in low cell growth (figure 4.18 A-1) and FAN consumption (figure 4.19 B-1 and figure 4.19 B-2); this suggests that high concentrations of glycerol can be detrimental to cell growth and a limiting factor in nitrogen transport (when the ratio of C is greater than that of N), which results in nitrogen accumulation. Carbon is required to generate energy, while nitrogen is a component of proteins and amino acids. A high C/N ratio (excess carbon) will retard protein and amino acid formation (Martin, 2007); therefore, the carbon to nitrogen (C/N) ratio is an important parameter that should be maintained at appropriate levels as it is essential for growth. As a result, in media with high glycerol concentrations, reactions for the formation of amino acids and protein are slower, and free nitrogen may accumulate.

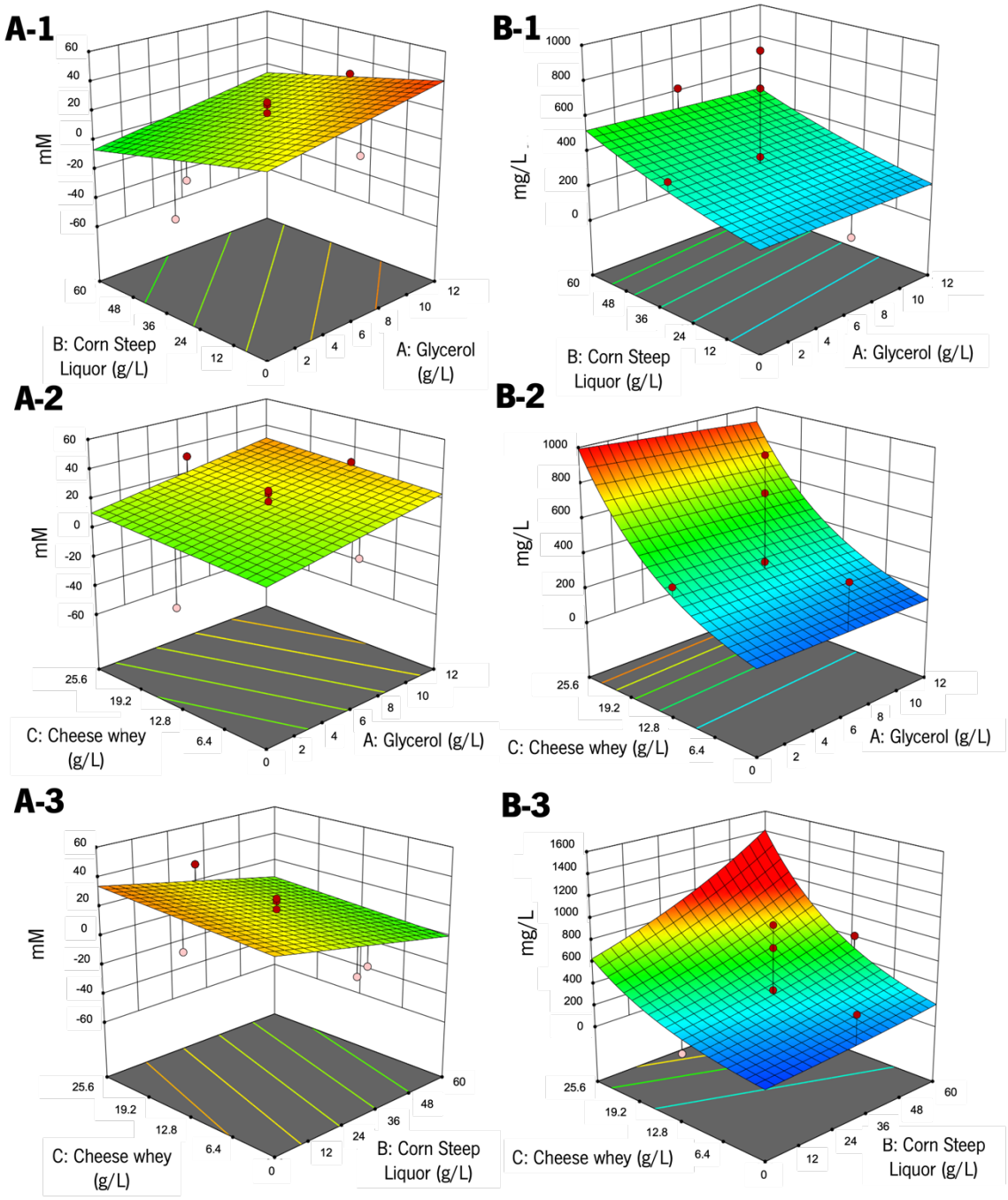

Figure 4.19 – 3D contour plots representing the variations in phosphate (left column) and nitrogen (right column) consumption for non-mutated *E. coli* BL21(DE3) at different concentrations of CW, CSL and glycerol after 24 h EFT. The consumption was determined by subtracting the initial value at 0 h EFT to the values obtained after 24 h EFT. In dark red (●) are the points above the surface and in light red (●), the points below the surface.

As observed in the previous section with the OFAT approach, the highest protein expression levels were observed after 4 h of induction (12 h EFT). The variations of cell density (OD_{600nm}) and total protein content with glycerol, CW and CSL, were also assessed after 12 h of fermentation (figure 4.20). Although displaying lower OD_{600nm} values and except for the pair CSL/glycerol, the variations in cell density followed a similar profile to that of 24 h EFT (figure 4.20, left column). However,

analysis of total protein content revealed distinct results. The amount of total protein demonstrated to be highly dependent of CW concentration, independently of CSL and glycerol concentration (figure 4.20, right column).

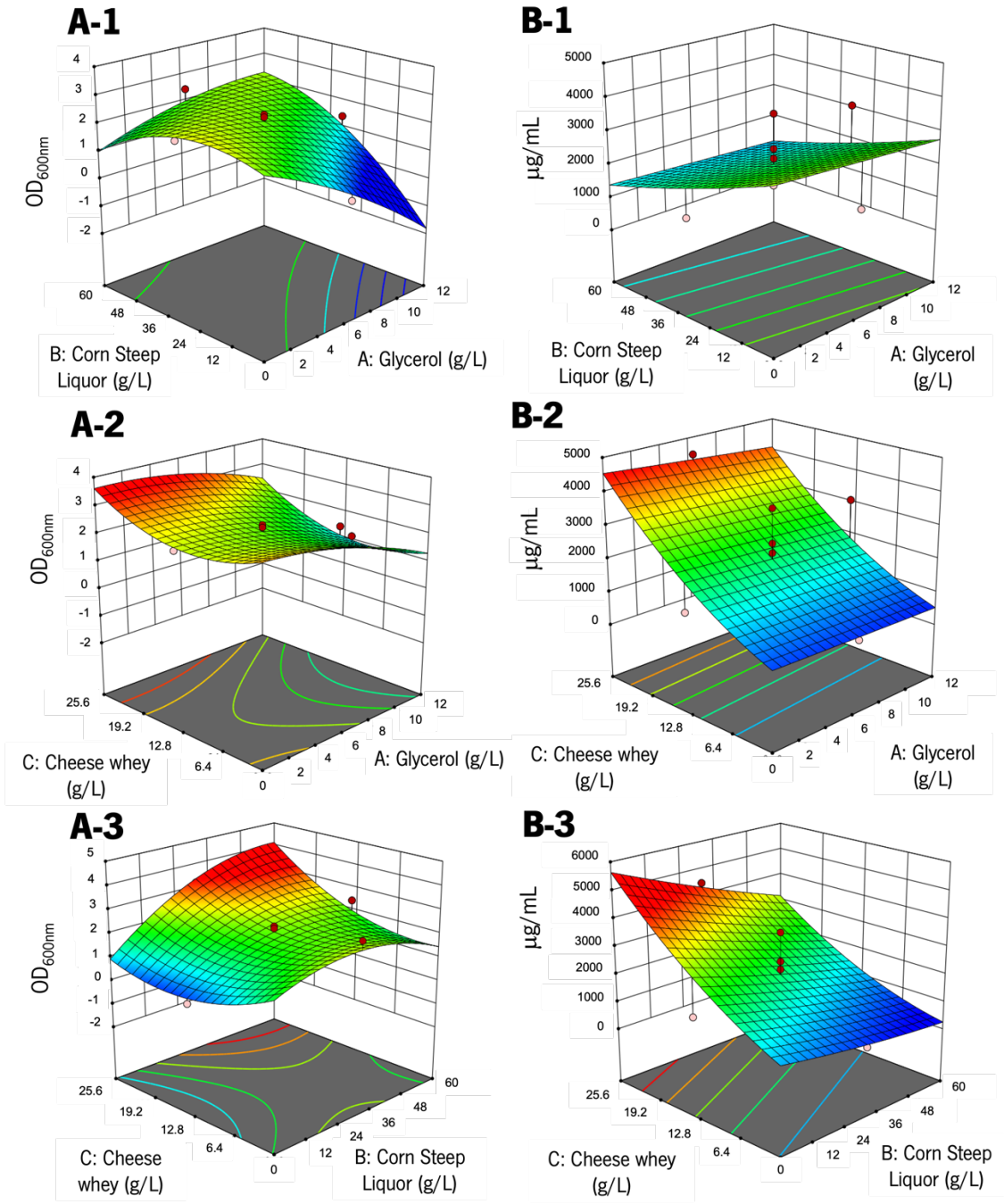

Figure 4.20 – 3D contour plots representing the variations in cell density (left column) and total protein content (right column) of non-mutated *E. coli* BL21(DE3) at different concentrations of CW, CSL and glycerol after 12 h EFT. A) Cell densities of the 28 different conditions defined in the CCD were determined by assessing the optical density at 600 nm (OD_{600nm}). B) The protein levels (µg/mL) of the 28 different conditions defined in the CCD were quantified using the Pierce BCA Protein Assay (Thermo Scientific). In dark red (●) are the points above the surface and in light red (●), the points below the surface.

Since biomass production is related with mixed-acid fermentation (Collins *et al.*, 2013; Xu *et al.,* 1999), the concentration of acetic acid was determined in representative samples to provide a better picture of the growth and protein expression profile. The conditions with low concentrations of CSL (conditions 15 and 17; specified in table 3.2) demonstrated to result in low acetic acid production. In contrast, conditions with a high concentration of CSL (conditions 18, 22, 27 and 28; specified in table 3.2) demonstrated to result in higher production of acetic acid up to the end of the exponential phase of growth, being posteriorly reconsumed (figure 4.21). The CCD analysis of acetic acid production in conditions with variable concentrations of CSL, CW and glycerol is presented in appendix I, demonstrating a positive relation between acetic acid and CSL concentration.

When *E. coli* intake of a primary carbon source exceeds its conversion into CO_2 and biomass, acetate is produced due to a rate-limiting factor generated by either the electron transport system, the TCA cycle, or both (Holms, 1986). A high acetate concentration can have a negative impact on the cell's physiology, limiting growth and potentially lowering the amount of recombinant protein generated. Kleman *et al.,* (1994) also reported that the presence of low concentrations of glucose could trigger an unknown switch mechanism for the consumption of the accumulated acetic acid (Kleman *et al.*, 1994). In media formulations with high concentrations of CSL and CW (3 g/L glycerol, 45 - 60 g/L CSL, 19.2 g/L CW; specified in table 3.2), there was the production of high amounts of acetic acid, which remained long after the exponential phase ended (figure 4.21). While there was a higher concentration of carbon source, the cell was unable to convert it all to biomass, resulting in the production of more acetic acid. At the end of the exponential phase, even though there was likely still carbon source to be consumed, the acetic acid concentration inhibited further growth. On the other hand, conditions 13 and 15 showed low production of acetic acid, suggesting that the lower concentrations of CSL could not be sufficient to sustain a high growth rate (acetic acid is produced as a consequence of cell's inability to convert the exceeding amount of carbon into CO_2 and biomass).

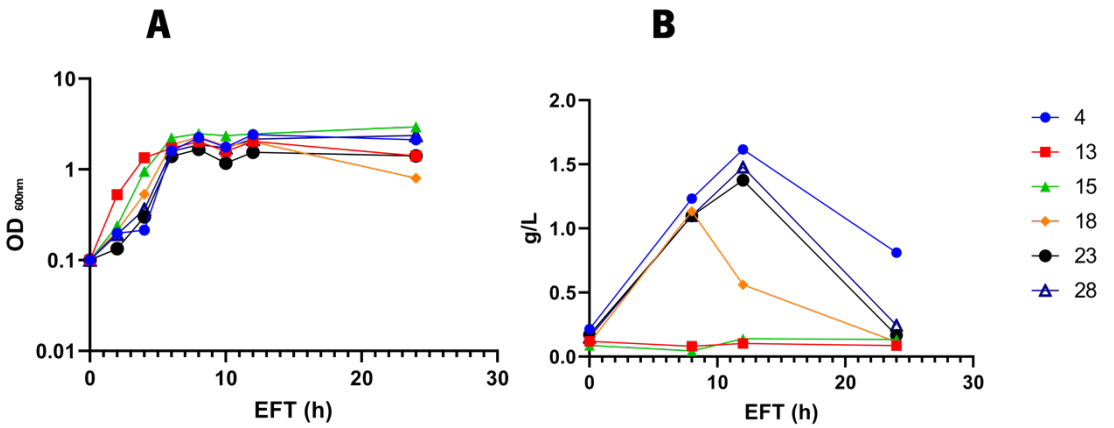

Figure 4.21 – Variations of (A) cell density and (B) acetic acid production for the non-mutant *E. coli* BL21(DE3) using representative media formulations. A few examples were chosen based on better cell growth: 4 (–●–) 6 g/L glycerol, 60 g/L CSL and 12.8 CW; 13 (–■–) 3 g/L glycerol, 15 g/L CSL and 6.4 CW; 15 (–▲–) 3 g/L glycerol, 15 g/L CSL and 19.2 CW; 18 (–◆–) 6 g/L glycerol, 30 g/L CSL and 12.8 CW; 23 (–●–) 9 g/L glycerol, 45 g/L CSL and 6.4 CW and 28 (–▲–) 3 g/L glycerol, 45 g/L CSL and 19.2 CW.

4.3.1.2. Analysis of SELP-59-A production levels

Quantification of SELP-59-A produced after 12 h and 24 h of EFT was initially carried out by densitometry analysis of SDS-PAGE gels using a known concentration of SELP-59-A as reference (figure 4.22 A), and further compared with pure lyophilized SELP-59-A (figure 4.22 B). However, due to operational limitations (*e.g.* number of experiments), assessment of SELP-59-A production after 12 h of EFT was completed by densitometry only. Although the determination of the weight of pure lyophilized SELP-59-A samples is much more reliable and accurate, it is also highly time-consuming. As such, analysis of protein expression was firstly carried out by assessing protein production levels by densitometry. This analysis, if used with caution, represents a convenient approach for the determination of volumetric productivities, especially for comparison purposes. In this work, SDS-PAGE analysis (appendix J) was used for the direct comparison of protein expression bands between gels, using a known concentration of SELP-59-A as internal control.

Similarly, to the results described in section 4.2.1 (figure 4.15), the best expression levels were observed after 4 h of induction (12 h EFT) (appendix J). The 3D contour plots of densitometry analysis after 12 h EFT reveals that protein expression is highly influenced by CSL content, being higher in media with elevated concentrations of CSL (figure 4.22). Estimation of volumetric productivities by densitometry was further evaluated after 24 EFT and compared with the mass of pure lyophilized SELP-59-A. Overall, analysis of the 3D contour plots obtained by densitometry and

weight measurement reveals a general trend: high concentrations of CSL result in higher SELP-59--A production, especially in conditions with high content of CW (figure 4.23). The discrepancy between the volumetric productivity values determined by densitometry or weight measurement are a consequence of the method used for staining the SDS-PAGE gels. As previously mentioned, the limited amino acid variability in SELP-59-A composition (reduced number of charged and aromatic amino acids) hinders the use of more adequate staining methods such as Coomassie blue. Therefore, copper chloride negative staining (the gel is stained except for proteins) was preferred, as it allows the proper visualization of the recombinant protein; nevertheless, it presents limitations due to saturation of protein bands.

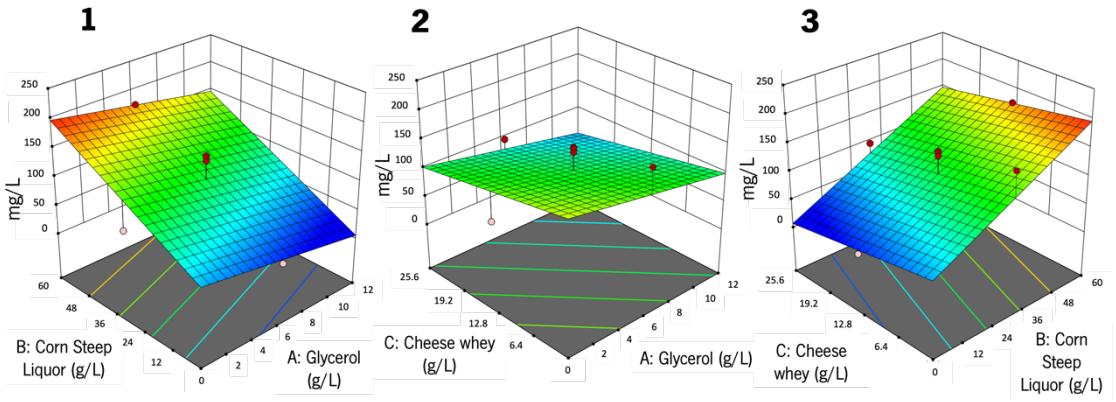

Figure 4.22 – 3D contour plots representing the variations in SELP-59-A production by the non-mutant *E. coli* BL21(DE3) after 12 h of EFT. Protein quantification was determined by densitometry analysis of SDS-PAGE gels. In dark red (●) are the points above the surface and in light red (●), the points below the surface.

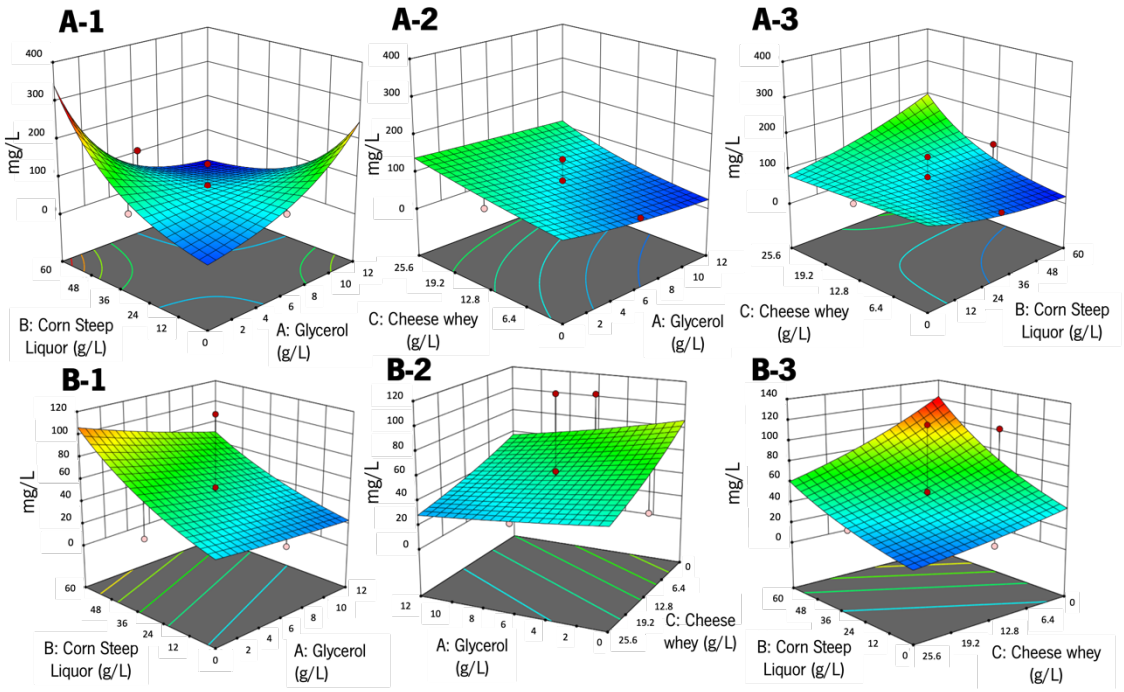

Figure 4.23 – 3D contour plots representing the amount of SELP-59-A produced by the non-mutant *E. coli* BL21(DE3) after 24 h EFT. Protein quantification was evaluated by A) densitometry or by B) weighing pure lyophilized protein. In dark red (●) are the points above the surface and in light red (●), the points below the surface.

4.3.1.3. Optimization of media conditions

The optimal concentration points of CSL, glycerol and CW, expected to yield the best volumetric productivities and biomass, were determined by RSM optimization after 12 h and 24 h of EFT using constraints for the parameters (appendix K). CCD analysis resulted in 63 possible solutions for the optimal points after 12 h EFT and 68 possible solutions for the optimal points after 24 h EFT (appendix L). Figure 4.24 shows the contour plot with the optimal points for 12 h and 24 h EFT (indicated by desirability box), based on the parameter desirability (0.705 and 0.917 for 12 h and 24 h, respectively). According to the CCD analysis, the best medium formulation for 12 h of EFT comprises 1.00 g/L of glycerol, 41.89 g/L of corn steep liquor and 19.20 g/L of cheese whey, corresponding to a predicted volumetric productivity for SELP-59-A of 138.64 mg/L and a corresponding OD_{600nm} of 2.71 (appendix L, table 7.4). As mentioned above, it should be noted that the prediction for 12 h of EFT was based on the protein production values determined by densitometry, which are prone to an overestimation. Regarding the CCD results for 24 h of EFT, the model indicates that the best media formulation comprises 2.07 g/L of glycerol, 60 g/L of

corn steep liquor and 19.2 g/L of cheese whey, with a predicted SELP-59-A production of 72.53 mg/L and a corresponding OD_{600nm} of 2.86 (appendix L, table 7.5).

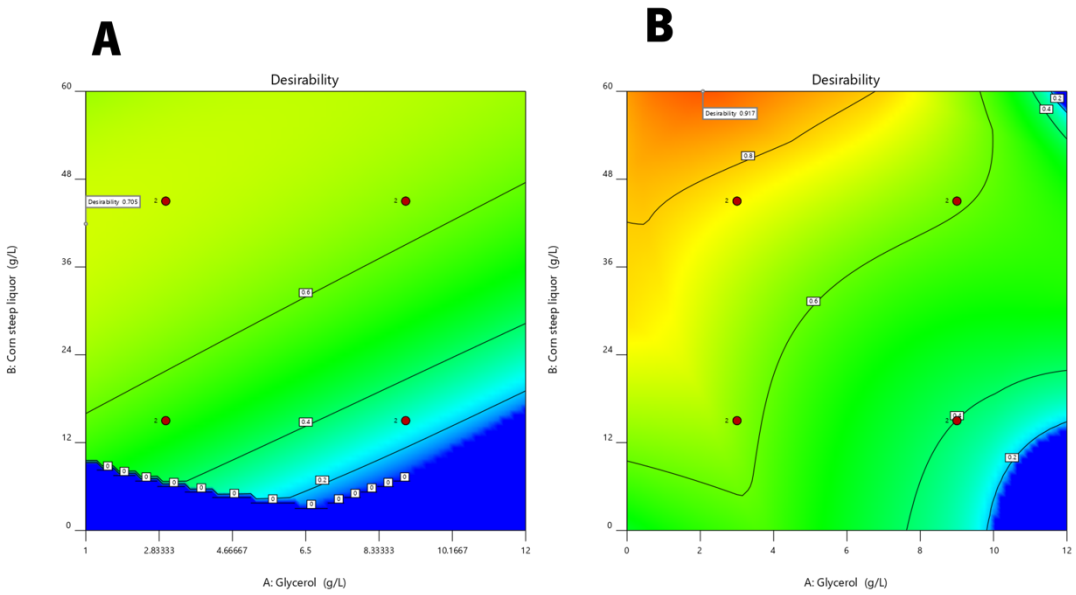

Figure 4.24 – 2D contour plot for the best optimal point based on desirability. The factor cheese whey is fixed at 19.2. The optimization occurred at A) 12 h and B) 24 h. The dark red dots (●) represent design points above the surface. The white box showing the desirability (0.723 and 0.900 for 12 h and 24 h of EFT, respectively) indicates the best formulation. According to the model, the best formulations were determined as 1.00 g/L of glycerol, 41.89 g/L of corn steep liquor and 19.20 g/L of cheese whey after 12 h, and 2.07 g/L of glycerol, 60 g/L of corn steep liquor and 19.2 g/L of cheese whey after 24 h of EFT.

4.3.2. Mutated BL21(DE3) variant P.S.5

4.3.2.1. CCD analysis of growth conditions

The CCD study was also extended to the *E. coli* BL21(DE3) mutant P.S.5, obtained from the proton suicide method, to compare the performance with the non-mutant strain. In general, at 24 h of EFT (figure 4.25), cell density showed a similar trend to the non-mutated strain with the concentration of CW and CSL playing a major role to sustain cell growth. On the other hand, significant changes on total protein content were observed for mutant P.S.5. This parameter demonstrated to be strongly affected by the concentration of CW, and at a lower extent by CSL or glycerol. For instance, at conditions with a fixed concentration of CW, the total protein content remained fairly constant within the range of 3 g/L, independently of variations in the concentrations of CSL and glycerol (figure 4.25 B1). In opposition, increasing the concentration of CW while

keeping constant the concentrations of CSL (figure 4.25 B-2) or glycerol (figure 4.25 B-3), showed to dramatically increase the total protein content up to values higher than 6 g/L.

Similarly to the non-mutated *E. coli*, no remarkable changes were observed for the total values of phosphates and FAN after 24 h (appendix H). Analysis of phosphate and FAN consumption, assessed by subtracting the initial concentration of phosphates and FAN (EFT at 0 h), also revealed a similar trend to the non-mutated *E. coli* – increasing the concentration of CSL showed to result in lower levels of phosphate consumption. Regarding FAN consumption, while the concentrations of CW and CSL demonstrated to greatly impact FAN consumption in the non-mutated *E. coli* (figure 4.19 B-2 and B-3), changes were more modest for mutant P.S.5 (figure 4.26 B-2 and B-3). In the non-mutated sample, FAN consumption reached values of 1,000 mg/L at the highest value of CW and a fixed concentration of CSL (30 g/L), and even greater values at the highest concentrations of CW and CSL. In opposition, for mutant P.S.5, FAN consumption reached a maximum of around 300 – 400 mg/L at the same conditions. The highest change was observed by increasing the concentration of CW and CSL (figure 4.26 B-3) while maintaining the concentration of glycerol constant at the central point (6 g/L). However, it should be noted that the negative values observed at low concentrations of CW and CSL suggest the possibility of an experimental error.

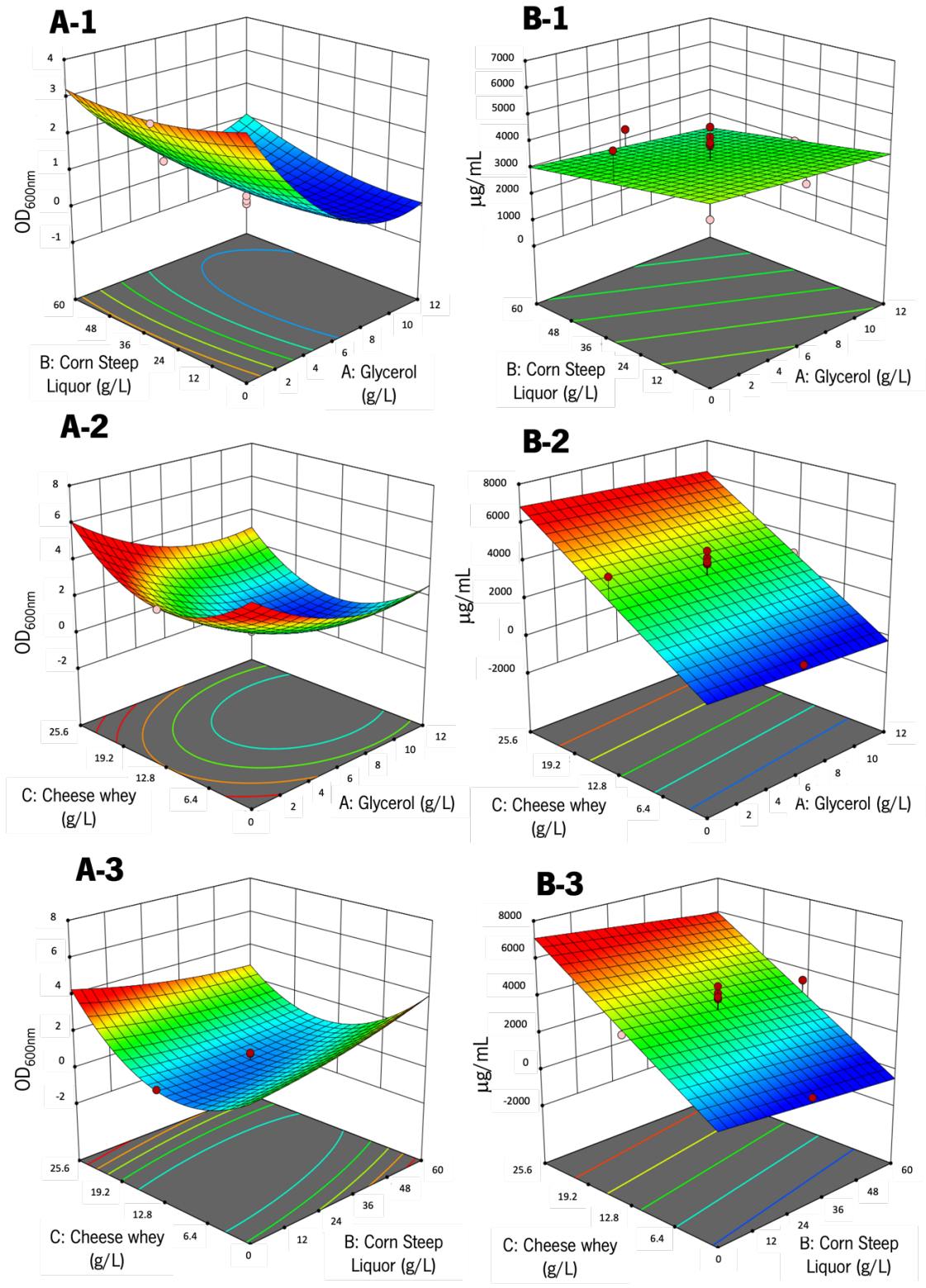

Figure 4.25 – 3D contour plots representing the variations in cell density (left column) and total protein content (right column) of mutated *E. coli* BL21(DE3) P.S.5 at different concentrations of CW, CSL and glycerol after 24 h EFT. A) Cell densities of the 28 different conditions defined in the CCD were determined by assessing the optical density at 600 nm (OD_{600nm}). B) The protein levels (µg/mL) of the 28 different conditions defined in the CCD were quantified using the Pierce BCA Protein Assay (Thermo Scientific). In dark red (●) are points (runs) that are above the surface and in light red (●), the points below the surface.

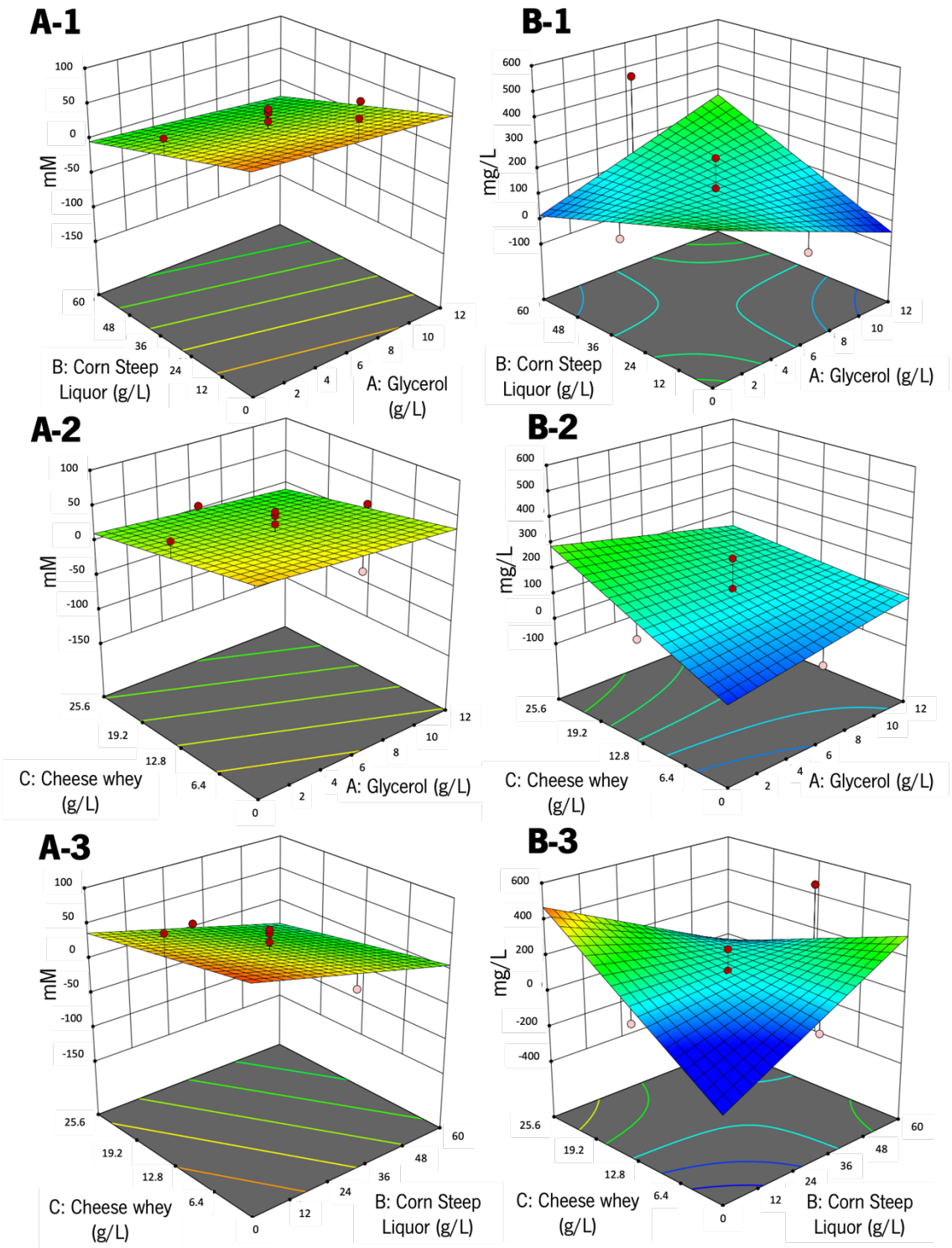

Figure 4.26 – 3D contour plots representing the variation in the consumption of phosphates (left column) and nitrogen (right column) of mutated *E. coli* BL21(DE3) P.S.5 at different concentrations of CW, CSL and glycerol after 24 h EFT. The consumption was determined by subtracting the initial value at 0 h EFT to the values obtained after 24 h EFT. In dark red (●) are points (runs) that are above the surface and in light red (●), the points below the surface.

Analysis of CCD results for mutant P.S.5 after 12 h of EFT revealed remarkable differences in comparison to the non-mutated sample, especially at the level of total protein content. Although cell density remained at relatively similar values, evaluation of total protein content revealed to be greatly impacted by the concentration of CW. As observed in figure 4.27 B-2, increasing the concentration of CW demonstrated to result in total protein values higher than 8 g/L (figure 4.27 B-2).

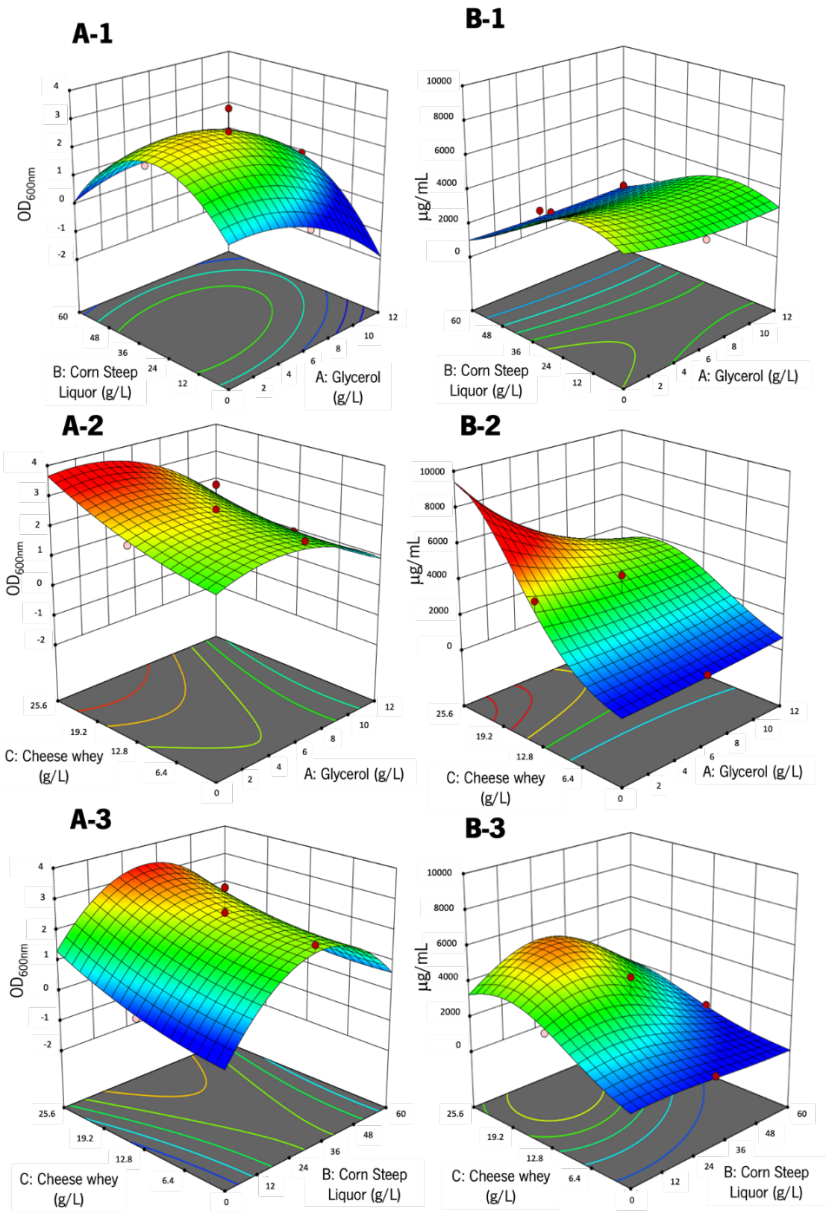

Figure 4.27 – 3D contour plots representing the variations in cell density (left column) and total protein content (right column) of mutated *E. coli* BL21(DE3) P.S.5 at different concentrations of CW, CSL and glycerol after 12 h EFT. A) Cell densities of the 28 different conditions defined in the CCD were determined by assessing the optical density at 600 nm (OD_{600nm}). B) The protein levels (µg/mL) of the 28 different conditions defined in the CCD were quantified using the Pierce BCA Protein Assay (Thermo Scientific). In dark red (●) are points (runs) that are above the surface and in light red (●), the points below the surface.

A comparison of some selected conditions for mutant P.S.5 (conditions 4, 13, 15, 17, 28, 23, 27 and 28; specified in table 3.2) in terms of optical density and acetic acid accumulation was performed. As observed in figure 4.28, the acetic acid accumulation in the supernatant is higher for the conditions with higher CSL concentration (conditions 4, 18, 27 and 28), with the highest observed for condition 4, 23 and 28 with 45 – 60 g/L of CSL. On the other hand, with the exceptions of 4 and 28, the highest cell densities were observed for the samples with low amounts of CSL (conditions 13, 15 and 17). In conclusion, the mutated strain apparently favors media formulations with higher concentrations of cheese whey, lower concentrations of glycerol and average concentrations of corn steep liquor (24 – 37 g/L).

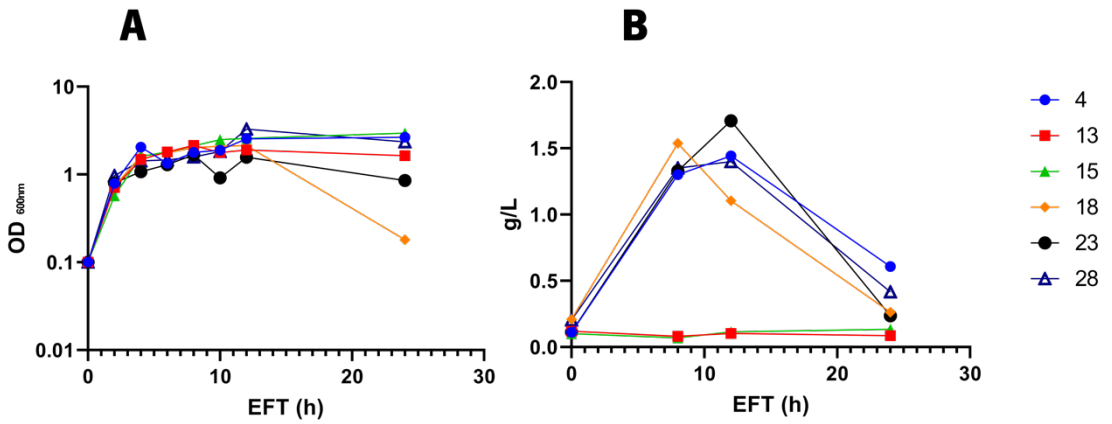

Figure 4.28 – Linear representation of mutant *E. coli* BL21(DE3) P.S. 5, A) DO and B) acetic acid variation along the EFT. A few examples were chosen based on better cell growth as: 4 ( ) 6 g/L glycerol, 60 g/L CSL and 12.8 CW; 13 ( ) 3 g/L glycerol, 15 g/L CSL and 6.4 CW; 15 ( ) 3 g/L glycerol, 15 g/L CSL and 19.2 CW; 18 ( ) 6 g/L glycerol, 30 g/L CSL and 12.8 CW; 23( ) 9 g/L glycerol, 45 g/L CSL and 6.4 CW and 28( ) 3 g/L glycerol, 45 g/L CSL and 19.2 CW.

4.3.2.2. Analysis of SELP-59-A production levels

Following the same procedure as described above for the non-mutated sample, the quantification of SELP-59-A produced by mutant P.S.5 after 12 h and 24 h of EFT was carried out by densitometry analysis of SDS-PAGE gels (appendix J), and by weighting pure lyophilized SELP-59-A after 24 h of EFT.

The 3D contour plots relating SELP-59-A production with the CCD experimental design after 12 h and 24 h of EFT are depicted in figure 4.29 and 4.30, respectively. SDS-PAGE analysis indicates that the highest expression levels are observed after 12 h of EFT (appendix J), showing a decline of SELP-59-A production after 24 of EFT. This is also observed by comparing the 3D representation

graphs of densitometry analysis after 12 h (figure 4.29) and 24 h of EFT (figure 4.30 A1-3). After 12 h, densitometry indicates estimated volumetric productivities near 250 mg/L for the best condition (figure 4.29 1) whereas, values near 100 mg/L are observed in the same condition after 24 h of EFT (figure 4.30 A-1). These values are in general higher than those obtained for the non-mutant strain, in which, the highest volumetric productivity was around 200 mg/L after 12 h of EFT (figure 4.22 1).

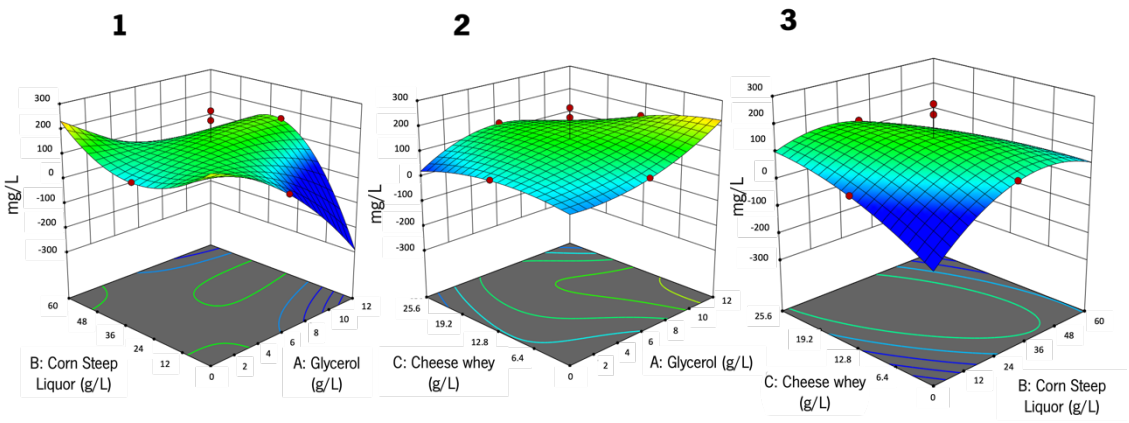

Figure 4.29 – 3D contour plots representing the amount of SELP-59-A produced by mutant P.S.5 after 12 h of EFT. Protein quantification was determined by densitometry analysis of SDS-PAGE gels. In dark red (●) are the points above the surface and in light red (●), the points below the surface.

As mentioned earlier, despite the utility of densitometry for comparison purposes, determination of the weight for pure lyophilized SELP-59-A is more reliable and accurate than comparing band intensity in SDS-PAGE gels. The volumetric productivities of pure recombinant protein after 24 h of EFT are represented in figure 4.30 B1-3. The highest volumetric productivities were found for the conditions with high amounts of CSL and glycerol while maintaining the concentration of CW constant (figure 4.30 B-1). Overall, comparing the volumetric productivities between the non-mutated BL21 and mutant P.S.5, it is possible to observe a considerable improvement of protein production for the mutated variant. The non-mutated strain resulted in volumetric productivities around 120 mg/L whereas, the P.S.5 allowed reaching values around 150 mg/L.

In comparison to the original strain, the expression of recombinant protein was much higher in the new mutant strain with an increase from 117 mg/L (condition 22) to 293 mg/L (condition 18).

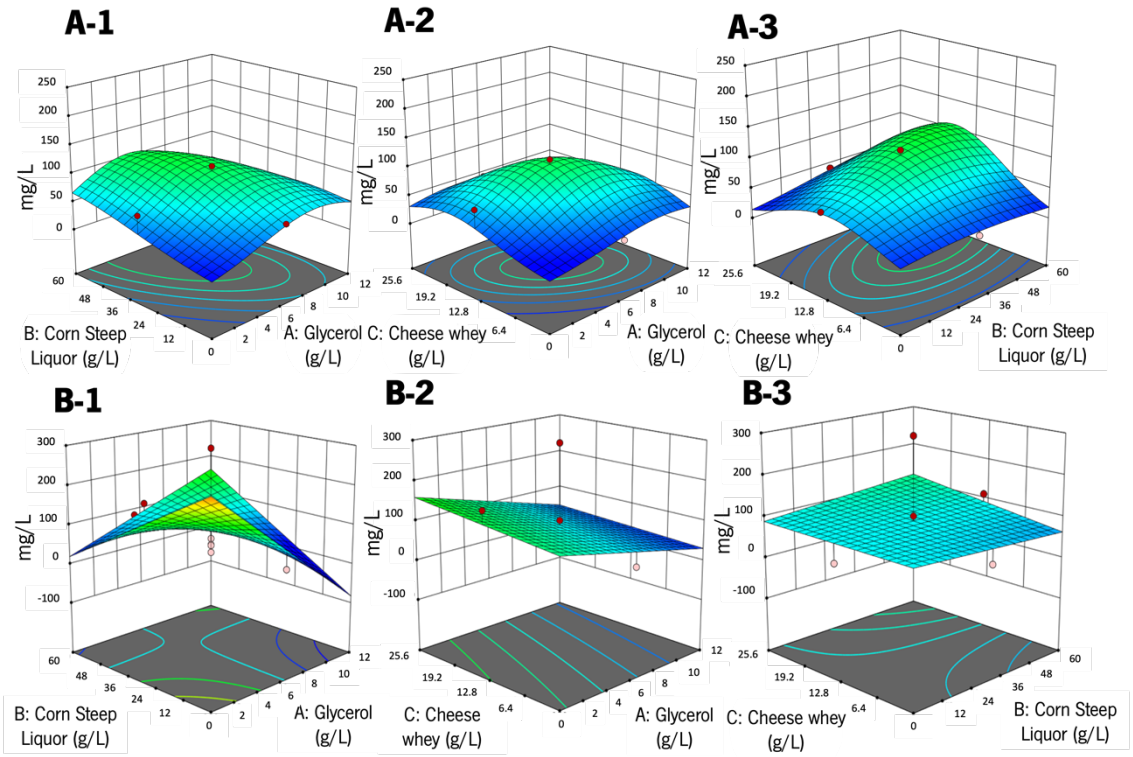

Figure 4.30 – 3D contour plots representing the amount of SELP-59-A produced by mutant P.S.5 after 24 h of EFT. Protein quantification was evaluated by A) densitometry or by B) weighing pure lyophilized protein. In dark red (●) are the points above the surface and in light red (●), the points below the surface.

4.3.2.3. Optimization of media conditions

The optimal concentration point for each of the media ingredients – CSL, glycerol and CW –, after 12 h and 24 h of EFT, was optimized by RSM using the constraint points defined in appendix M. After CCD analysis, 31 possible solutions were found after 12 h of EFT and 17 possible solutions after 24 h of EFT (appendix N). Figure 4.31 represents the optimal points for 12 h and 24 h of EFT, based on the parameter desirability (0.76 and 0.63 for 12 h and 24 h, respectively). Following CCD analysis, the best medium formulation for 12 h of EFT comprises 3.79 g/L of glycerol, 22.39 g/L of corn steep liquor and 19.2 g/L of cheese whey, with a predicted volumetric productivity for SELP-59-A of 148.10 mg/L (estimated by densitometry) and a corresponding OD_{600nm} of 2.99 (appendix N, table 7.8). According to the CCD model, the best medium formulation for 24 h of EFT consists of 1.14 g/L of glycerol, 22.27 g/L of corn steep liquor and 19.74 g/L of cheese whey, with a predicted SELP-59-A production of 163.93 mg/L (determined by weight measurement) and a corresponding OD_{600nm} of 3.56.

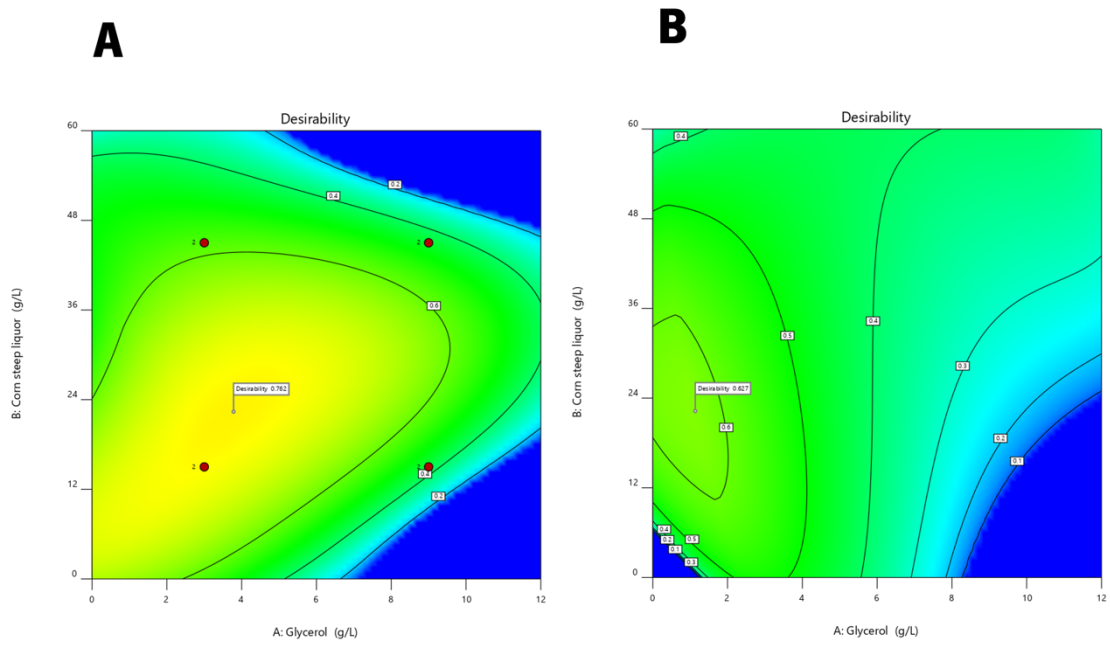

Figure 4.31 – 2D contour plot for the best optimal point based on desirability. The factor cheese whey is fixed at A) 19.2 g/L and B) 19.74 g/L. The optimization occurred at A) 12 h and B) 24 h. The dark red dots (●) represent design points above the surface. The white box showing the desirability (0.740 and 0.591 for 12 h and 24 h of EFT, respectively) indicates the best formulation. According to the model, the best formulations were determined as 3.79 g/L of glycerol, 22.39 g/L of corn steep liquor and 19.2 g/L of cheese whey after 12 h, and 1.14 g/L of glycerol, 22.27 g/L of corn steep liquor and 19.74 g/L of cheese whey after 24 h of EFT.

4.4. Considerations on the cost-efficiency of the fermentation bioprocesses

Comparing the results obtained with the non-mutated BL21 with mutant P.S.5, the profiles of production, cell growth and media requirements are distinctive. Due to a better cell growth and higher protein expression, the mutant P.S.5 demonstrated to be more efficient for the production of SELP-59-A. Moreover, the utilization of industrial by-products/residues as media ingredients results in a decrease of the overall costs associated with fermentation, thus improving the cost-efficiency of SELP-59-A production. For instance, considering similar volumetric productivities, the price of a representative pre-formulated commercial TB medium accounts for 5.29 €/L, whereas the price is reduced to 2.73 €/L with in-house/homemade formulations (figure 4.32). This greatly contrasts with the cost of media using industrial residues/by-products. Here, the optimized media formulations for the non-mutated *E. coli* were extrapolated with a value of approximately 0.056 €/L and 0.044 €/L for 12 h and 24 h of EFT, respectively (figure 4.32). By employing a proton-suicide approach, the costs were reduced even more, with an estimated value around 0.022 - 0.011 €/L for mutant P.S.5 (figure 4.32). Overall, the use of fermentation medium with a combination of by-

products is much cheaper than commercial media, and could have a meaningful impact in reducing the costs associated with fermentation, with the additional advantage of contributing to a circular economy.

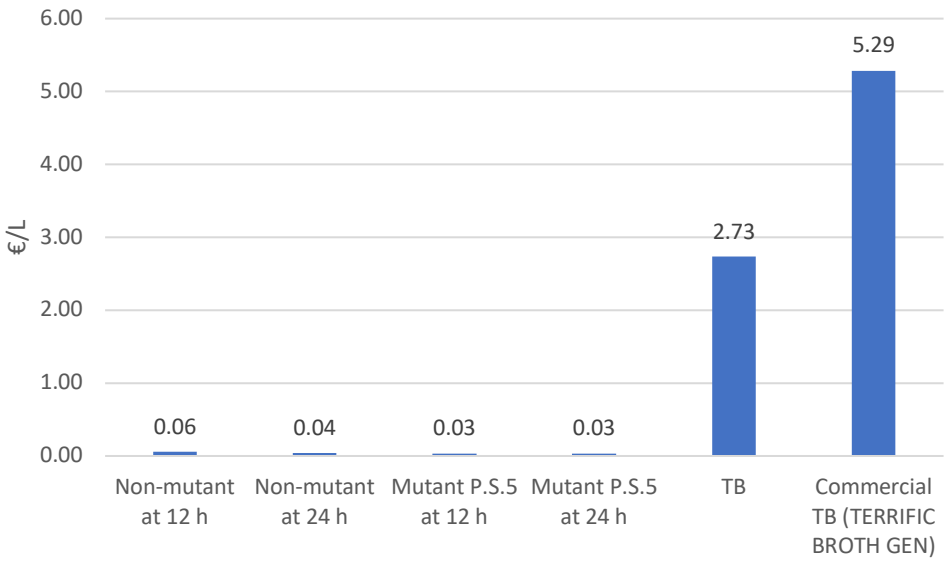

Figure 4.32 – Average cost of fermentation broths using media formulations optimized by CCD for the non-mutated *E. coli* BL21(DE3) and the mutated variant PS.5, versus the costs of homemade and commercial TB (TERRIFIC BROTH GEN).

5. Conclusion

The research and development of recombinant protein polymers (rPPs) have gained a tremendous momentum in recent years, driven by the need to develop novel bio-based, sustainable and biocompatible "green" materials. Silk-elastin-like proteins are an example of such innovation-driven advances, gathering in the same polypeptide chain the remarkable properties of silk fibroin and elastin, paving the way for a new set of applications. Until now, SELPs have been mainly produced at a laboratory scale, with complex media formulations and commercial ingredients; but in order to scale up to industrial and economically viable levels, it is necessary to improve the efficiency of the bioprocesses by lowering the costs of protein synthesis. As a result, agro-industrial residues/by-products such as glycerol, cheese whey, and corn steep liquor, classified as waste pollutants, can be used as source materials in the fermentative processes to reduce costs. In fact, the selection of industrial by-products/residues as media ingredients is an idea of reciprocal value: not only

contributes to the economic sustainability of the bioprocess but is also embedded in the circular economy framework.

In this study, we followed an integrative approach to reduce costs associated with the fermentation bioprocesses by employing two approaches while using SELP-59-A as model protein: enhance recombinant protein expression by inducing a mutagenic pressure on *E. coli* and, optimize media formulation by introducing low-cost ingredients for induction and growth.

To improve protein production, the expression host strain (*E. coli*) was subjected to mutagenic pressure via direct selection using a proton-suicide approach. The results revealed that the novel *E. coli* mutant was able to overexpress SELP at higher levels than the original strain. This demonstrates the potential of the method for the ultra-high expression of SELPs, which also find application for other recombinant proteins. Nevertheless, we do believe that a greater number of cycles with bromide/bromate may boost protein production even further, representing an opportunity to develop highly efficient microbial cell factories. To the best of our knowledge, this work represents the first time that proton-suicide is used to improve the production of rPPs.

With the aim to reduce the costs associated with fermentation media, we also evaluated the potential of using cheese whey (CW) permeate as inducer. This by-product from the dairy industry demonstrated to be a good replacement for lactose or IPTG, stimulating growth and recombinant protein production because of its higher nutritional composition, comprising lactose, soluble proteins, lipids, and mineral salts. In this dissertation, we demonstrated that CW may be successfully employed as inducer for the production of recombinant proteins based on the Lac promoter, hence minimizing pollution discharges to the environment. In addition, we also evaluated the feasibility of using glycerol and corn steep liquor (CSL) as cost-efficient media ingredients. Production of SELP-59-A in medium containing glycerol (5 g/L), CSL (60 g/L) and a small amount of yeast extract (0.12 g/L) demonstrated to yield volumetric productivities higher than those obtained with conventional TB and even with commercial TBAIM.

Optimization of media formulation was achieved by employing a factorial experimental design and an empirical model building approach by central composite design (CCD), to find the optimal concentrations for glycerol, CW and CSL. We found that high CW and CSL concentrations appear to promote a rapid cell proliferation and protein production, with similar results for both original and mutated variant of *E. coli*. According to the CCD, the best operational conditions are 12 h of EFT (corresponding to 4 h of induction) with 3.79 g/L of glycerol, 22.39 g/L of corn steep liquor

and 19.2 g/L of cheese whey, with a predicted volumetric productivity of 148.10 mg/L of SELP-59-A. Overall, the optimization studies conducted in this dissertation have a high impact in the development of cost-efficient fermentation bioprocesses by lowering the total fermentation to 12 h, and reducing the costs of the fermentation broth by near 45 to 90-fold, compared with conventional homemade TB (more than 170-fold if compared with a representative commercial formulation).

A limitation of the present study is the absence of a validation of the proposed optimal media formulations and the use of densitometry analysis to assess protein production yields after 12 h of EFT. This should be assessed in the future. Also, future experiments could extend the results from a laboratorial to a pilot or industrial scale. It would be interesting to see if the optimal point obtained from the CCD is adaptable to a scale-up process. As already mentioned, additional future work could also comprise testing the effect of more cycles of bromide/bromate on the cell would be of value, since it could boost the cells capabilities. Finally, additional studies focused on metabolomic and genomic analyses of the obtained mutant would be of interest, as these would provide insights of the effect of the protein-suicide method in the cell genome, transcriptome or metabolome.

6. References

Abad, S., Pérez, X., Planas, A., & Turon, X. (2014). Rapid monitoring of glycerol in fermentation growth media: Facilitating crude glycerol bioprocess development. Talanta, 121, 210-214.

Abbad-Andaloussi S, Manginot-Durr C, Amine J, Petitdemange E, Petitdemange H. (1995). Isolation and Characterization of *Clostridium butyricum* DSM 5431 Mutants with Increased Resistance to 1,3-Propanediol and Altered Production of Acids. Appl Environ Microbiol., 61(12):4413-7.

Ahmad, M. S., Ab Rahim, M. H., Alqahtani, T. M., Witoon, T., Lim, J.-W., & Cheng, C. K. (2021). A review on advances in green treatment of glycerol waste with a focus on electro-oxidation pathway. Chemosphere, 276, 130128.

Ait-Amir, Bouzid (2015). Embedded Mechatronic Systems 2.Meta-Model Development,151–179.

Akash, M. S. H., Rehman, K. And Chen S. (2015). Natural and Synthetic Polymers as Drug Carriers for Delivery of Therapeutic Proteins. Polymer Reviews, 55 371–406.

Alakomi, H. L., Skytta, E., Saarela, M., Mattila-Sandholm, T., Latva-Kala, K., & Helander, I. M. (2000). Lactic acid permeabilizes Gram-negative bacteria by disrupting the outer membrane. Applied and environmental microbiology, 66(5), 2001-2005.

Alexandri, M., Schneider, R., & Venus, J. (2018). Membrane Technologies for Lactic Acid Separation from Fermentation Broths Derived from Renewable Resources. Membranes, 8(4), 94.

Álvarez-Cao, M. E., Rico-Díaz, A., Cerdán, M. E., Becerra, M., & González-Siso, M. I. (2018). Valuation of agro-industrial wastes as substrates for heterologous production of α-*galactosidase*. Microbial Cell Factories, 17(1), 137.

Arlyapov, V.A., Kharkova, A.S., Kurbanaliyeva, S.K., Kuznetsova, L.S., Machulin, A.V., Tarasov, S.E., Melnikov, P.V., Ponamoreva, O.N., Alferov, V.A., Reshetilov, A.N. (2021). Use of biocompatible redox-active polymers based on carbon nanotubes and modified organic matrices for development of a highly sensitive BOD biosensor. Enzyme and Microbial Technology, 143, 109706

Ashby, Richard D., Solaiman, Daniel K. Y., Foglia, Thomas A. (2005). Synthesis of Short-/Medium-Chain-Length Poly(hydroxyalkanoate) Blends by Mixed Culture Fermentation of Glycerol.

Biomacromolecules, 6(4), 2106–2112.

Azizi-Shotorkhoft, A., Sharifi, A., Mirmohammadi, D., Baluch-Gharaei, H., Rezaei, J. (2016). Effects of feeding different levels of corn steep liquor on the performance of fattening lambs. Journal of Animal Physiology and Animal Nutrition, 100(1), 109–117.

Bacha, U., & Nasir, M. (2011). Comparative assessment of various agro-industrial wastes for *Saccharomyces cerevisiae* biomass production and its quality evaluation as single cell protein. The Journal of Animal & Plant Sciences, 21(4), 844-849.

Bakeland, L. (1909). The synthesis, constitution, and uses of Bakelite. The journal of industrial and engineering chemistry, (1) 150-161.

Balbas, P., & Lorence, A. (2004). Recombinant Gene Expression. Humana Press, 15-49.

Barroca, M., Rodrigues, P., Sobral, R., Costa, M. M. R., Chaves, S. R., Machado, R., Collins, T. (2016). Antibiotic free selection for the high-level biosynthesis of a silk-elastin-like protein. Scientific Reports, 6 (1), 39329.

Basavarajaiah, D. M., & Murthy, B. N. (2020). Design of Experiments and Advanced Statistical Techniques in Clinical Research. Springer.

Berg, P. (1971). The Viral Genome in Transformed Cells. Proceedings of the Royal Society B: Biological Sciences, 177(1046), 65–76.

Bonnet, M., Lagier, J. C., Raoult, D., & Khelaifia, S. (2019). Bacterial culture through selective and non-selective conditions: the evolution of culture media in clinical microbiology. New Microbes and New Infections, 34, 100622.

Boze, H., Moulin, G. and Galzy, P. (1995). Production of Microbial Biomass. Biotechnology Second, Completely Revised Edition, pp 168- 220.

Brar, S., Das, R. & Sarma, S. (2019). Microbial Sensing in Fermentation. John Wiley & Sons, 334.

Bren, A., Park, O., Towbin, D., Dekel, E., Rabinowitz, D., & Alon, U. (2016). Glucose becomes one of the worst carbon sources for *E. coli* on poor nitrogen sources due to suboptimal levels of cAMP. Scientific Reports, 6(1), 24834.

Burcin Y., Laura C., David L. (2019). Extended release formulations using silk proteins for controlled delivery of therapeutics. Expert Opinion on Drug Delivery 16 (7), 741-756.

Cappello, J., Crissman, J., Crissman, M., Ferrari, F., Textor, G., Wallis, O., Stedronsky, E. (1998). *In-situ* self-assembling protein polymer gel systems for administration, delivery, and release of drugs. Journal of Controlled Release, 53 (1-3) 105-117.

Carvalho, F., Prazeres, A. R., & Rivas, J. (2013). Cheese whey wastewater: Characterization and treatment. Science of the total environment, 445, 385-396.

Casal, M., Cunha, A. M., & Machado, R. (2013). Future Trends for Recombinant Protein-Based Polymers: The Case Study of Development and Application of Silk-Elastin-Like Polymers. Bio-Based Plastics, 311–329.

Cavero-Olguin, V. H., Rahimpour, F., Dishisha, T., Alvarez-Aliaga, M. T., & Hatti-Kaul, R. (2021). Propionic acid production from glycerol in immobilized cell bioreactor using an acid-tolerant strain of *Propionibacterium acidipropionici* obtained by adaptive evolution. Process Biochemistry, 110, 223–230.

Cereghino, G. P. L., Cereghino, J. L., Ilgen, C., & Cregg, J. M. (2002). Production of recombinant proteins in fermenter cultures of the yeast *Pichia pastoris*. Current opinion in biotechnology, 13(4), 329-332.

Chambre, L. Martã-Moldes, Z., Parker, R. N.; Kaplan, D. L. (2020). Bioengineered elastin- and silk-biomaterials for drug and gene delivery. Advanced Drug Delivery Reviews, Volume 160, 186-198.

Chen, L., Zhou, L., Qian, G., Kaplan, D., & Xia, X. (2017). Fabrication of Protein Films from Genetically Engineered Silk-Elastin-Like Proteins by Controlled Cross-Linking. ACS Biomaterials Science & Engineering, 3(3), 335–341.

Cheng, H., Chen, L., McClements, D. J., Yang, T., Zhang, Z., Ren, F., Jin, Z. (2021). Starch-based biodegradable packaging materials: A review of their preparation, characterization and diverse applications in the food industry. Trends in Food Science & Technology, 114, 70–82.

Chouhan, Dimple; Mandal, Biman B. (2019). Silk Biomaterials in Wound Healing and Skin Regeneration Therapeutics: from Bench to Bedside. Acta Biomaterialia, 103, 24-51.

Ciani, M., Comitini, F., & Mannazzu, I. (2008). Fermentation. Encyclopedia of Ecology, Five-Volume Set, 1548–1557.

Clark, D. P. (1989). The fermentation pathways of *Escherichia coli*. FEMS Microbiology Letters,

63(3), 223–234.

Cohen, S. N., Chang, A. C. Y., Boyer, H. W., & Helling, R. B. (1973). Construction of biologically functional bacterial plasmids in vitro. Proceedings of the National Academy of Sciences USA, 70(11), 3240–3244.

Collins, T., Barroca, M., Branca, F., Padrão, J., Machado, R., & Casal, M. (2014). High Level Biosynthesis of a Silk-Elastin-like Protein in *E. coli*. Biomacromolecules, 15(7), 2701–2708.

Collins, T., Silva, J. A., Costa, A. da, Branca, F., Machado, R., & Casal, M. (2013). Batch production of a silk-elastin-like protein in *E. coli* BL21(DE3): key parameters for optimisation. Microbial Cell Factories, 12 (1), 21.

Commission, E. (2021). EU averages of main dairy commodities. Milk Market Observatory, 2017, 1–7.

Correia, D. M., Ribeiro, S., da Costa, A., Ribeiro, C., Casal, M., Lanceros-Mendez, S., & Machado, R. (2019). Development of bio-hybrid piezoresistive nanocomposites using silk-elastin protein copolymers. Composites Science and Technology, 172, 134–142.

Costa, Ohana Y. A., Oguejiofor, Chidinma; Zahlke, Daniela; Barreto, Cristine C., Wansche, Christine; Riedel, Katharina; Kuramae, Eiko E. (2020). Impact of Different Trace Elements on the Growth and Proteome of Two Strains of Granulicella, Class “Acidobacteriia”. Frontiers in Microbiology, 11, 1227.

Crowley, Erika L., Rafferty, Steven P. (2019). Review of lactose-driven auto-induction expression of isotope-labelled proteins. Protein Expression and Purification, S1046592819300257

da Costa, A., Machado, R., Ribeiro, A., Collins, T., Thiagarajan, V., Neves-Petersen, M. T., Carlos Rodriguez-Cabello, J., Gomes, A. C., & Casal, M. (2015). Development of Elastin-Like Recombinamer Films with Antimicrobial Activity. Biomacromolecules, 16 (2), 625–635.

Dias Junior, E. M., Dias, D. dos R. C., Rodrigues, A. P. D., Dias, C. G. B. T., Bastos, G. de N. T., Oliveira, J. A. R. de, Passos, M. F. (2021). SIPNs polymeric scaffold for use in cartilaginous tissue engineering: physical-chemical evaluation and biological behavior. Materials Today Communications, 26, 102111.

Diaz, A. B., Blandino, A., & Caro, I. (2018). Value added products from fermentation of sugars derived from agro-food residues. Trends in Food Science & Technology, 71, 52-74.

Djoudi, W., Aissani-Benissad, F., & Bourouina-Bacha, S. (2007). Optimization of copper cementation process by iron using central composite design experiments. Chemical Engineering Journal, 133(1-3), 1-6.

Dubey C. (2014). Advanced Biotechnology. R C Dubey, 1161.

Ducheyne, P., Healy, K., Hutmacher, D. W., Grainger, D. W., Kirkpatrickpp. C. J., (2015). Comprehensive Biomaterials, Volume 1, 300-349.

Eckerle, G. J., Pacheco, L. A., Olson, K. C., & Jaeger, J. R. (2012). Effects of corn steep liquor supplementation on voluntary selection of tallgrass prairie hay contaminated with *sericea lespedeza* and uncontaminated tallgrass prairie hay. Kansas Agricultural Experiment Station Research Reports, 1, 58–61.

Eckert, A. & Trinh T. (2016). Biotechnology for Biofuel Production and Optimization. Elsevier, 572.

Elnashar, M. (2010). Biopolymers. Sciyo, 1° Edition, 13-219.

Enjalbert, B., Millard, P., Dinclaux, M., Portais, J-C. Létisse, F. (2017). Acetate fluxes in *Escherichia coli* are determined by the thermodynamic control of the *Pta-AckA* pathway. Scientific Reports, 7, 42135

Enzymatic, (2022). Consulted October 31, (2022). Available in http://www.enzymatic.pt/index.html

Estevez, Enrique G. (1984). Bacteriologic Plate Media: Review of Mechanisms of Action. Laboratory Medicine, 15(4), 258–262.

Fahnestock SR, Bedzyk LA. (1997). Production of synthetic spider dragline silk protein in *Pichia pastoris*. Appl Microbiol Biotechnol.,47(1).

Fernandes, M. M., Correia, D. M., da Costa, A., Ribeiro, S., Casal, M., Lanceros-Méndez, S., & Machado, R. (2018). Multifunctional magnetically responsive biocomposites based on genetically engineered silk-elastin-like protein. Composites Part B: Engineering, 153 (15), 413-419.

Förster, A. H., & Gescher, J. (2014). Metabolic engineering of *Escherichia coli* for production of mixed-acid fermentation end products. Frontiers in Bioengineering and Biotechnology,

2(MAY), 1–12.

Frandsen, J. L. and Ghandehari, H. (2012). Recombinant protein-based polymers for advanced drug delivery. Chem. Soc. Rev. 41 (7), 2696-2706.

Fu, X. Dong-Zhi Wei; Wang-Yu Tong (2006). Effect of yeast extract on the expression of thioredoxin–human parathyroid hormone from recombinant *Escherichia coli*., 81(12), 1866–1871.

Georgilis, E., Abdelghani, M., Pille, J., Aydinlioglu, E., Hest, J., Lecommandoux, S., & Garanger, E. (2020). Nanoparticles based on natural, engineered or synthetic proteins and polypeptides for drug delivery applications. International Journal of Pharmaceutics, 11 (9), 119537.

Gerba, Charles P. (2015). Environmental Microbiology. Disinfection, 645–662.

Ghasemi, K., Emadi, S. M., & Ghasemi, Y. (2018). Effect of different culture media on *broccoli* (*Brassica oleracea var. italica*) yield components and mineral elements concentration in soilless culture. Journal of Horticulture Science, 31(4).

Gnanasekaran, D. (2019). Green Biopolymers and their Nanocomposites. Materials Horizons: From Nature to Nanomaterials, 1st Edition, 1-29.

Godard, P., Urrestarazu, A., Vissers, S., Kontos, K., Bontempi, G., van Helden, J., & Andre, B. (2007). Effect of 21 Different Nitrogen Sources on Global Gene Expression in the Yeast *Saccharomyces cerevisiae*. Molecular and Cellular Biology, 27 (8), 3065–3086.

Gombert, A. K., & Kilikian, B. V. (1998). Recombinant gene expression in *Escherichia coli* cultivation using lactose as inducer. Journal of biotechnology, 60(1-2), 47-54.

Gonzalez-Obeso, C., Rodriguez-Cabello, J. C., & Kaplan, D. L. (2021). Fast and reversible crosslinking of a silk elastin-like polymer. Acta biomaterialia. in press.

Greish, K, Araki, K, Li, D, O'Malley, BW, Jr, Dandu, R, Frandsen, J, Cappello, J & Ghandehari, H (2009). Silk-Elastin-like Protein Polymer Hydrogels for Localized Adenoviral Gene Therapy of Head and Neck Tumours. Biomacromolecules, 10 (8), 2183–2188.

Guimarães, P. M., Teixeira, J. A., & Domingues, L. (2010). Fermentation of lactose to bio-ethanol by yeasts as part of integrated solutions for the valorisation of cheese whey. Biotechnology advances, 28(3), 375-384.

Gustafson, J. A., & Ghandehari, H. (2010). Silk-elastinlike protein polymers for matrix-mediated cancer gene therapy. Advanced drug delivery reviews, 62(15), 1509-1523.

Haider, Mohamed; Leung, Vivian; Ferrari, Franco; Crissman, John; Powell, James; Cappello, Joseph; Ghandehari, Hamidreza (2005). Molecular Engineering of Silk-Elastinlike Polymers for Matrix-Mediated Gene Delivery: Biosynthesis and Characterization. Molecular Pharmaceutics, 2(2), 139–150.

Han, K., Lim, H. C., & Hong, J. (1992). Acetic acid formation in *Escherichia coli* fermentation. Biotechnology and bioengineering, 39(6), 663-671

Haugaard, N. (1959). D-and L-Lactic acid oxidase of *Escherichia coli.* Biochimica *et Biophysica* Acta, 31(1), 66-72.

Herendeen, S.L., Vanbogelen, R.A., And Neidhardt, F. C. (1978). Levels of major proteins of *Escherichia coli* during growth at different temperatures. Journal of bacteriology, 139 (1), 185-194.

Herzog, R., Singh, N., Urry, D. *et al.*, Expression of a synthetic protein-based polymer (elastomer) gene in *Aspergillus nidulans*. Appl Microbiol Biotechnol 47, 368–372 (1997).

Hofer, Alexandra; Hauer, Stefan; Kroll, Paul; Fricke, Jens; Herwig, Christoph (2018). In-depth characterization of the raw material corn steep liquor and its bioavailability in bioprocesses of *Penicillium chrysogenum*. Process Biochemistry, S1359511318302733

Holms, W. H. (1986). The central metabolic pathways of *Escherichia coli*: relationship between flux and control at a branch point, efficiency of conversion to biomass, and excretion of acetate. Current topics in cellular regulation, 28, 69-105.

Huang, W., Rollett, A. and Kaplan, D. L. (2015). Silk-elastin-like protein biomaterials for the controlled delivery of therapeutics. Expert Opinion on Drug Delivery, 12 (5), 779-791.

Hui Y.H. & Khachatourians, G. (1996). Food Biotechnology: Microorganisms. Food science and technology, John Wiley & Sons, pp 54.

Hull, S. R., Yang, B. Y., Venzke, D., Kulhavy, K., & Montgomery, R. (1996). Composition of corn steep water during steeping. Journal of agricultural and food chemistry, 44(7), 1857-1863.

Itakura, K; Hirose, T; Crea, R; Riggs, A., Heyneker, H., Bolivar, F; Boyer, H. (1977). Expression in *Escherichia coli* of a chemically synthesized gene for the hormone somatostatin. Science, 198(4321), 1056–1063.

Jacyna, J., Kordalewska, M., & Markuszewski, M. J. (2018). Design of Experiments in metabolomics-related studies: An overview. Journal of Pharmaceutical and Biomedical Analysis, 164, 598-606.

Jana, Maiti, S., Jana, S. (2017). Biopolymer-Based Composites: Drug Delivery and Biomedical Applications. Woodhead Publishing, 1st Edition.

Jenkins, R. and Maddocks S. (2019). Bacteriology Methods for the Study of Infectious Diseases. Academic Press, 1° edition, 20-29.

Jensen, M. M., Jia, W., Isaacson, K. J., Schults, A., Cappello, J., Prestwich, G. D., Ghandehari, H. (2017). Silk-elastin-like protein polymers enhance the efficacy of a therapeutic glycosaminoglycan for prophylactic treatment of radiation-induced proctitis. Journal of Controlled Release, 263, 46–56.

Jian, J., Zhang, S. Q., Shi, Z. Y., Wang, W., Chen, G. Q., & Wu, Q. (2010). Production of polyhydroxyalkanoates by *Escherichia coli* mutants with defected mixed acid fermentation pathways. Applied microbiology and biotechnology, 87(6), 2247-2256.

Jung, H. R., Yang, S. Y., Moon, Y. M., Choi, T. R., Song, H. S., Bhatia, S. K., ... & Yang, Y. H. (2019). Construction of efficient platform *Escherichia coli* strains for polyhydroxyalkanoate production by engineering branched pathway. Polymers, 11(3), 509.

Jurtshuk P Jr. (1996). Bacterial Metabolism. Medical Microbiology. 4th edition. Galveston (TX): University of Texas Medical Branch at Galveston.

Karigidi, K. O., & Olaiya, C. O. (2019). Antidiabetic activity of corn steep liquor extract of *Curculigo pilosa* and its solvent fractions in streptozotocin-induced diabetic rats. Journal of Traditional and Complementary Medicine, in Press.

Kaur, J., Sarma, A. K., Jha, M. K., & Gera, P. (2020). Valorisation of crude glycerol to value-added products: Perspectives of process technology, economics and environmental issues. Biotechnology Reports, 27, e00487.

Kavetskyy, T., Smutok, O., Demkiv, O., Kasetaite, S., Ostrauskaite, J., Švajdlenková, H., ... & Gonchar, M. (2019). Dependence of operational parameters of laccase-based biosensors on structure of photocross-linked polymers as holding matrixes. European Polymer Journal, 115, 391-398.

Khalaf N. (2016). Green Polymers and Environmental Pollution Control. CRC Press, 1st edition, 436.

Khani, M. H., & Bagheri, M. (2020). Skimmed milk as an alternative for IPTG in induction of recombinant protein expression. Protein Expression and Purification, 170, 105593.

Kim, S., Lee, D., Lim, D., Lim, S., Park, S., Kang, C., Lee, T. (2020). Paramylon production from heterotrophic cultivation of *Euglena gracilis* in two different industrial by-products: Corn steep liquor and brewer's spent grain. Algal Research, 47, 101826.

Kim, T. S., Jung, H. M., Kim, S. Y., Zhang, L., Li, J., Sigdel, S., ... & Lee, J. K. (2015). Reduction of acetate and lactate contributed to enhancement of a recombinant protein production in *E. coli* BL21. Journal of Microbiology and Biotechnology, 25(7), 1093-1100.

Kinikoglu, B., Rodríguez-Cabello, J. C., Damour, O., & Hasirci, V. (2011). The influence of elastin-like recombinant polymer on the self-renewing potential of a 3D tissue equivalent derived from human lamina propria fibroblasts and oral epithelial cells. Biomaterials, 32(25), 5756-5764.

Kleman, G. L., & Strohl, W. R. (1994). Acetate metabolism by *Escherichia coli* in high-cell-density fermentation. Applied and environmental microbiology, 60(11), 3952-3958.

Kopp J, Slouka C, Ulonska S, Kager J, Fricke J, Spadiut O, Herwig C. (2018). Impact of Glycerol as Carbon Source onto Specific Sugar and Inducer Uptake Rates and Inclusion Body Productivity in *E. coli* BL21(DE3). Bioengineering.; 5(1):1.

Kotik, M., Kočanová M., Marešová, H., Kysĺík P., (2004). High-level expression of a fungal pyranose oxidase in high cell-density fed-batch cultivations of *Escherichia coli* using lactose as inducer, 36(1), 0–69.

Kumar, L. R., Yellapu, S. K., Tyagi, R. D., & Zhang, X. (2019). A review on variation in crude glycerol composition, bio-valorization of crude and purified glycerol as carbon source for lipid production. Bioresource Technology, 293, 122155.

Kundu, K., Afshar, A., Katti, D. R., Edirisinghe, M., & Katti, K. S. (2021). Composite nanoclay-hydroxyapatite-polymer fiber scaffolds for bone tissue engineering manufactured using pressurized gyration. Composites Science and Technology, 202, 108598.

Lee, S. Y. (1996). High cell-density culture of *Escherichia coli*. Trends in biotechnology, 14(3), 98-

105.

Lee, X. J., Hiew, B. Y. Z., Lai, K. C., Tee, W. T., Thangalazhy-Gopakumar, S., Gan, S., & Lee, L. Y. (2021). Applicability of a novel and highly effective adsorbent derived from industrial palm oil mill sludge for copper sequestration: Central composite design optimisation and adsorption performance evaluation. Journal of Environmental Chemical Engineering, 9(5), 105968.

Leong, Y. K., Show, P. L., Ooi, C. W., Ling, T. C., & Lan, J. C.W. (2014). Current trends in polyhydroxyalkanoates (PHAs) biosynthesis: Insights from the recombinant *Escherichia coli*. Journal of Biotechnology, 180, 52–65.

Li, S. H. J., Li, Z., Park, J. O., King, C. G., Rabinowitz, J. D., Wingreen, N. S., & Gitai, Z. (2018). *Escherichia coli* translation strategies differ across carbon, nitrogen and phosphorus limitation conditions. Nature microbiology, 3(8), 939-947.

Li, X., Xu, W., Yang, J., Zhao, H., Xin, H., & Zhang, Y. (2016). Effect of different levels of corn steep liquor addition on fermentation characteristics and aerobic stability of fresh rice straw silage. Animal Nutrition, 2(4), 345-350.

Liggett, R. W., & Koffler, H. (1948). Corn steep liquor in microbiology. Bacteriological reviews, 12(4), 297-311.

Liu, S. (2020). Bioprocess engineering: kinetics, sustainability, and reactor design. Elsevier.

Loy, D. D., & Lundy, E. L. (2019). Nutritional properties and feeding value of corn and its coproducts. In Corn (pp. 633-659). AACC International Press.

Lu, H. J., Breidt, F., Pérez-Díaz, I. M., & Osborne, J. A. (2011). Antimicrobial Effects of Weak Acids on the Survival of *Escherichia coli* O157:H7 under Anaerobic Conditions. Journal of Food Protection, 74(6), 893–898.

Luo, Xiaolan; Ge, Xumeng; Cui, Shaoqing; Li, Yebo (2016). Value-added processing of crude glycerol into chemicals and polymers. Bioresource Technology,215, 144-154.

Lutz, S. and Bornscheuer U. T. (2012). Protein Engineering Handbook. John Wiley & Sons. Volume 1, 502.

Lyons, R. E., Lesieur, E., Kim, M., Wong, D. C., Huson, M. G., Nairn, K. M., & Elvin, C. M. (2007). Design and facile production of recombinant resilin-like polypeptides: gene construction

and a rapid protein purification method. Protein Engineering, Design & Selection, 20(1), 25-32.

Machado, R., Azevedo-Silva, J., Correia, C., Collins, T., Arias, F. J., Rodrguez-Cabello, J. C., & Casal, M. (2013a). High level expression and facile purification of recombinant silk-elastin-like polymers in auto-induction shake flask cultures. Amb Express, 3 (1), 11.

Machado, R., da Costa, A., Sencadas, V., Garcia-Arévalo, C., Costa, C. M., Padrão, J., Gomes, Lanceros-Mendez, Rodríguez-Cabello, Casal, M. (2013b). Electrospun silk-elastin-like fibre mats for tissue engineering applications. Biomedical Materials, 8 (6), 065009.

Machado, R., da Costa, A., Sencadas, V., Pereira, A. M Collins, T., Rodríguez-Cabello, Lanceros-Mendez, Casal, M. (2015). Exploring the Properties of Genetically Engineered Silk-Elastin-Like Protein Films. Macromolecular bioscience, 15(12), 1698-1709.

Machado, R., Ribeiro, A. J., Padrão, J., Silva, D., Nobre, A., Teixeira, J. A., ... & Casal, M. (2009). Exploiting the sequence of naturally occurring elastin: construction, production and characterization of a recombinant thermoplastic protein-based polymer. In Journal of Nano Research (Vol. 6, pp. 133-145). Trans Tech Publications Ltd.

Made-in-China (2021). Consulted October 28, 2021. Available in https://www.made-in-china.com/showroom/6744ea61201b60f1/product-detailzXFQZxyWAbUr/China-Corn-Steep-Liquor.html

Mahr-Un-Nisa, Khan, M. A., Sarwar, M., Lee, W. S., Lee, H. J., Ki, K. S., Ahn, B. S., & Kim, H. S. (2006). Influence of corn steep liquor on feeding value of urea treated wheat straw in buffaloes fed at restricted diets. Asian-Australasian Journal of Animal Sciences, 19(11), 1610–1616.

Martin, A.M. (2007). Maximising the Value of Marine By-Product. Composting of seafood wastes. Food Science, Technology and Nutrition, 486–515.

Meikle J.L. (1995). American Plastic: A Cultural History. Rutgers University Press, 1° edition.

Miller, I., Crawford, J., & Gianazza, E. (2006). Protein stains for proteomic applications: which, when, why?. Proteomics, 6(20), 5385-5408.

Mitsui, R., Yamada R., (2021). *Saccharomyces cerevisiae* as a microbial cell factory. Microbial Cell Factories Engineering for Production of Biomolecules, 319-333.

Mobayed, F. H., Nunes, J. C., Gennari, A., de Andrade, B. C., Ferreira, M. L. V., Pauli, P., ... & Volken de Souza, C. F. (2021). Effect of by-products from the dairy industry as alternative inducers of recombinant *β-galactosidase* expression. Biotechnology Letters, 43(3), 589-599.

Monteiro, M. R., Kugelmeier, C. L., Pinheiro, R. S., Batalha, M. O., & da Silva César, A. (2018). Glycerol from biodiesel production: Technological paths for sustainability. Renewable and Sustainable Energy Reviews, 88, 109-122.

Mordor intelligence, (2021). Recombinant Protein Market - Growth, Trends, Covid-19 Impact, And Forecasts (2021 - 2026). Consulted October 12, 2022. Available in : https://www.mordorintelligence.com/industry-reports/recombinant-protein-market

Moulton, G. G. (2014). Fed-Batch Fermentation: A Practical Guide to Scalable Recombinant Protein Production in *Escherichia coli*. Elsevier, 63–108.

Nagarsekar, A., Crissman, J., Crissman, M., Ferrari, F., Cappello, J., & Ghandehari, H. (2002). Genetic synthesis and characterization of pH- and temperature-sensitive silk-elastin-like protein block copolymers. Journal of Biomedical Materials, 62(2):195-203.

Nair, R., Salvi, P., Banerjee, S., Raiker, V. A., Bandyopadhyay, S., Soorapaneni, S., ... & Padmanabhan, S. (2009). Yeast extract mediated autoinduction of *lacUV5* promoter: an insight. New biotechnology, 26(6), 282-288.

Ner, Y., Stuart, J. A., Whited, G., & Sotzing, G. A. (2009). Electrospinning nanoribbons of a bioengineered silk-elastin-like protein (SELP) from water. Polymer, 50 (24), 5828–5836.

Neubauer, P., Hofmann, K., Holst, O., Mattiasson, B., & Kruschke, P. (1992). Maximizing the expression of a recombinant gene in *Escherichia coli* by manipulation of induction time using lactose as inducer. Applied microbiology and biotechnology, 36(6), 739-744.

Nielsen, J. (2013). Production of biopharmaceutical proteins by yeast: advances through metabolic engineering. Bioengineered, 4(4), 207-211.

Novagen, (2006). (EMD Biosciences) pET System Manual. 11. Novagen (EMD Biosciences), Gibbstown, NJ.

Numata, K. (2020). How to define and study structural proteins as biopolymer materials. Polym J 52, 1043–1056.

Othman, A. M., Mahmoud, M., Abdelraof, M., Karim, G. S. A., & Elsayed, A. M. (2021). Enhancement of laccase production from a newly isolated *Trichoderma harzianum* S7113 using submerged fermentation: Optimization of production medium via central composite design and its application for hydroquinone degradation. International Journal of Biological Macromolecules, 192, 219-231.

Padinjakkara, A., Thankappan, A., Souza, Jr., F., Thomas, S. (2019). Biopolymers and Biomaterials. New York: Apple Academic Press, 370.

Pais, J., Farinha, I., Freitas, F., Serafim, L. S., Martínez, V., Martínez, J. C., Arévalo-Rodríguez, M., Auxiliadora Prieto, M., & Reis, M. A. M. (2014). Improvement on the yield of polyhydroxyalkanotes production from cheese whey by a recombinant *Escherichia coli* strain using the proton suicide methodology. Enzyme and Microbial Technology, 55, 151–158.

Panesar, R., Kaur, S., & Panesar, P. S. (2015). Production of microbial pigments utilizing agro-industrial waste: a review. Current Opinion in Food Science, 1, 70–76.

Parker, Wu, McKay, Xu, Kaplan, (2019). Design of Silk-Elastin-Like Protein Nanoparticle Systems with Mucoadhesive Properties. Journal of Functional Biomaterials, 10(4), 49.

Pereira, A.M., Machado, R., da Costa, A., Ribeiro, A., Collins, T., Gomes, A.C., Leonor, B. Kaplan, D.L., Reis, R.L., Casal, M. (2016). Silk-based biomaterials functionalized with fibronectin type II promotes cell adhesion. Acta Biomaterialia, (47), 50-59.

Pereira, A.M.; Gomes, D.; da Costa, A.; Dias, S.C.; Casal, M.; Machado, R., (2021). Protein-Engineered Polymers Functionalized with Antimicrobial Peptides for the Development of Active Surfaces. Appl. Sci., 11, 5352.

Pham, Phuc V. (2018). Omics Technologies and Bio-Engineering. Medical Biotechnology, 449–469.

Pinhal, S., Ropers, D., Geiselmann, J., & de Jong, H. (2019). Acetate metabolism and the inhibition of bacterial growth by acetate. Journal of bacteriology, 201(13), e00147-19.

Pontrelli, S., Chiu, T.-Y., Lan, E.I., Chen, F.Y.-H., Chang, P., Liao, J.C. (2018). *Escherichia coli* as a host for metabolic engineering, Metabolic Engineering, 50, pp. 16-46.

Poursaid, A.; Price, R., Tiede, A., Olson, E., Huo, E., McGill, L., Ghandehari, H., Cappello, J. (2015). *In situ* gelling silk-elastin-like protein polymer for transarterial chemoembolization.

Biomaterials, 57, 142–152.

Pradhan, S., Rajamani S., Agrawal G., Dash M., Samal S.K. (2017). Characterization of Polymeric Biomaterials. NMR, FT-IR and raman characterization of biomaterials, 147–173.

Presser, K. A., Ratkowsky, D. A., & Ross, T. (1997). Modelling the growth rate of *Escherichia coli* as a function of pH and lactic acid concentration. Applied and environmental microbiology, 63(6), 2355-2360.

Qiu W, Huang Y, Teng W, Cohn CM, Cappello J, Wu X. (2010). Complete recombinant Silk-Elastin-like protein-based tissue scaffold. Biomacromolecules, 11, 3219–3227.

Quispe, C. A., Coronado, C. J., & Carvalho Jr, J. A. (2013). Glycerol: Production, consumption, prices, characterization and new trends in combustion. Renewable and sustainable energy reviews, 27, 475-493.

Roberts, E. G., Rim, N., Huang, Wenwen; Tarakanova, A., Yeo, J., Buehler, M. J., Kaplan, D. L., Wong, J. Y. (2018). Fabrication and Characterization of Recombinant Silk-Elastin-Like-Protein (SELP) Fiber. Macromolecular Bioscience, 18(12), 1800265.

Rosano, G. L., & Ceccarelli, E. A. (2014). Recombinant protein expression in *Escherichia coli*: advances and challenges. Frontiers in Microbiology, 5, 172, 1-17.

Roy, R.M. (2006). A Modern Approach to Operations Management. New Age International, 344.

Runnels, C. M., Lanier, K. A., Williams, J. K., Bowman, J. C., Petrov, A. S., Hud, N. V., & Williams, L. D. (2018). Folding, assembly, and persistence: The essential nature and origins of biopolymers. Journal of molecular evolution, 86(9), 598-610.

Ruy, A. D. da S., Ferreira, A., Bresciani, A., Alves, R. & Pontes L. (2021). Market Prospecting and Assessment of the Economic Potential of Glycerol from Biodiesel. Biotechnological Applications of Biomass, first edition. IntechOpen.

Sallach, R. E., Conticello, V. P., & Chaikof, E. L. (2009). Expression of a recombinant elastin-like protein in *Pichia pastoris*. Biotechnology progress, 25(6), 1810–1818.

Sambrook, S., & Russel, D. W. (2006). The Condensed Protocols from Molecular Cloning: A Laboratory Manual (1st edition). Cold SprinngHarbor Laboratory Press.

Sanchez, S., & Demain, A. L. (2002). Metabolic regulation of fermentation processes. Enzyme and Microbial Technology, 31 (7), 895–906.

Scheel, R. A., Ho, T., Kageyama, Y., Masisak, J., McKenney, S., Lundgren, B. R., & Nomura, C. T. (2021). Optimizing a Fed-Batch High-Density Fermentation Process for Medium Chain-Length Poly(3-Hydroxyalkanoates) in *Escherichia coli*. Frontiers in bioengineering and biotechnology, 9, 618259.

Scheller, J., Henggeler, D., Viviani, A., & Conrad, U. (2004). Purification of spider silk-elastin from transgenic plants and application for human chondrocyte proliferation. Transgenic research, 13(1), 51-57.

Schipperus, R., Eggink, G., & de Wolf, F. A. (2012). Secretion of elastin-like polypeptides with different transition temperatures by *Pichia pastoris*. Biotechnology progress, 28(1), 242-247.

Schipperus, R., Teeuwen, R.L.M., Werten, M.W.T. (2009) Secreted production of an elastin-like polypeptide by *Pichia pastoris*. Appl Microbiol Biotechnol 85, 293–301.

Schneider, C. A., Rasband, W. S., & Eliceiri, K. W. (2012). NIH Image to ImageJ: 25 years of image analysis. Nature methods, 9(7), 671-675.

Sekar, N., Veetil, S. K., & Neerathilingam, M. (2013). Tender coconut water an economical growth medium for the production of recombinant proteins in *Escherichia coli*. BMC biotechnology, 13, 70.

Selvakumari, I. A. E., Jayamuthunagai, J., & Bharathiraja, B. (2021). Exploring the potential of biodiesel derived crude glycerol into high value malic acid: Biosynthesis, process optimization and kinetic assessment. Journal of the Indian Chemical Society, 98(6), 100075.

Shiekh, P. A., Andrabi, S. M., Singh, A., Majumder, S., & Kumar, A. (2021). Designing cryogels through cryostructuring of polymeric matrices for biomedical applications. European Polymer Journal, 144, 110234.

Sidoruk, K. V., Davydova, L. I., Kozlov, D. G., Gubaidullin, D. G., Glazunov, A. V., Bogush, V. G., Debabov, V. G. (2015). Fermentation optimization of a *Saccharomyces cerevisiae* strain producing 1F9 recombinant spidroin. Applied Biochemistry and Microbiology, 51(7), 766–773.

Singh, V., Haque, S., Niwas, R., Srivastava, A., Pasupuleti, M., & Tripathi, C. K. M. (2017). Strategies for Fermentation Medium Optimization: An In-Depth Review. Frontiers in Microbiology, 7, 2087.

Smolke C. (2009). The Metabolic Pathway Engineering Handbook: Tools and Applications, Volume 1. CRC Press, 582.

Sohl, J. L.; Splittgerber, A. G. (1991). The binding of Coomassie brilliant blue to Bovine Serum Albumin: A physical biochemistry experiment. Journal of Chemical Education, 68(3), 262.

Soini, J., Ukkonen, K., & Neubauer, P. (2008). High cell density media for *Escherichia coli* are generally designed for aerobic cultivations–consequences for large-scale bioprocesses and shake flask cultures. Microbial Cell Factories, 7(1), 1-11.

Song, H., & Lee, S. Y. (2006). Production of succinic acid by bacterial fermentation. Enzyme and microbial technology, 39(3), 352-361.

Soni, S. S., & Rodell, C. B. (2021). Polymeric materials for immune engineering: Molecular interaction to biomaterial design. Acta Biomaterialia, 133, 139-152.

Sørensen, H. P., & Mortensen, K. K. (2005). Advanced genetic strategies for recombinant protein expression in *Escherichia coli*. Journal of Biotechnology, 115 (2), 113–128.

Spedding, G. (2013). The World's most popular assay? a review of the ninhydrin-based free amino nitrogen reaction (FAN assay) emphasizing the development of newer methods and conditions for testing alcoholic beverages. Journal of the American Society of Brewing Chemists, 71(2), 83-89.

Stanbury P.F. (1998). Principles of Fermentation Technology. Elsevier Science & Technology, 2° edition, pp 104-110.

Stanbury, P., Whitaker, A. & Hall S. (2013). Principles of Fermentation Technology. Elsevier, 2nd edition, 243-227.

Stephens, J.S., Fahnestock, S.R., Farmer, R.S., Kiick, K.L.G., Chase, D.B., Rabolt J.F. (2005) Biomacromolecules, 6 (3) (2005), pp. 1405-1413.

Stevens, C. V. (2013). Bio-based plastics: materials and applications. John Wiley & Sons pp. 312-328.

Studier FW, (2005). Protein production by auto-induction in high-density shaking cultures. Protein Expr Purif,41(1):207–234.

Suástegui, M., Ng, C. Y., Chowdhury, A., Sun, W., Cao, M., House, E., & Shao, Z. (2017). Multilevel engineering of the upstream module of aromatic amino acid biosynthesis in *Saccharomyces*

cerevisiae for high production of polymer and drug precursors. Metabolic engineering, 42, 134-144.

Sun, S., Ding, Y., Liu, M., Xian, M., & Zhao, G. (2020). Comparison of Glucose, Acetate and Ethanol as Carbon Resource for Production of Poly(3-Hydroxybutyrate) and Other Acetyl-CoA Derivatives. Frontiers in Bioengineering and Biotechnology, 8.

Sun, Z., Qin, G., Xia, X., Cronin-Golomb, M., Omenetto, F. G., & Kaplan, D. L. (2013). Photoresponsive Retinal-Modified Silk–Elastin Copolymer. Journal of the American Chemical Society, 135(9), 3675–3679.

Tamang, N., Shrestha, P., Khadka, B., Mondal, M. H., Saha, B., & Bhattarai, A. (2021). A Review of Biopolymers' Utility as Emulsion Stabilizers. Polymers, 14(1), 127.

Tan, J.S., Ramanan, R.N., Ling, T.C. (2012). The role of *lac* operon and *lac* repressor in the induction using lactose for the expression of periplasmic human interferon-α2b by *Escherichia coli.* Ann Microbiol 62, 1427–1435

Tănase, Râpă, M, Popa, O. (2014). Biopolymers based on renewable resources - a review. Scientific Bulletin. Series F. Biotechnologies, 17, 188-195.

Tang, X. Z., Kumar, P., Alavi, S., & Sandeep, K. P. (2012). Recent Advances in Biopolymers and Biopolymer-Based Nanocomposites for Food Packaging Materials. Critical Reviews in Food Science and Nutrition, 52(5), 426–442.

Tang, X., Ye, X., Wang, X. (2021). High mechanical property silk produced by transgenic silkworms expressing the spidroins *PySp1* and *ASG1*. Sci Rep 11, 20980.

Tanner, F., & Pitner, G. (1939). Germicidal action of bromine. Proceedings of the Society for Experimental Biology and Medicine, 40(1), 143-145.

Tarakanova, A., Huang, W., Qin, W., Kaplan, D. L. and Buehler M.J. (2017). Modeling and Experiment Reveal Structure and Nanomechanics across the Inverse Temperature Transition in *B. mori* Silk-Elastin-like Protein Polymers. ACS Biomater. Sci. Eng., 3, 2889-2899.

Teng, W., Huang, Y., Cappello, J., & Wu, X. (2011). Optically Transparent Recombinant Silk-Elastin like Protein Polymer Films. The Journal of Physical Chemistry B, 115(7), 1608–1615.

Tjin, M., Low, P. & Fong, E. (2014). Recombinant elastomeric protein biopolymers: progress and

prospects. Polym J 46, 444–451.

Torrezan, G. S., Polaquini, C. R., Lima, M. F., & Regasini, L. O. (2020). Use of glycerol, waste glycerol from biodiesel production and other protic solvents in bioactive α, β-unsaturated ketones synthesis. Sustainable Chemistry and Pharmacy, 16, 100250.

Tran, L., Kwon, S., Kim, Z.H., Oh, Y., & Lee, (2010). Statistical optimization of culture media for growth and lipid production of *Botryococcus braunii* LB572. Biotechnology and Bioprocess Engineering, 15(2), 277–284.

Trefil, J. S., Morowitz, H., Ceruzzi, P. (2001). Encyclopedia of Science and Technology, Taylor & Francis.

Ukkonen, K., Veijola, J., Vasala, A. (2013). Effect of culture medium, host strain and oxygen transfer on recombinant Fab antibody fragment yield and leakage to medium in shaken *E. coli* cultures. Microb Cell Fact 12, 73.

Vandamme, E. (2009). Agro-Industrial Residue Utilization for Industrial Biotechnology Products. Springer Science+Business Media B.V, 3-11.

Vasconcelos A., Gomes A., Cavaco-Paulo A., (2012). Novel silk fibroin/elastin wound dressings. Acta Biomaterialia, 8(8).

Vollrath, F., & Porter, D. (2009). Silks as ancient models for modern polymers. Polymer, 50(24), 5623-5632.

Walker, G. M. (2014). Fermentation (Industrial): media for industrial fermentations. In Encyclopedia of food microbiology (pp. 769-777). Academic Press.

Wang, C., Chang, T., Yang, H., & Cui, M. (2014a). Surface physiological changes induced by lactic acid on pathogens in consideration of *pKa* and pH. Food Control, 46, 525-531.

Wang, Qin; Xia, Xiaoxia; Huang, Wenwen; Lin, Yinan; Xu, Qiaobing; Kaplan, David L. (2014b). High Throughput Screening of Dynamic Silk-Elastin-Like Protein Biomaterials. Advanced Functional Materials, 24(27), 4303–4310.

Wanger, A., Chavez, V., Huang, R., Wahed, A., Dasgupta, A., & Actor, J. K. (2017). Microbiology and molecular diagnosis in pathology: a comprehensive review for board preparation, certification and clinical practice.

Wanner, B. L. (1993). Gene regulation by phosphate in enteric bacteria. Journal of cellular

biochemistry, 51(1), 47-54.

Warnecke, T., & Gill, R. T. (2005). Organic acid toxicity, tolerance, and production in *Escherichia coli* biorefining applications. Microbial cell factories, 4(1), 1-8.

Werten, M. W., Wisselink, W. H., Jansen-van den Bosch, T. J., de Bruin, E. C., & de Wolf, F. A. (2001). Secreted production of a custom-designed, highly hydrophilic gelatin in *Pichia pastoris*. Protein engineering, 14(6), 447-454.

Werten, T.J. van den Bosch, R.D. Wind, H. Mooibroek, F.A. de Wolf, (1999). High-yield secretion of recombinant gelatins by *Pichia pastoris* Yeast, 15, pp. 1087-1096.

White, G. (1998). Bromine, bromine chloride, and iodine. In G. White, Handbook of Chlorination and Alternative Disinfectants (4th ed., pp. 1347-1384). Hoboken: Wiley-Interscience.

Willems, L., Roberts, S., Weitzhandler, I., Chilkoti, A., Mastrobattista, E., Van Der Oost, J., & De Vries, R. (2019). Inducible Fibril formation of silk–elastin diblocks. ACS *omega*, 4(5), 9135-9143.

Winkelman, J. W., & Clark, D. P. (1984). Proton suicide: General method for direct selection of sugar transport- and fermentation-defective mutants. Journal of Bacteriology, 160(2), 687–690.

Woyskit, D., & Cupp-Vickery, J. R. (2001). Enhanced expression of cytochrome P450s from *lac*-based plasmids using lactose as the inducer. Archives of Biochemistry and Biophysics, 388(2), 276-280.

Wu, W., Pang, B., Yang, R., Liu, G., Ai, C., Jiang, C., & Shi, J. (2020). Improvement of the probiotic potential and yield of *Lactobacillus rhamnosus* cells using corn steep liquor. LWT, 131, 109862.

Wurm DJ, Veiter L, Ulonska S, Eggenreich B, Herwig C, Spadiut O. (2016). The *E. coli* pET expression system revisited-mechanistic correlation between glucose and lactose uptake. Appl Microbiol Biotechnol, 100(20):8721-9.

Xia, X., Xu, Q., Hu, X., Qin, G. and Kaplan D. L. (2011). Tunable Self-Assembly of Genetically Engineered Silk–Elastin-like Protein Polymers. Biomacromolecules, 12, 11, 3844–3850.

Xinming, L., Yingde, C., Lloyd, A. W., Mikhalovsky, S. V., Sandeman, S. R., Howel, C. A., & Liewen, L. (2008). Polymeric hydrogels for novel contact lens-based ophthalmic drug delivery

systems: A review. Contact Lens and Anterior Eye, 31(2), 57-64.

Xu, B., Jahic, M., Blomsten, G., & Enfors, S. O. (1999). Glucose overflow metabolism and mixed-acid fermentation in aerobic large-scale fed-batch processes with *Escherichia coli*. Applied microbiology and biotechnology, 51(5), 564-571.

Yadav, P., Yadav, H., Shah, V. G., Shah, G., & Dhaka, G. (2015). Biomedical Biopolymers, their Origin and Evolution in Biomedical Sciences: A Systematic Review. Journal of Clinical & Diagnostic Research, 9(9), 21–25.

Yang, Y. J., Holmberg, A. L., & Olsen, B. D. (2017). Artificially engineered protein polymers. Annual review of chemical and biomolecular engineering, 8, 549-575.

Zhai, Y.; F.Z. Cui (2006). Recombinant human-like collagen directed growth of hydroxyapatite nanocrystals, 291(1), 202–206.

Zhang, J., Reddy J., Buckland, B. and Greasham, R. (2003). Toward consistent and productive complex media for industrial fermentations: Studies on yeast extract for a recombinant yeast fermentation process. 82(6), 640–652.

Zhang, X., Jantama, K., Moore, J. C., Jarboe, L. R., Shanmugam, K. T., & Ingram, L. O. (2009). Metabolic evolution of energy-conserving pathways for succinate production in *Escherichia coli.* Proceedings of the National Academy of Sciences, 106(48), 20180-20185.

Zhang, Y., Gladyshev, V. N. (2010). dbTEU: a protein database of trace element utilization. Bioinformatics, 26(5), 700–702.

Zhu, Jingxin; Huang, Wenwen; Zhang, Qiang; Ling, Shengjie; Chen, Ying; Kaplan, David (2016). Aqueous-Based Coaxial Electrospinning of Genetically Engineered Silk Elastin Core-Shell Nanofibers. Materials, 9(4), 221.

7. Appendixes

Appendix A. Competent cells

Competent cells were made, by growth of the *E. coli* strain BL21(DE3) in 5 mL of Lysogeny Broth (LB) overnight at 37 °C until stationary phase. The overnight culture was diluted to 1:100 in fresh LB, grown at 37 °C at 200 rpm until it reached ≈ 0.6 (OD_{600nm}) nm. The cells were incubated on ice for 10 min, and then centrifuge at 3170 xg for 10 min at 4 °C, followed by the resuspension of the pellet in 32 mL of ice-cold TB (10 mM HEPES; 15 mM $CaCl_2$; 250 mM KCl and adjusted the pH to 6.7 with KOH, 55 mM $MnCl_2$ was dissolved in TB Buffer, sterilized and stored at 4 °C), and the incubation in ice for another 10 min.

The pellet was gently resuspended in 8 mL of ice-cold TB and DMSO was added to a final concentration of 7 % with gently swirling on an ice bath for 10 min. 100 µL of the cell suspension was distributed in Eppendorf's and immediately flash-freeze in liquid N_2. The cells were frozen at -80 °C for posterior use.

Appendix B. Quantification of protein by BCA method

Following the standard protocol provide by Pierce™, the BCA Protein Assay Kit for microplates (Thermo scientific™ - by number of catalog) was used for detection and quantitation of total protein in samples. The working reagent (WR) was prepared by mixing 50 parts of BCA Reagent A with 1 part of BCA Reagent B. The samples were diluted in water (1:10) and pipetted 25 µL of each sample with 200 µL of the WR to each well and mixed well in the plate. The plate was covered and incubated at 37 °C for 30 min. The absorbance was measured at or near 562 nm on a plate reader.

For the standard curve, BSA solutions (Bovine Serum Albumin) with concentrations ranging from 20–2,000 µg/mL were prepared by diluting BSA in ultrapure water and used to determine protein concentration of each unknown sample.

Appendix C. List of reagents used for SDS-PAGE

Table 7.1 – Recipe for the 10 % acrylamide gel used in SDS-PAGE.

Reagents	Running gel	Staking gel
Acrylamide/Bis-acrylamide, 30 % solution	2.8 mL	0.55 mL
1.875 M Tris, pH 8.8	5.6 mL	-
0.5 M Tris, pH 6.8	-	2.2 mL
ddH_2O	2.7 mL	1.8 mL
10 % APS	75 µL	35 µL
TEMED	12 µL	10 µL

Appendix D. Selection of mutants via proton suicide approach

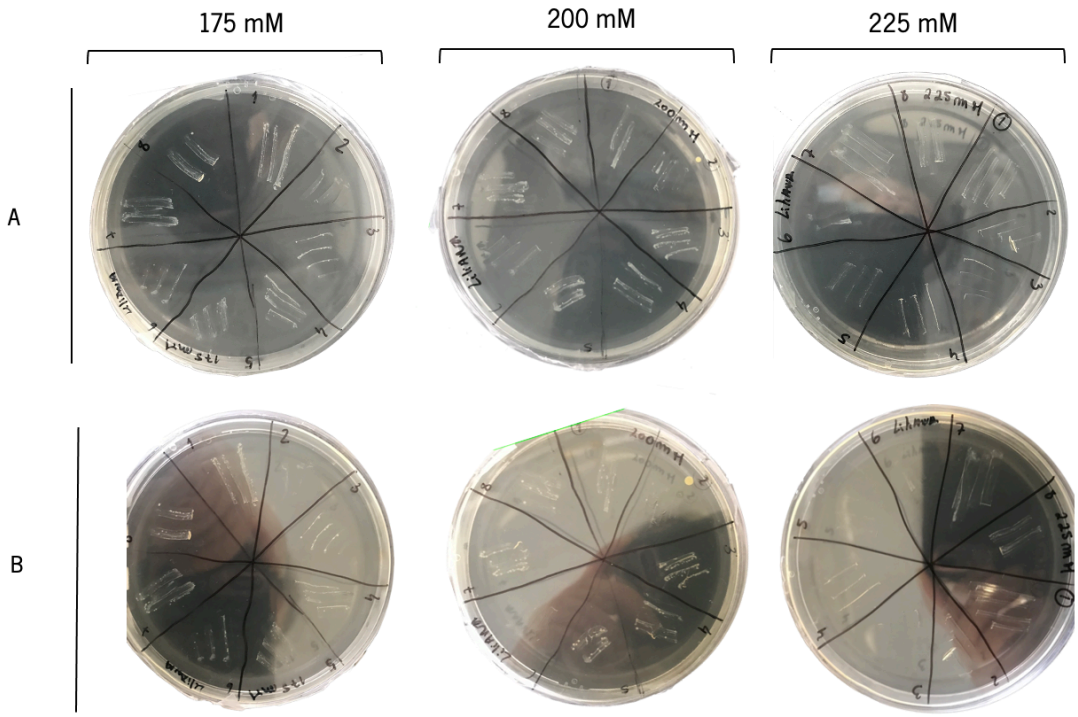

Figure 7.1 – The 8 colonies selected were plated in fresh LB plates supplements with equimolar concentrations of Bromate and Bromide (175, 200 and 225 mM). The plates incubated for A) 48 and B) 144 h.

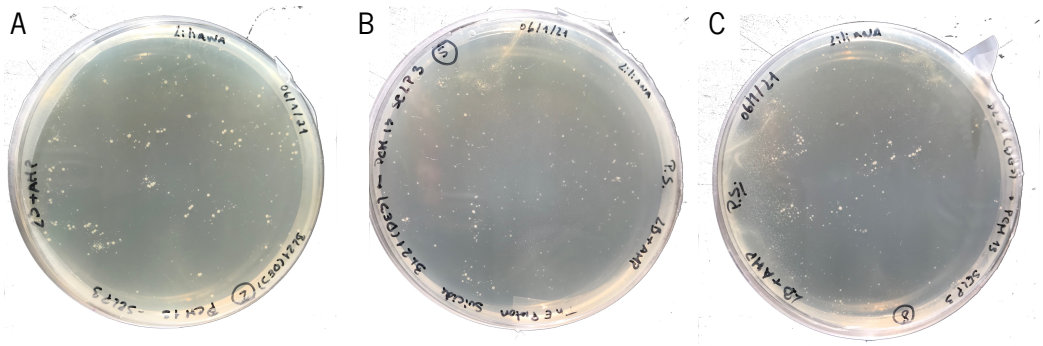

Figure 7.2 – The TSS tranformation of the seleted mutants, resulting in the creation of A) *E. coli* BL21(DE3) P.S.2, B) mutant *E. coli* BL21(DE3) P.S.8 and C) mutant *E. coli* BL21(DE3) P.S.8.

Appendix E. Optimization of phosphate quantification for microplate reading

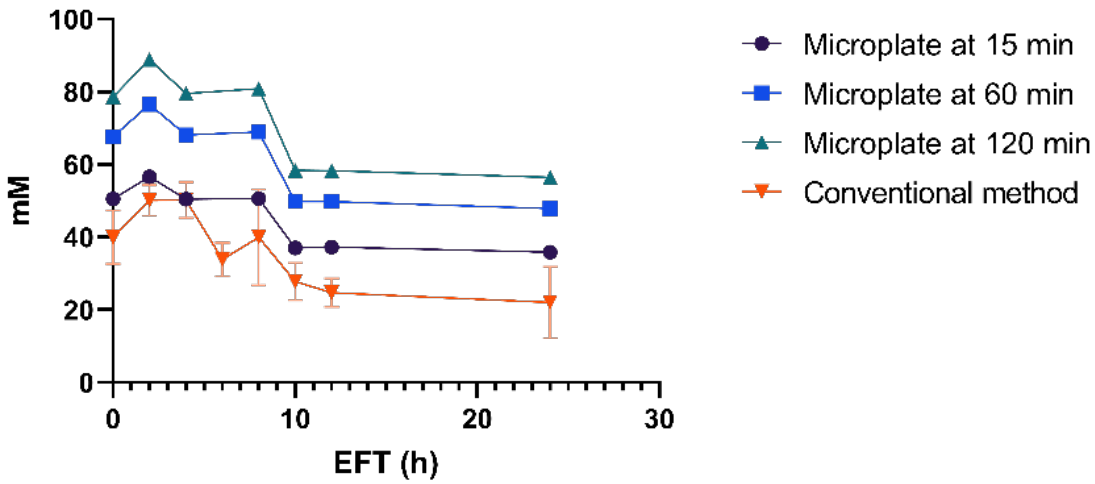

Figure 7.3– Optimization of the phosphates protocol to microplate reading. The samples were compared to the conventional method to a microplate format. The microplate was read at different point at 15, 60 and 120 min.

To adapt the conventional method using higher volumes in cuvettes, the protocol for phosphate determination was adapted for microplates. Figure 7.3 displays a comparison of the traditional approach using cuvettes with the adaptation to microplates. Results demonstrate that readings after 15 min of incubation were comparable to the traditional method.

Appendix F. Optimization of FAN quantification for microplate reading

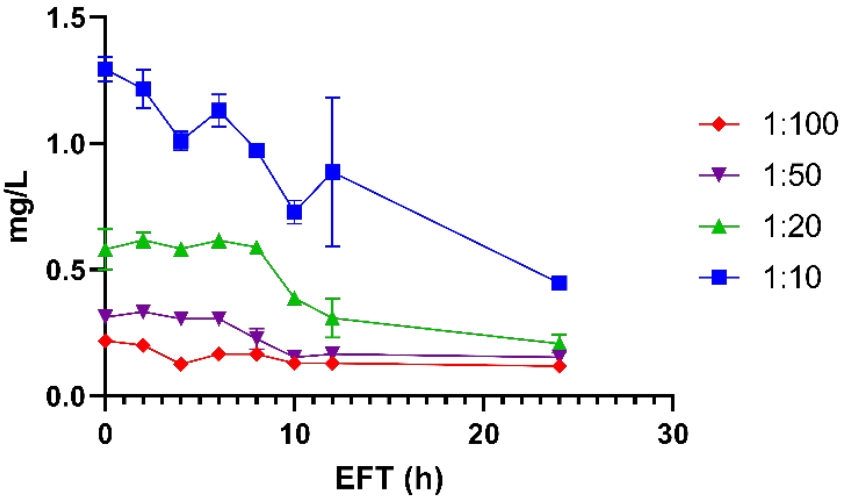

Figure 7.4 – Optimization of the protocol of FAN in a microplate format. The samples were diluted to 1:10, 1:20, 1:50 and 1:100.

Since the medium broth is highly rich in nitrogen, the use of undiluted broth samples impairs the quantification of free amino nitrogen as values are above the detection limit. To optimize the method, a nitrogen-rich sample (60 g/L CSL) was utilized and diluted to 1:10, 1:20, 1:50, and 1:100. The findings revealed that a higher dilution resulted in a more accurate estimation of the nitrogen content of the sample. Accordingly, the samples were diluted to 1:100 for FAN determination (figure 7.4).

Appendix G. Purification of SELP-59-A

Purification of SELP-59-A was achieved via well-established methodologies previously described by our group, involving an initial acidification process followed by salting out with ammonium sulfate for a 25 % saturation (Machado *et al.*, 2013a). After ultrasonic disruption, the resulting cell lysate (figure 7.5, lane 6) was precipitated by adjusting the pH to 3.5 (figure 7.5, lane 2). This acidification step functions as a pre-purification process, allowing to eliminate most of *E. coli* endogenous proteins, without affecting the stability of SELP-59-A (Machado *et al.*, 2013a). The next step of the purification process relies on the salting out with 25 % ammonium sulfate saturation to precipitate and concentrate SELP-59-A, separating it from the persisting cell contaminants. After precipitation and centrifugation, the supernatant is discarded (figure 7.5, lane 4) and the SELP-59-A-enriched pellet (figure 7.5, lane 3) is dissolved in deionized water. The protein polymer fraction is then centrifuged to remove insoluble bodies, allowing to achieve a highly pure protein polymer fraction (figure 7.5, lane 5), followed by dialysis and lyophilization.

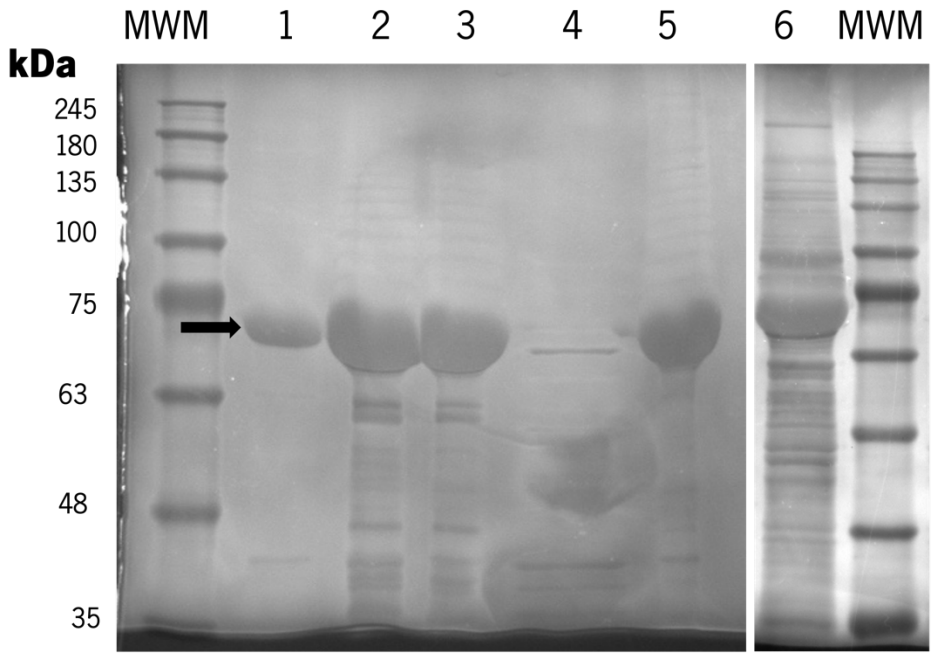

Figure 7.5 – Optimization of purification process of SELP-59-A by ammonium sulfate precipitation. 1) pure SELP-59-A (10 μg) used as control; 2) supernatant resulting from the acidification step; 3) the supernatant resulted acidification was added ammonium sulfate for 30 min to the crude soluble lysate; 4) after adding ammonium sulfate for 30 min to the crude soluble lysate and centrifuged, the supernatant was saved and represented in lane 4; 5) then the pellet was resuspended in ultra-pure water and left overnight and 6) The cell crude extracts of SELP-59-A before purification. Target recombinant protein is indicated by arrows and molecular weight marker is represented in of each gel by MWM

Appendix H. 3D contour plots of phosphates and FAN concentration at 24 h EFT

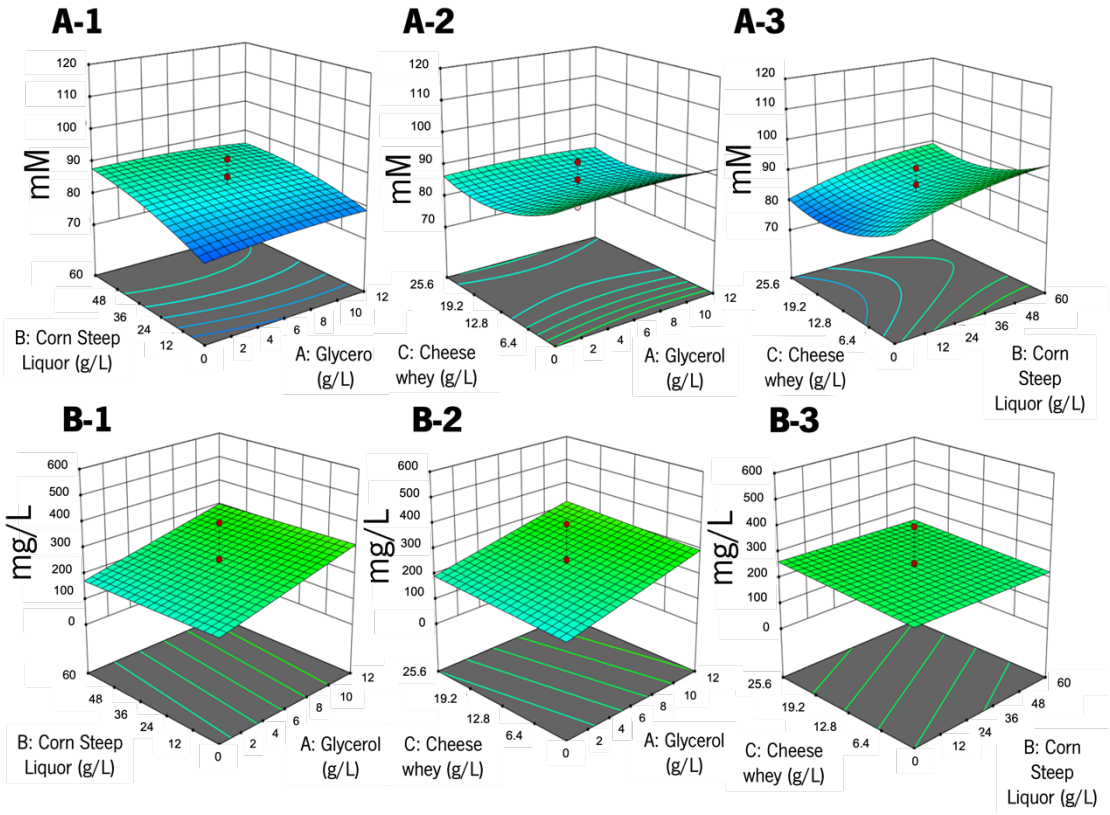

Figure 7.6 – 3D contour plots representing the variations of (A) phosphate and (B) FAN concentration for non-mutated *E. coli* BL21(DE3) after 24 h EFT. In dark red (●) are the points above the surface and in light red (●), the points below the surface.

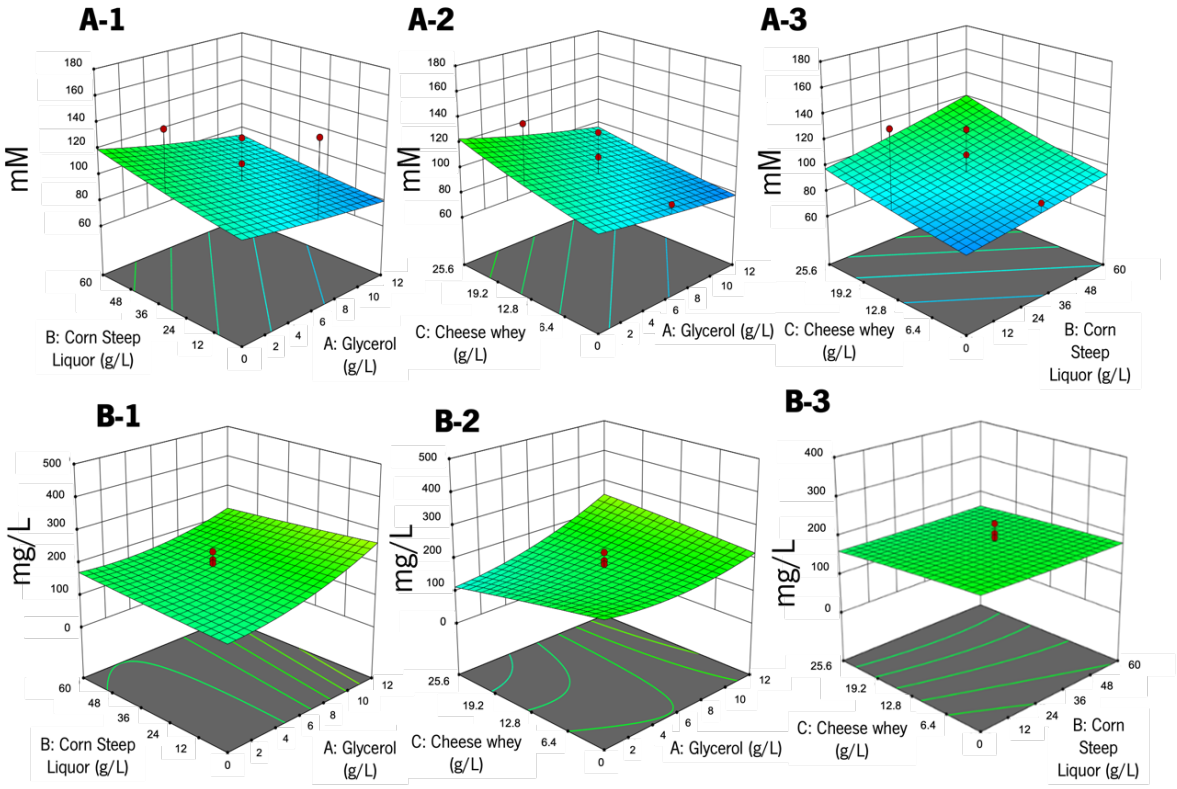

Figure 7.7 – 3D contour plots representing the variations of phosphate (A) and FAN (B) concentration for mutated *E. coli* BL21(DE3) PS.5 after 24 h EFT. In dark red (●) are the points above the surface.

Appendix I. 3D contour plots of acetic acid production after 24 h EFT

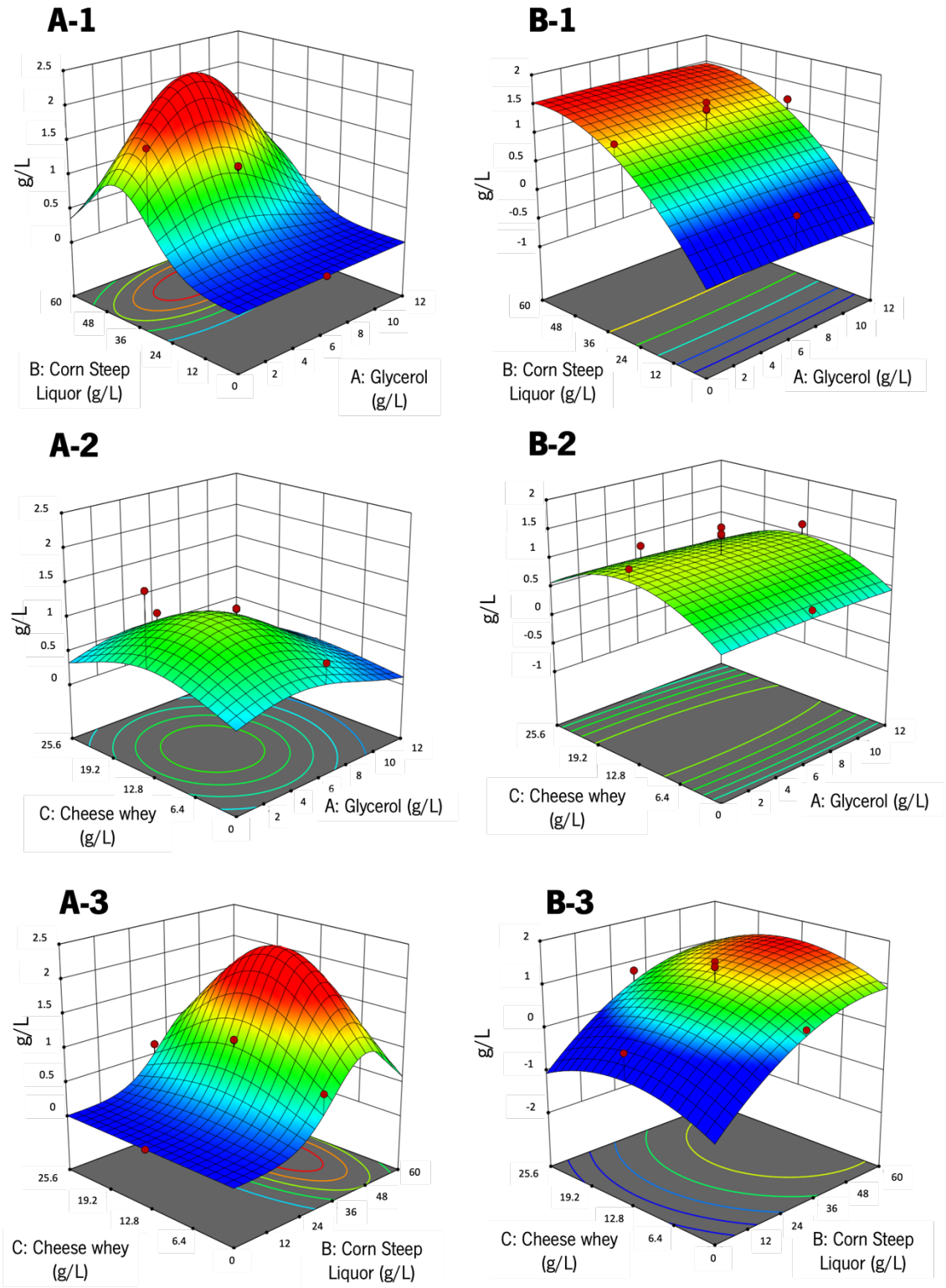

Figure 7.8 – 3D contour plots representing the variations of acetic acid production (g/L) after 24 h EFT for A) non-mutated *E. coli* BL21(DE3) and B) *E. coli* BL21(DE3) mutant P.S.5. In dark red (●) are the points above the surface.

Appendix J. Assessment of protein production

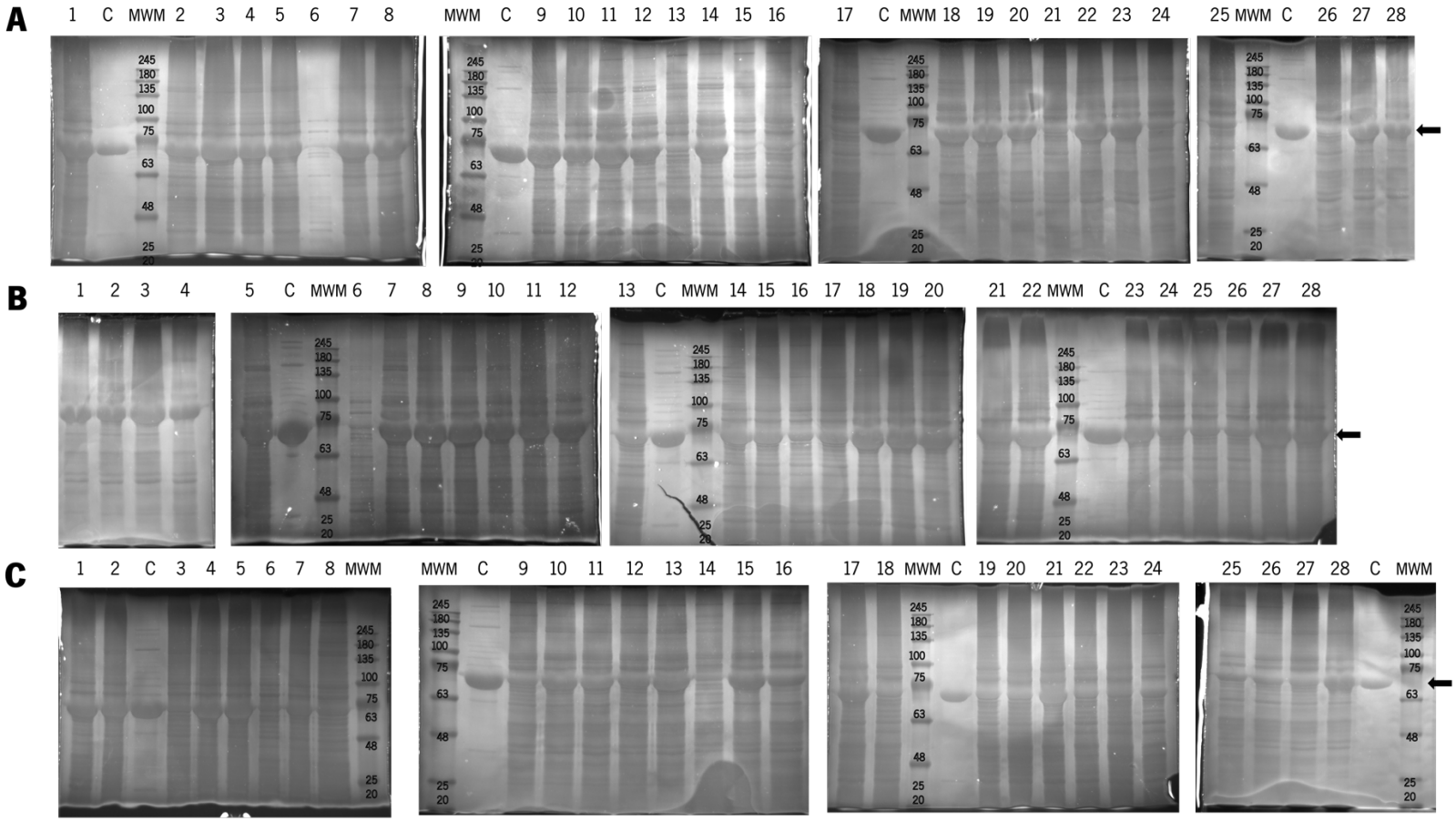

Figure 7.9 – Electrophoretic patterns of cell crude extracts at different time points for non-mutated *E. coli* BL21(DE3). A) 8 h, B) 12 h and C) 24 h. The cell crude extracts from condition 1 to 28 were assessed with non-mutant *E. coli* BL21(DE3) transformed with pCM13::SELP-59-A. All samples were normalised for the same quantity (5 µL) before loading on gel. Target recombinant protein is indicated by arrows and molecular weight marker is represented in of each gel by MWM.

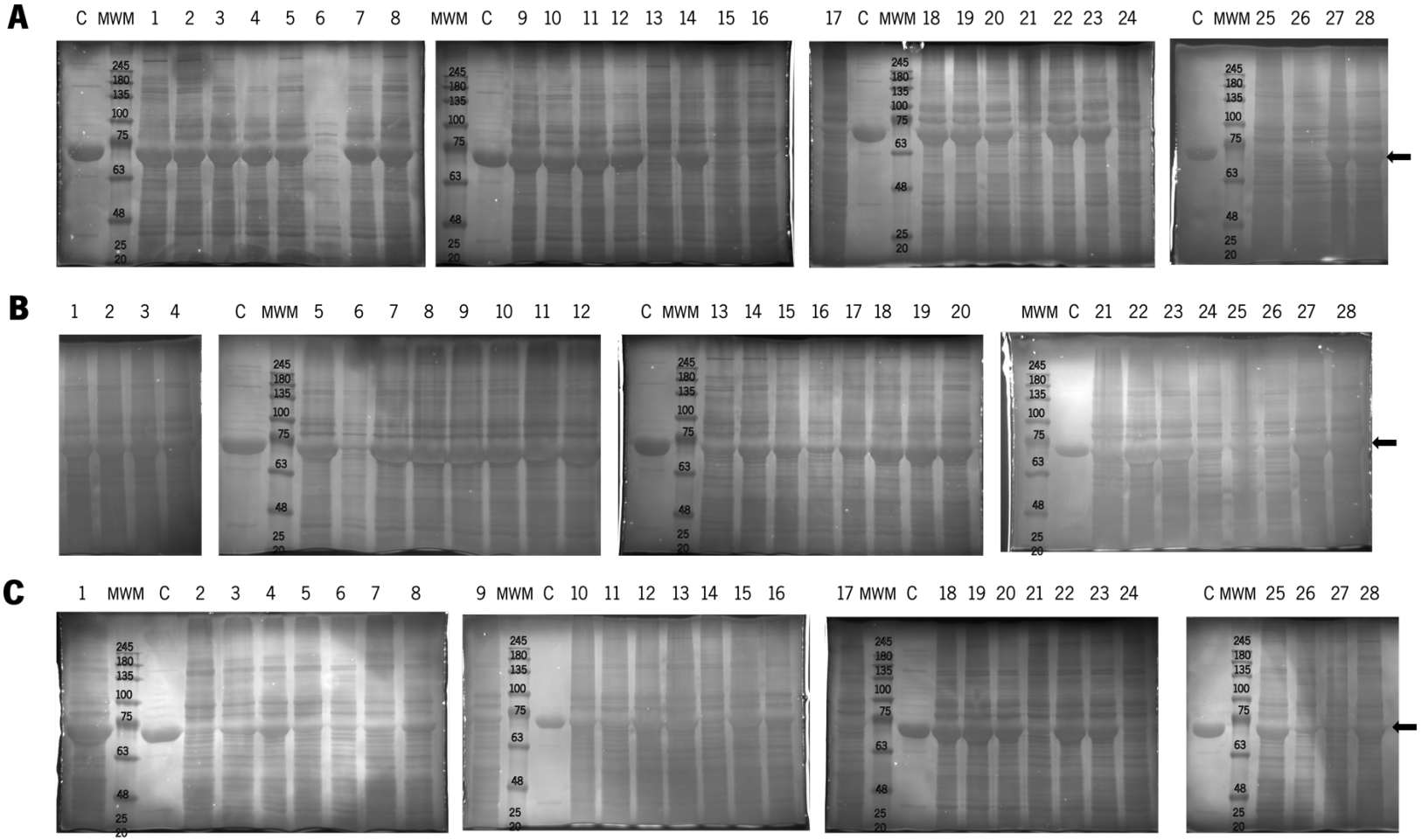

Figure 7.10 – Electrophoretic patterns of cell crude extracts at different time points for *E. coli* BL21(DE3) mutant P.S.5. A) 8 h, B) 12 h and C) 24 h. The cell crude extracts from conditions 1 to 28 were assessed with mutant *E. coli* BL21(DE3) P.S.5 transformed with pCM13::SELP-59-A. All samples were normalised for the same quantity (5 µL) before loading on gel. Target recombinant protein is indicated by arrows and molecular weight marker is represented in of each gel by MWM.

Appendix K. Constraints used for optimization of RSM model after 12 h and 24 h EFT for the non-mutated *E. coli* BL21(DE3)

Table 7.2 – Constraints used in the RSM model for optimization of media components considering 12 h EFT for the non-mutated *E. coli* BL21(DE3). Values of volumetric productivity were determined by densitometry analysis.

Name	Goal	Lower Limit	Upper Limit	Lower Weight	Upper Weight	Importance
A: Glycerol (g/L)	is in range	1.00	12.00	1	1	3
B: Corn steep liquor (g/L)	is in range	0.00	60.00	1	1	3
C: Cheese whey (g/L)	is in range	6.40	19.20	1	1	3
Volumetric productivity (mg/L)	maximize	23.31	202.63	1	1	4
OD_{600nm}	maximize	0.30	3.34	1	1	4
BCA (µg/mL)	maximize	408.70	4471.49	1	1	5
FAN (mg/L)	is in range	26.228	543	1	1	3
Phosphates	is in range	73.56	114.29	1	1	3

Table 7.3 – Constraints used in the RSM model for optimization of media components considering 24 h EFT for the non-mutated *E. coli* BL21(DE3). Volumetric productivity based on the weight of pure lyophilized SELP-59-A.

Name	Goal	Lower Limit	Upper Limit	Lower Weight	Upper Weight	Importance
A: Glycerol (g/L)	is in range	0.00	12.00	1	1	3
B: Corn steep liquor (g/L)	is in range	0.00	60.00	1	1	3
C: Cheese whey (g/L)	is in range	6.40	19.20	1	1	3
Protein Expression (mg/L)	maximize	11.11	117.78	1	1	5
OD_{600nm}	maximize	0.30	2.99	1	1	5
BCA (µg/mL)	maximize	735.37	5112.34	1	1	4
FAN (mg/L)	is in range	26.23	543.00	1	1	3
Phosphates (mM)	is in range	73.56	114.29	1	1	3

Appendix L. Optimal points obtained by RSM optimization using the CCD approach, after 12 h and 24 h EFT for the non-mutated *E. coli* BL21(DE3)

Table 7.4 – Optimal point solutions and predicted values obtained with RSM optimization for the non-mutant *E. coli* BL21(DE3), after 12 h EFT. Formulation #1 (in bold) was selected as the best formulation. Predicted values for volumetric productivity were computed based on densitometry results.

Number	Glycerol (g/L)	Corn steep liquor (g/L)	Cheese whey (g/L)	Predicted values			Desirability
				Volumetric productivity (mg/L)	OD_{600nm}	BCA (µg/mL)	
1	**1.00**	**41.90**	**19.20**	**138.65**	**2.71**	**2749.16**	**0.71**
2	1.00	41.92	19.20	138.70	2.71	2748.51	0.71
3	1.00	41.87	19.20	138.59	2.71	2749.98	0.71
4	1.00	41.99	19.20	138.89	2.71	2745.94	0.71
5	1.00	41.73	19.20	138.26	2.71	2754.62	0.71
6	1.00	42.08	19.20	139.10	2.71	2743.01	0.71
7	1.00	41.66	19.20	138.10	2.72	2756.84	0.71
8	1.00	42.38	19.20	139.80	2.70	2733.15	0.71
9	1.02	42.05	19.20	138.93	2.71	2743.34	0.71
10	1.00	41.13	19.20	136.84	2.73	2774.44	0.71
11	1.01	41.80	19.19	138.40	2.71	2751.04	0.71
12	1.00	41.49	19.19	137.71	2.72	2761.28	0.71
13	1.07	41.80	19.20	138.14	2.72	2750.36	0.71
14	1.00	40.50	19.20	135.34	2.74	2795.45	0.71
15	1.00	40.35	19.20	134.99	2.74	2800.35	0.71
16	1.13	42.12	19.20	138.66	2.72	2738.16	0.71
17	1.00	41.41	19.17	137.55	2.72	2760.56	0.70
18	1.18	42.90	19.20	140.28	2.70	2710.74	0.70
19	1.20	42.47	19.20	139.18	2.71	2724.20	0.70
20	1.00	42.18	19.16	139.41	2.70	2733.37	0.70
21	1.24	42.46	19.20	139.00	2.72	2723.69	0.70
22	1.24	42.30	19.20	138.60	2.72	2728.98	0.70
23	1.21	43.74	19.20	142.14	2.69	2682.69	0.70
24	1.29	42.11	19.20	137.98	2.73	2733.63	0.70

25	1.42	43.03	19.20	139.62	2.72	2699.70	0.70
26	1.00	45.00	19.20	146.01	2.64	2647.88	0.70
27	1.45	42.99	19.20	139.37	2.72	2699.85	0.70
28	1.62	44.35	19.20	141.89	2.71	2651.13	0.70
29	1.67	43.87	19.20	140.52	2.72	2665.04	0.70
30	1.00	37.96	19.20	129.33	2.78	2880.29	0.70
31	1.56	45.31	19.20	144.43	2.68	2621.82	0.70
32	1.75	44.38	19.20	141.42	2.72	2646.12	0.70
33	1.76	44.15	19.20	140.83	2.73	2653.50	0.70
34	1.76	43.95	19.20	140.36	2.73	2659.66	0.70
35	1.00	41.90	19.08	138.88	2.70	2727.78	0.70
36	1.86	44.48	19.20	141.19	2.73	2639.70	0.70
37	1.00	37.54	19.20	128.33	2.78	2894.53	0.70
38	1.85	45.10	19.20	142.71	2.71	2620.24	0.70
39	1.89	44.55	19.20	141.22	2.73	2636.69	0.70
40	1.92	43.73	19.20	139.20	2.74	2662.40	0.70
41	1.00	41.98	19.05	139.15	2.69	2719.63	0.70
42	1.00	42.36	19.02	140.10	2.68	2702.45	0.70
43	1.79	47.73	19.20	149.20	2.65	2537.89	0.70
44	2.47	45.90	19.20	142.05	2.75	2576.83	0.70
45	2.54	45.74	19.20	141.33	2.76	2580.06	0.70
46	2.61	45.99	19.20	141.62	2.76	2570.00	0.70
47	2.85	47.34	19.20	143.84	2.76	2520.54	0.70
48	1.00	35.43	19.20	123.33	2.80	2966.29	0.70
49	2.96	49.19	19.20	147.77	2.73	2459.25	0.70
50	3.04	49.08	19.20	147.18	2.74	2460.37	0.70
51	3.39	49.46	19.20	146.62	2.77	2438.93	0.70
52	3.43	49.71	19.20	147.04	2.76	2430.00	0.70
53	4.39	51.89	19.20	148.24	2.81	2337.02	0.70
54	4.75	53.36	19.20	150.19	2.82	2283.12	0.69

55	4.78	53.97	19.20	151.54	2.82	2263.99	0.69
56	5.22	56.04	19.20	154.56	2.83	2190.87	0.69
57	5.52	55.03	19.20	150.93	2.87	2212.86	0.69
58	5.79	57.63	19.20	155.99	2.86	2129.71	0.69
59	1.00	31.42	19.20	113.83	2.82	3105.07	0.69
60	7.36	60.00	18.96	155.48	2.95	1986.80	0.68
61	9.60	60.00	19.20	145.73	3.15	1965.60	0.68
62	9.86	60.00	19.20	144.64	3.16	1959.10	0.67
63	1.00	20.71	19.20	88.44	2.72	3491.49	0.64

Table 7.5 – Optimal point solutions and predicted values obtained with RSM optimization for the non-mutant *E. coli* BL21(DE3), after 24 h EFT. Formulation #1 (in bold) was selected as the best formulation. Predicted values for volumetric productivity were computed based on the weight of pure lyophilized SELP-59-A.

Number	Glycerol (g/L)	Corn steep liquor (g/L)	Cheese whey (g/L)	Predicted values			Desirability
				Volumetric productivity (mg/L)	OD_{600nm}	BCA (μg/mL)	
1	**2.07**	**60.00**	**19.20**	**72.53**	**2.86**	**4733.20**	**0.92**
2	2.07	60.00	19.20	72.53	2.86	4733.38	0.92
3	2.11	60.00	19.20	72.44	2.86	4776.93	0.92
4	2.13	60.00	19.20	72.38	2.86	4803.58	0.92
5	2.06	59.93	19.20	72.46	2.86	4710.63	0.92
6	2.27	60.00	19.20	72.03	2.85	4961.26	0.92
7	1.98	60.00	19.19	72.76	2.87	4629.62	0.92
8	2.30	60.00	19.20	71.97	2.85	4985.25	0.92
9	2.05	59.87	19.20	72.40	2.86	4690.70	0.92
10	2.05	60.00	19.15	72.67	2.85	4682.51	0.92
11	2.39	60.00	19.20	71.75	2.84	5084.65	0.92
12	2.42	60.00	19.20	71.68	2.84	5114.75	0.92
13	2.04	59.76	19.20	72.29	2.86	4658.70	0.92
14	2.03	59.69	19.20	72.22	2.86	4636.18	0.91
15	2.04	60.00	19.09	72.83	2.84	4626.98	0.91
16	2.01	59.52	19.20	72.05	2.85	4583.93	0.91
17	2.06	59.53	19.20	71.94	2.85	4646.82	0.91
18	2.02	59.99	19.04	72.95	2.84	4576.10	0.91
19	1.99	59.59	19.11	72.37	2.84	4516.23	0.91
20	1.97	59.26	19.20	71.80	2.85	4505.90	0.91

21	1.96	59.15	19.20	71.69	2.85	4474.33	0.91
22	2.53	60.00	18.98	71.83	2.79	5090.06	0.91
23	1.41	60.00	19.20	74.20	2.92	3959.56	0.91
24	1.97	59.95	18.88	73.36	2.81	4404.10	0.91
25	1.30	60.00	19.20	74.47	2.93	3832.87	0.90
26	1.27	60.00	19.20	74.54	2.93	3800.54	0.90
27	1.25	60.00	19.20	74.59	2.94	3776.84	0.90
28	1.22	60.00	19.20	74.69	2.94	3733.54	0.90
29	1.13	60.00	19.20	74.90	2.95	3632.31	0.90
30	1.82	58.23	19.20	70.80	2.84	4206.16	0.90
31	1.07	60.00	19.20	75.07	2.96	3557.58	0.90
32	1.00	59.91	19.20	75.12	2.96	3463.65	0.90
33	2.55	60.00	18.61	72.54	2.72	4862.36	0.89
34	1.86	60.00	18.49	74.52	2.74	4044.81	0.89
35	0.78	59.85	19.20	75.61	2.99	3208.08	0.89
36	0.73	60.00	19.20	75.95	3.00	3160.96	0.89
37	1.79	56.92	19.20	69.19	2.81	4018.38	0.88
38	1.73	58.57	18.73	72.40	2.76	3869.57	0.88
39	1.54	56.41	19.20	69.13	2.83	3726.44	0.88
40	0.47	59.90	19.20	76.49	3.03	2865.61	0.87
41	0.31	60.00	19.20	77.05	3.06	2693.52	0.87
42	1.16	54.23	19.20	67.28	2.85	3226.02	0.86
43	0.18	60.00	19.20	77.37	3.08	2562.46	0.86
44	0.11	60.00	19.20	77.58	3.09	2482.77	0.85

45	0.07	60.00	19.20	77.68	3.09	2445.97	0.85
46	0.02	60.00	19.20	77.83	3.10	2387.82	0.85
47	0.01	60.00	19.11	78.03	3.08	2338.94	0.85
48	0.00	59.90	19.11	77.91	3.08	2326.31	0.84
49	1.45	59.15	17.49	76.44	2.59	2988.98	0.84
50	0.00	60.00	18.99	78.32	3.06	2268.65	0.84
51	0.02	57.93	19.20	74.91	3.08	2328.37	0.84
52	5.18	60.00	19.20	65.20	2.81	6415.25	0.84
53	0.33	51.11	19.20	65.37	2.99	2519.92	0.84
54	0.00	59.95	18.45	79.43	2.95	2027.17	0.82
55	0.00	46.68	19.20	60.92	3.09	2432.65	0.81
56	0.00	32.12	19.20	46.58	3.38	4115.90	0.78
57	0.00	31.40	19.20	45.98	3.41	4279.41	0.78
58	0.00	29.05	19.20	44.02	3.49	4913.35	0.78
59	0.35	27.34	19.20	42.14	3.40	5114.32	0.76
60	0.38	27.25	19.20	42.03	3.39	5112.34	0.76
61	0.24	23.04	19.20	39.09	3.62	6915.84	0.73
62	0.00	22.75	19.20	39.20	3.74	7597.80	0.73
63	0.00	21.26	19.20	38.14	3.81	8543.31	0.72
64	0.00	18.74	15.12	40.74	3.24	5112.42	0.71
65	0.00	10.15	10.20	39.84	3.32	5111.78	0.66
66	0.00	7.33	8.32	39.84	3.47	5112.23	0.65
67	0.00	6.57	7.78	39.87	3.53	5112.34	0.65
68	4.05	60.00	7.26	94.23	2.02	1776.12	0.61

Appendix M. Constraints used for optimization of RSM model after 12 h and 24 h EFT for the mutated *E. coli* BL21(DE3) variant P.S.5

Table 7.6 – Constraints used in the RSM model for optimization of media components considering 12 h EFT for the mutated *E. coli* BL21(DE3) variant P.S.5. Values of volumetric productivity were determined by densitometry analysis.

Name	Goal	Lower Limit	Upper Limit	Lower Weight	Upper Weight	Importance
A: Glycerol (g/L)	is in range	0.00	12.00	1	1	3
B: Corn steep liquor (g/L)	is in range	0.00	60.00	1	1	3
C: Cheese whey (g/L)	is in range	6.40	19.20	1	1	3
Volumetric productivity (mg/L)	maximize	22.98	272.97	1	1	5
OD_{600nm}	maximize	0.19	3.39	1	1	5
BCA (µg/mL)	maximize	562.28	6148.95	1	1	4
FAN (mg/L)	is in range	0	397.80	1	1	3
Phosphates (mM)	is in range	64.22	172.18	1	1	3

Table 7.7 – Constraints used in the RSM model for optimization of media components considering 24 h EFT for the mutated *E. coli* BL21(DE3) variant P.S.5. Volumetric productivity based on the weight of pure lyophilized SELP-59-A.

Name	Goal	Lower Limit	Upper Limit	Lower Weight	Upper Weight	Importance
A: Glycerol (g/L)	is in range	0.00	12.00	1	1	3
B: Corn steep liquor (g/L)	is in range	0.00	60.00	1	1	3
C: Cheese whey (g/L)	is in range	0.00	25.60	1	1	3
Volumetric productivity (mg/L)	maximize	20.00	293.33	1	1	5
OD_{600nm}	maximize	0	3.56	1	1	5
BCA (µg/mL)	maximize	356.67	6167.12	1	1	1
FAN (mg/L)	is in range	0	397.79	1	1	3
Phosphates (mM)	is in range	64.22	172.18	1	1	3

Appendix N. Optimal points obtained by RSM optimization using the CCD approach, after 12 h and 24 h EFT for the mutated *E. coli* BL21(DE3) variant P.S.5

Table 7.8 – Optimal point solutions and predicted values obtained with RSM optimization for mutant *E. coli* BL21(DE3) P.S.5, after 12 h EFT. Formulation #1 (in bold) was selected as the best formulation. Predicted values for volumetric productivity were computed based on densitometry results.

Number	Glycerol (g/L)	Corn steep liquor (g/L)	Cheese whey (g/L)	Predicted values			Desirability
				Volumetric productivity (mg/L)	OD_{600nm}	BCA (µg /L)	
1	**3.79**	**22.39**	**19.20**	**148.10**	**3.00**	**5747.79**	**0.76**
2	3.78	22.35	19.20	148.08	3.00	5752.41	0.76
3	3.80	22.39	19.20	148.19	3.00	5743.06	0.76
4	3.80	22.43	19.20	148.16	3.00	5740.38	0.76
5	3.77	22.30	19.20	148.08	3.00	5756.90	0.76
6	3.78	22.29	19.20	148.18	2.99	5752.76	0.76
7	3.82	22.50	19.20	148.18	3.00	5733.46	0.76
8	3.76	22.19	19.20	148.22	2.99	5760.07	0.76
9	3.79	22.57	19.20	147.87	3.00	5741.18	0.76
10	3.83	22.40	19.20	148.44	2.99	5730.04	0.76
11	3.82	22.31	19.20	148.48	2.99	5737.13	0.76
12	3.76	22.48	19.20	147.74	3.00	5755.80	0.76
13	3.86	22.60	19.20	148.35	3.00	5715.63	0.76
14	3.82	22.25	19.20	148.58	2.99	5737.49	0.76
15	3.85	22.46	19.20	148.52	2.99	5720.70	0.76
16	3.83	22.26	19.20	148.66	2.99	5732.74	0.76
17	3.70	22.03	19.20	147.97	2.99	5788.14	0.76
18	3.85	22.80	19.20	148.02	3.00	5712.45	0.76
19	3.73	21.93	19.20	148.36	2.99	5777.81	0.76
20	3.65	22.08	19.20	147.51	3.00	5804.64	0.76
21	3.82	22.01	19.20	148.96	2.98	5741.38	0.76
22	3.69	22.67	19.20	146.89	3.01	5776.44	0.76
23	3.67	21.49	19.20	148.58	2.98	5808.48	0.76
24	4.05	23.84	19.20	148.11	3.02	5610.28	0.76

25	3.45	20.83	19.20	148.00	2.97	5900.87	0.76
26	3.37	22.14	19.20	144.85	3.02	5913.66	0.76
27	4.17	21.72	19.20	151.59	2.94	5620.60	0.76
28	2.85	19.33	19.20	145.82	2.95	6155.91	0.76
29	2.74	17.68	19.20	149.02	2.88	6185.55	0.76
30	2.72	19.08	19.20	145.24	2.94	6209.87	0.76
31	2.43	16.39	19.20	150.10	2.82	6297.74	0.75

Table 7.9 – Optimal point solutions and predicted values obtained with RSM optimization for mutant *E. coli* BL21(DE3) P.S.5, after 24 h EFT. Formulation #1 (in bold) was selected as the best formulation. Predicted values for volumetric productivity were computed based on the weight of pure lyophilized SELP-59-A.

Number	Glycerol (g/L)	Corn steep liquor (g/L)	Cheese whey (g/L)	Predicted values			Desirability
				Volumetric productivity (mg/L)	OD_{600nm}	BCA (μg/mL)	
1	**1.14**	**22.27**	**19.74**	**163.93**	**3.56**	**5446.24**	**0.63**
2	1.14	22.32	19.74	163.80	3.56	5446.38	0.63
3	1.14	22.22	19.73	164.08	3.56	5445.80	0.63
4	1.14	22.38	19.75	163.64	3.56	5446.59	0.63
5	1.12	22.33	19.72	163.92	3.56	5439.81	0.63
6	1.13	22.16	19.71	164.37	3.56	5439.94	0.63
7	1.12	22.53	19.73	163.38	3.56	5438.84	0.63
8	1.14	22.56	19.77	163.11	3.56	5447.51	0.63
9	3.52	57.73	25.60	95.47	3.56	6162.85	0.55
10	3.51	58.31	25.60	94.67	3.56	6152.95	0.55
11	4.00	59.77	25.60	98.31	3.37	6102.07	0.54
12	6.96	60.00	25.60	131.19	2.67	5949.39	0.52
13	11.41	60.00	7.81	147.87	1.64	1222.48	0.37
14	11.41	60.00	7.79	147.76	1.65	1218.12	0.37
15	11.38	60.00	7.78	147.42	1.64	1214.57	0.37
16	11.41	60.00	7.76	147.75	1.65	1208.07	0.37
17	11.64	60.00	7.94	150.90	1.67	1242.91	0.37